NASA Contractor Report 4733

Advanced Technology Composite Fuselage—Repair and Damage Assessment Supporting Maintenance

B. W. Flynn, J. B. Bodine, B. Dopker, S. R. Finn, K. H. Griess, C. T. Hanson, C. G. Harris, K. M. Nelson, and T. H. Walker
The Boeing Company • Seattle, Washington

T. C. Kennedy and M. F. Nahan
Oregon State University • Corvallis, Oregon

National Aeronautics and Space Administration
Langley Research Center • Hampton, Virginia 23681-0001

Prepared for Langley Research Center
under Contracts NAS1-18889 and NAS1-20013

April 1997

Printed copies available from the following:

NASA Center for AeroSpace Information
800 Elkridge Landing Road
Linthicum Heights, MD 21090-2934
(301) 621-0390

FOREWORD

This document is one of nine complementary final technical reports on the development of advanced composite transport fuselage concepts. The work described was performed by the Boeing Commercial Airplane Group, Seattle, Washington, from May 1989 through December 1995 under contracts NAS1-18889 and NAS1-20013, Task 2. The contracts were sponsored by the National Aeronautics and Space Administration, Langley Research Center (NASA-LaRC) as part of the Advanced Composite Technology (ACT) program. Direction from NASA-LaRC was provided by M.J. Shuart, J.G. Davis, W.T. Freeman, and J.B. Nelson.

The nine documents comprising the final documentation for the NASA/Boeing ATCAS program include:

Advanced Technology Composite Fuselage

- **Program Overview** (CR-4734). *Synopsis of program approach, timeline and significant findings. Design synthesis considering manufacturing, materials, processes, structural performance, maintenance, and cost.*
- **Manufacturing** (CR-4735). *Baseline manufacturing and assembly approaches. Process and tooling developments, and manufacturing demonstration activities to address critical manufacturing issues.*
- **Materials and Processes** (CR-4731). *Baseline and alternative materials and processes. Material and process developments. Material performance.*
- **Structural Performance** (CR-4732). *Methods used for design sizing. Analysis and test activities supporting assessment of design development methodologies for critical performance issues.*
- **Repair and Damage Assessment Supporting Maintenance** (CR-4733). *Maintenance considerations in design. Detailed repair concepts for quadrant design. Fabrication, inspection, and analytical developments.*

Cost Optimization Software for Transport Aircraft Design Evaluation (COSTADE)

- **Overview** (CR-4736). *Synopsis of COSTADE initiative, including integration of cost, weight, manufacturing, design, structural analysis, load redistribution, optimization, and blending.*
- **Design Cost Methods** (CR-4737). *Components of cost analysis and their interactions. Theoretical framework for process-time prediction. Methods for developing and maintaining cost equations. Applications to ATCAS quadrant designs.*
- **User's Manual** (CR-4738). *COSTADE user instructions, including hardware requirements and installation procedures. Program structure, capabilities, and limitations. Basis of cost model and structural analysis routines. Example problems.*
- **Process Cost Analysis Database** (CR-4739). *Rationale for database framework. Database user's guide, including capabilities and limitations. ATCAS process step equations.*

Use of commercial products or names of manufacturers in this report does not constitute official endorsement of such products or manufacturers, either expressed or implied, by the Boeing Company or the National Aeronautics and Space Administration.

At completion of these contracts, Boeing program management included Bjorn Backman as Program Manager, Peter Smith as Technical Manager, and Larry Ilcewicz as Principal Investigator. Authors listed for this contractor report prepared portions of the document. The members (past and present) of the Boeing ACT contract team who contributed to the work described in this document include:

Program Management:
Phil Whalley
Ron Johnson
Ray Horton
Jordan Olson
Bjorn Backman

Technical Management:
Peter Smith

Principal Investigators:
Randy Coggeshall
Larry Ilcewicz

Structural Design:
George Truslove
Chris Hanson
Ken Griess
Mike Schram
Stephen Metschan
Mike Morris
Tuan Le

Computing Support:
Bob Lundquist
Bill Koch
Sterling Johnston

Structural Analysis:
Tom Walker
Ernie Dost
Gary Swanson
Blake Flynn
Gerald Mabson
David Carbery
Scott Finn
Dan Murphy
Bernhard Dopker
David Polland
William Avery
Jerry Bodine
Doug Graesser
Andre Williams
Mark Fedro
Peter Grant
Adam Sawicki
Pierre Minguet

Technical Aide:
Bill Waltari

Materials and Processes:
Dodd Grande
David Scholz
Karl Nelson
Tony Falcone
Brian Perkins

Manufacturing Technology:
Tom May
Kurtis Willden
Val Starkey
Tim Davies
Mark Gessel
Joe Hafenrichter
Bob Matetich
Ken Goodno
Dick Curran
Ken Dull
Rob Biornstad
Peter Lohr
Stan Stawski
Chris Harris
Greg Bell
Jan Koontz
Rob Synder
Tom Cundiff
Gary Moon

Cost Estimating:
Kent Venters
Will Gaylord
Cal Pfahl
David Tervo
Len Witonsky
Odo Bormke
Robert Humphrey
Mike Proctor
Hans Fredrikson
Dennis Stogin

Fire Worthiness:
Jim Peterson
Thomas Murray

Developmental Manufacturing:
Jose Valdez
Ponci Puzon
Bonnie Luck

Test Laboratories:
Ron Slaminko
John Schneider
Carl Preuss
Joan Dufresne
Tony Phillips
Dan Moreillon
Bill Hardrath

Business Management:
Jeff Heineman
Marge Apeles
Kira Goerlich

QC and NDE Development:
Ken Mackey
Brian Lempriere
Bill Fortig
John Linn

Weights:
Glenn Parkan

Repair Development:
Bert Bannink
Mike Evens
Sherry Marrese

Customer Support:
Dave Berg
Jeff Kollgaard

Materiel:
Maureen Hughes
Mark Jones
Steve Ruth
Doug Wood
Christal Tyson-Winston
Howard Lanie
Mark McConnell
Tom Hesketh

Industry And University Design-Build-Team Members

University of Washington:
Kuen Y. Lin
James Seferis
Zelda Zabinsky
Mark Tuttle

Stanford University:
Fu-Kuo Chang

Oregon State University:
Tim Kennedy

M.I.T:
Paul Lagace
Tim Gutowski
David Hoult
Greg Dillon
Hugh McManus

Drexel University:
Jonathan Awerbuch
Albert Wang
Alan Lau
Frank Ko

University of Iowa:
Roderic Lakes

University of Utah:
William Bascom
John Nairn

University of Wyoming:
Donald Adams
Rhonda Coguill
Scott Coguill

U. of Cal. Santa Barbara:
Keith Kedward

Univ. of British Columbia:
Anoush Poursartip

Brigham Young University:
Ken Chase

San Jose State University:
Robert Anderson

Dow-UT:
Rich Andelman
Douglas Hoon

Sikorsky Aircraft:
Christos Kassapoglou

Northrop/Grumman:
Ravi Deo
Steve Russell
Bob Ley
Ram Vastava
Ram Ramkumar

McDonnell Douglas:
Benson Black

Lockheed Aero. Systems:
Tony Jackson
Ron Barrie
Bob Chu
Dan Skolnik
Jay Shukla
Bharat Shah
Lowell Adams
Lisa Ott

Fiber Innovations:
Steve Goodwin
Garrett Sharpless

Hercules Materials Co.:
Doug Cairns
David Cohen
Roger Stirling
Lynn Muir
Will McCarvill
Yas Tokita

Alliant Techsystems:
Carroll Grant
George Walker
Tammy Harris
Todd Brown
Mark Wheeler
Jon Poesch
Vern Benson

American Airlines:
Jim Epperson
Marcus Peter

Northwest Airlines:
Jim Oberg
Erik Restad
Mark Wolf

United Airlines:
Bob Bernicchi
John Player

Cherry Textron:
Howard Gapp

Sunstrand:
Glen Smith
Hossein Saatchi
Bill Durako

ICI Fiberite:
Erinann Corrigan
Russ Holthe

G.M.I:
Roland Chemana

Intec:
Brian Coxon
Chris Eastland
Rod Wishart
Shreeram Raj
Don Stobbe

Zetec:
Chuck Fitch
Gregg Colvin

Draper Laboratory:
Ed Bernardon

Hexcel:
Stacy Biel
Julaine Nichols
Kevin Marshal

E. I. Du Pont De Nemours:
Jim Pratte
Hal Loken
Ginger Gupton

Materials Science Corp.:
Walt Rosen
Anthony Caiazzo

Structural Consultant:
John McCarty

EBCO Tooling:
Rich Roberts

TABLE OF CONTENTS

1.0 SUMMARY

Under the NASA-sponsored contracts for Advanced Technology Composite Aircraft Structures (ATCAS) and Materials Development Omnibus Contract (MDOC), Boeing is studying the technologies associated with the application of composite materials to commercial transport fuselage structure. Included in the study is the incorporation of maintainability and repairability requirements of composite primary structure into the design. Such issues must be addressed to meet regulatory requirements and ensure that life-cycle costs are competitive with current metallic structure. This contractor report describes activities performed as part of the ATCAS program to address maintenance issues in composite fuselage applications.

A key aspect of the study was the development of a maintenance philosophy which included consideration of maintenance issues early in the design cycle, multiple repair options, and airline participation in design trades. Furthermore, fuselage design evaluations considered trade-offs between structural weight, damage resistance/tolerance (repair frequency), and inspection burdens. To support these design decisions, analysis methods were developed to assess structural residual strength in the presence of damage, and to evaluate repair design concepts.

Repair designs were created with a focus on mechanically fastened concepts for skin/stringer structure and bonded concepts for sandwich structure. Repair materials and processes were established in small-scale trials, then demonstrated on large panels. Both a large crown (skin/stringer) and keel (sandwich) panel were repaired. A compression test of the keel panel indicated the demonstrated repairs recovered ultimate load capability. In conjunction with the design and manufacturing developments, inspection methods were investigated for their potential to evaluate damaged structure and verify the integrity of completed repairs.

2.0 INTRODUCTION

Boeing's Advanced Technology Composite Aircraft Structures (ATCAS) program (contract NAS1-18889) was initiated in May 1989 as an integral part of the NASA sponsored Advanced Composites Technology (ACT) initiative. As an extension of this work, Task 2 of Materials Development Omnibus Contract (MDOC, contract NAS1-20013) was awarded in November 1993. Combined, these two contracts addressed concept selection and technology development (referred to as Phases A and B). An additional contract (NAS1-20553) has been initiated to verify this technology at a large scale (referred to as Phase C). The goal of the ACT initiative is to develop composite primary structure for commercial transport aircraft with 20-25% less cost and 30-50% less weight than equivalent metallic structure.

The ATCAS program activities within the ACT framework have focused on fuselage structure. More specifically, the primary objective of the program is to develop and demonstrate an integrated technology which enables the cost- and weight-effective use of composite materials in fuselage structures of future aircraft. The area of study is a pressurized aft fuselage section of a wide body airplane with a diameter of 244 inches (Figure 2-1). The structure, located immediately aft of the wing-to-body intersection and main landing gear wheel well, is designated Section 46 on Boeing aircraft. This section, highlighted in Figure 2-1, contains most of the structural details and critical manufacturing issues found throughout the fuselage. It has significant variations in design detail due to relatively high loads in the forward end which diminish toward the aft end, allowing a transition to minimum gage structure.

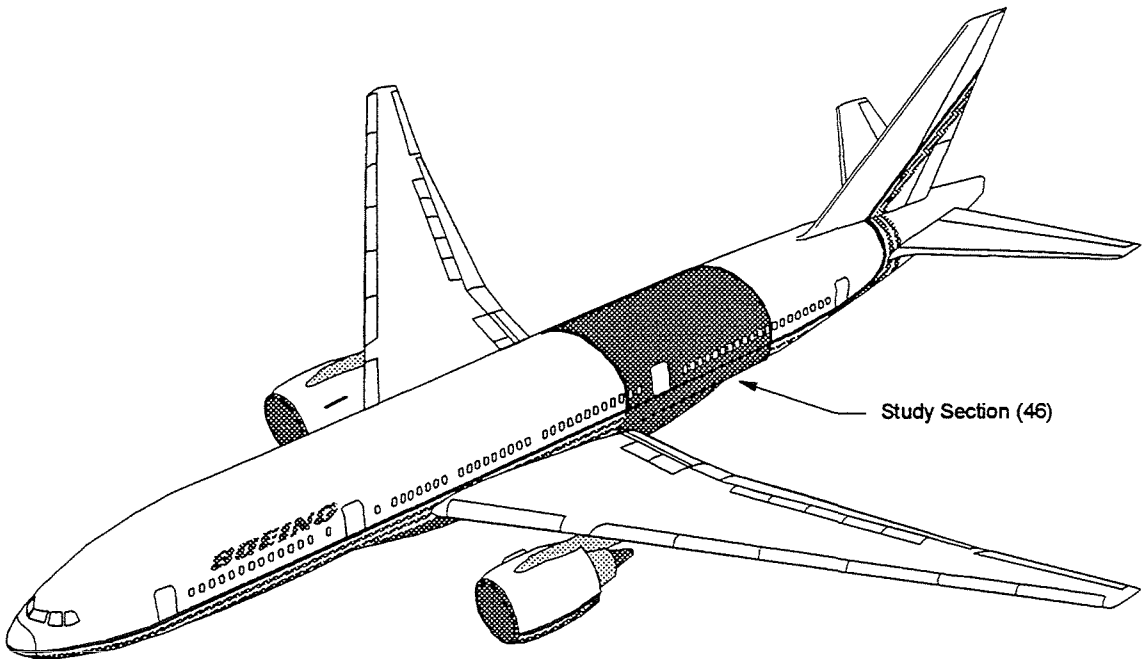

Figure 2-1: Baseline Vehicle and Study Section

The fuselage cross-section is divided into four circumferential segments in the baseline manufacturing approach. These "quadrants" consist of a crown, keel, and left and right side panels, as illustrated in Figure 2-2. The quadrant approach was adopted to reduce panel assembly costs (fewer longitudinal splices) and leverage the size-related efficiencies of the automated fiber placement (AFP) process for laminated skins, while maintaining design flexibility for regions with differing requirements [1, 2].

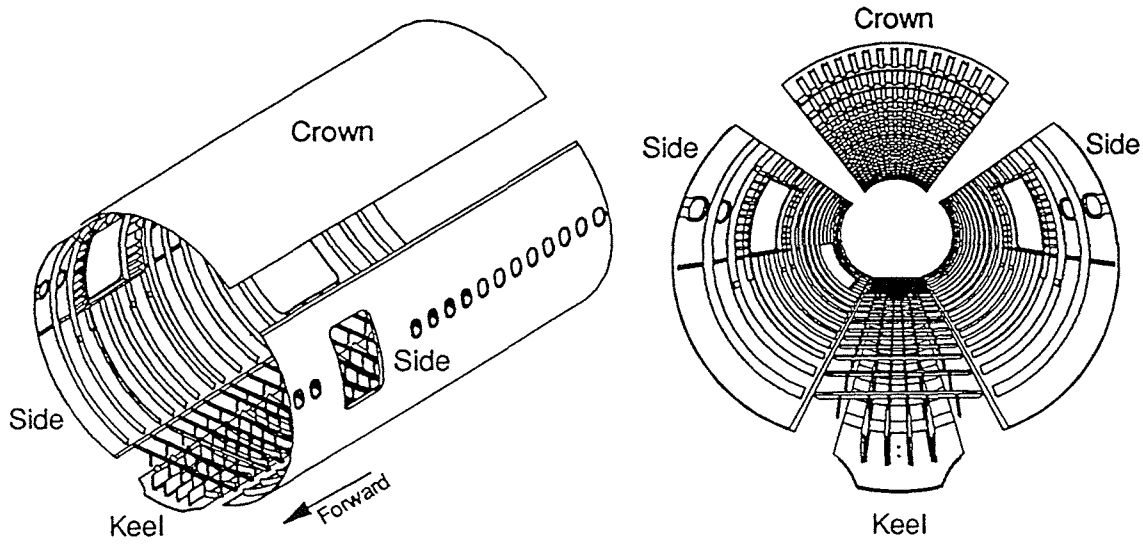

Figure 2-2: Fuselage Quadrants

Design Build Teams (DBTs), consisting of various disciplines responsible for creating aircraft structure (e.g., design, manufacturing, cost analysis, materials, structures, quality control) were formed to develop detailed designs and manufacturing plans for each quadrant, as well as the associated splices. Design trade studies resulted in the selection of a skin/stringer configuration for the crown, and sandwich construction for the keel and side quadrants [1, 3]. Large crown and keel subcomponent panels were subsequently fabricated to demonstrate manufacturability and to verify cost and weight efficiency of the respective designs. In addition to numerous small-scale repair trials, one subcomponent panel of each design was dedicated to demonstrate repair techniques and serve as a structural test panel.

Crucial to the success of composite fuselage design is the incorporation of maintainability and repairability requirements. These issues were addressed by the DBT throughout the ATCAS program. This report comprises the findings of this effort. Section 3.0 presents the general approach established for including maintenance considerations into the design, and describes specific repair designs for crown (skin/stringer) and keel (sandwich) panels. Section 4.0 details analysis and test efforts supporting the design of both maintainable quadrant panels and individual repairs. Developments and demonstrations of repair manufacturing processes and inspection methods are discussed in Sections 5.0 and 6.0, respectively.

Initial investigations of repair technology under Phases A and B of ATCAS were necessarily limited due to budget and schedule constraints. For this reason, a relatively narrow scope of damage scenarios, material options, processing and other design variables were demonstrated. Nevertheless, due to the building block nature of the approach, some scaling to other damage states is possible. Subsequent development under Phase C funding will expand composite repair technology, and will have as its goal the development of a general repair approach for a variety of damage which is likely to occur in service, with supporting process development and demonstration.

3.0 DESIGN FOR MAINTAINABILITY

3.1 In-Service Experience

The first step toward designing reliable and cost-effective design details is to understand the history of composite structure currently flying in the commercial aircraft fleet. Composite materials, as we know them today, were introduced into the commercial aircraft industry during the early 1960's and used mostly glass fiber. Development of more advanced fibers such as boron, aramid, and carbon offered the possibility of increased strength, reduced weight, improved corrosion resistance, and greater fatigue resistance than aluminum. These new material systems, commonly referred to as advanced composites, were introduced to the industry very cautiously to ensure their capabilities.

The early success of the first simple components such as wing spoilers and fairings led to the use of advanced composites in more complex components such as ailerons, flaps, nacelles, and rudders. The increased specific stiffness and strengths of composites over aluminum, coupled with weight-driven requirements caused by fuel shortages, led to the application of thin-skin sandwich structures. Long-term durability requirements of the original aluminum parts were not fully accounted for when these composite parts were originally designed. To compound the problem further, damage phenomena such as delamination and microcracking were new and complex in comparison to traditional aluminum structure.

The original composite parts, particularly thin-gage sandwich panels, experienced durability problems that could be grouped into three categories: low resistance to impact, liquid ingression, and erosion. Because the parts were secondary structure, and given the emphasis placed on weight and performance, the facesheets of honeycomb sandwich parts were often only three plies thick. This approach was adequate for stiffness and strength, but never considered the service environment where parts are crawled over, tools dropped, and where service personnel are often unaware of the fragility of thin-skinned sandwich parts. Because damage to these components is quite often difficult to detect with a visual inspection, service personnel did not want to delay aircraft departure or bring attention to their accidents, which might reflect poorly on their performance record. Therefore, small damages were allowed to go unchecked, often resulting in growth of the damage due to liquid ingression into the core. Nondurable design details (e.g., improper core edge close-outs) also led to liquid ingression.

The repair of parts due to liquid ingression can vary depending upon the liquid, of which water and Skydrol (hydraulic fluid) are the two most common. Water tends to create additional damage in repaired parts when cured unless all moisture is removed from the part. Most repair material systems cure at temperatures above the boiling point of water, which can cause a disbond at the skin-to-core interface wherever trapped water resides. For this reason, core drying cycles are typically included prior to performing any repair. Some airlines will take the extra step of placing a damaged but unrepaired part in the autoclave to preclude any additional damage from occurring during the cure of the repair.

This is done to assure they will only need to repair the part once. Skydrol presents a different problem. Once the core of a sandwich part is saturated, complete removal of Skydrol is almost impossible. The part continues to weep the liquid even in cure such that bondlines can become contaminated and full bonding does not occur.

Erosion capabilities of composite materials have been known to be less than that of aluminum and, as a result, their application in leading edge surfaces has been avoided. However, composites have been used in areas of highly complex geometry, but generally with an erosion coating. The durability and maintainability of erosion coatings are less than ideal. Another problem, not as obvious as the first, is that edges of doors or panels can erode if they are exposed to the air stream. This erosion can be attributed to improper design or installation/fitup.

Assessing airline experience with composite structure is, taken as a whole, an extremely difficult task. Depending on who is consulted from the airlines, the responses vary from horror stories to outstanding success. Given these limitations, the facts and data that are currently available are the detailed reports that were received from the airlines on parts involved in the NASA-sponsored Advanced Composites Energy Efficiency (ACEE) program, which supported the design and fabrication of composite parts such as those shown in Figure 3-1 to replace metal parts. Five shipsets of 727 elevators have accumulated more than 331,000 hrs. and 189,000 cycles; 108 737 spoilers have accumulated more than 2,888,000 hrs. and 3,781,000 cycles. Also included were five shipsets of 737 horizontal stabilizers which incorporated laminate torque boxes and sandwich ribs. These stabilizers have amassed over 133,500 flight hours and 130,000 landings as of May, 1995. The service exposure data collected for these parts has not indicated any durability or corrosion problems. (Some minor corrosion pitting was found in fastener holes of 737 stabilizer aluminum trailing edge fittings — this due to an obsolete sealing practice.) Several repairs have been satisfactorily performed on the 727 elevators and 737 horizontal stabilizers.

Production graphite-epoxy sandwich parts, such as trailing edge panels, cowls, landing gear doors, and fairings have demonstrated weight reduction, delamination resistance, fatigue improvement and corrosion prevention. The poor service records of some parts can be attributed to fragility or the inclusion of nondurable design details. Many of the design problems were a result of insufficient technology transfer from development programs such as NASA-ACEE. Fragility, so much an issue in thin-gage secondary structure, is expected to be much less important in thicker-gage primary structures such as the fuselage and wing. The thicker skins of the current 777 composite horizontal stabilizer, for instance, are much more damage resistant.

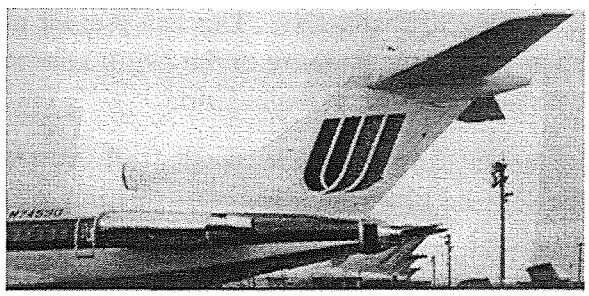

727 elevator

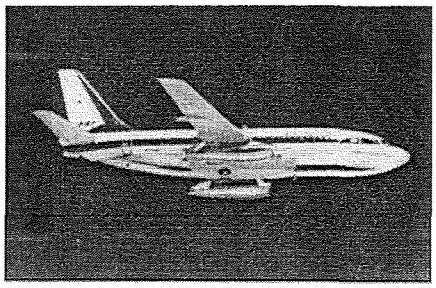

737 horizontal stabilizer

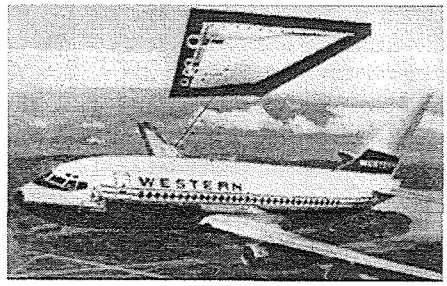

737 spoilers

Figure 3-1: Prototype Commercial Applications of Composite Primary and Secondary Structures

3.2 General Maintenance Approach

The maintenance approach for the ATCAS program was based upon input and knowledge gained from a working relationship established between the ATCAS team and airline maintenance personnel. This was accomplished through repair workshops with airline and customer support personnel, subcontracts with American Airlines for repair trials and demonstrations, and involvement with an international composite repair committee. The time spent within these efforts has provided a broader understanding of the overall environment in which airlines operate. Boeing's involvement in the Commercial Aircraft Composite Repair Committee (CACRC) has contributed considerably to addressing the problems that airlines voice. The CACRC is pioneering standards and recommendations for the design and maintenance of future composite structure based on current and past experience.

Figure 3-2 shows maintenance development philosophy established during Phase B of the ATCAS composite fuselage program. Maintenance procedures such as inspection and repair, which are applicable to a service environment, must be considered during design selection. Closed hat-section stringers, for instance, are compatible with inexpensive manufacturing techniques, but pose difficulties relative to inspection and attachment in repair applications. Material choices may also be affected. The designer should avoid the use of different material systems with different curing temperatures on one part. For instance, skins and stiffeners are sometimes precured at 350°F and then, for manufacturing

ease, secondarily bonded with 250°F adhesive. This can present problems when the skins or stiffeners are repaired at 350°F; the integrity of the 250°F adhesive at the bond interface may be compromised with no indication of degradation.

Design concept developments should include parallel efforts to establish maintenance procedures. As will be discussed later, the crown was the only ATCAS fuselage quadrant where maintenance procedures were established *after* design features for manufacturing scale-up were set, resulting in unnecessarily complex repair designs and processes. Skin layup changes were later found to simplify the crown repair without adding weight.

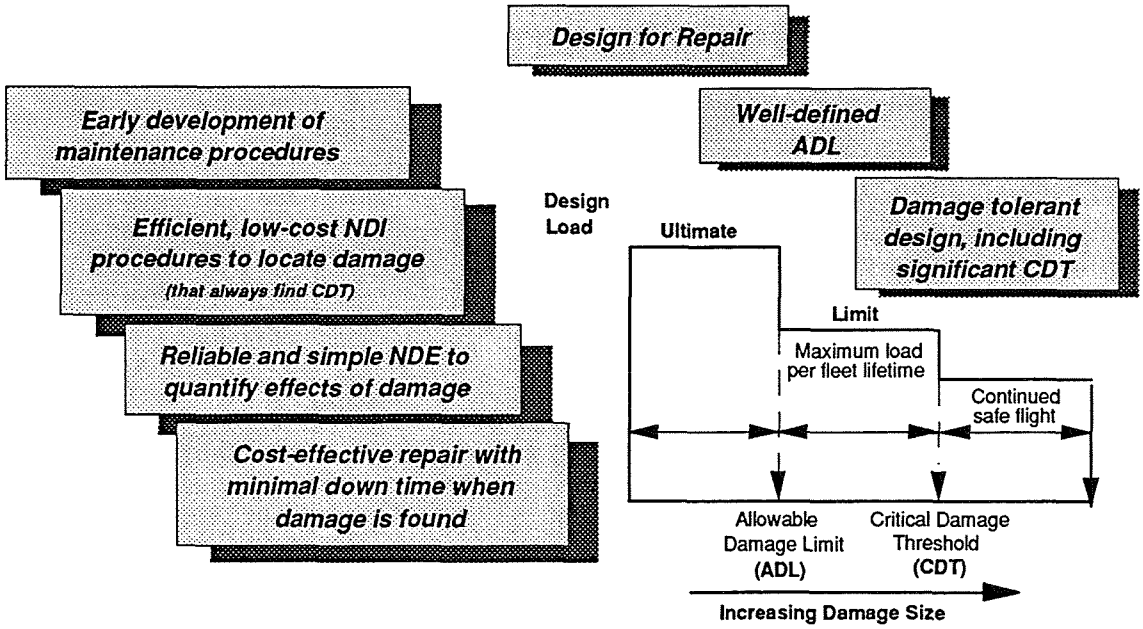

Figure 3-2: Rules for Maintainable Composite Structures

Another important aspect of concept development critical to maintenance is damage tolerant design practices. The allowable damage limits (ADL) and critical damage thresholds (CDT) defined in Figure 3-2 must be established to support the structural repair manual and inspection procedures. The former allows rapid determination of the need for repair during scheduled inspection, while the latter should be sufficiently large to allow safe aircraft operation between inspection intervals. Knowledge of residual strength and inspection capabilities should allow determination of both ADL and CDT as a function of structural location.

The design of some areas of the structure can be controlled by manufacturing and durability considerations. Specific examples of these considerations are minimum gage requirements (to provide a minimum of impact damage resistance and avoid knife-edge at countersink fasteners), and avoiding rapid ply drops and buildups. Areas of the structure designed to these considerations will therefore have higher margins for damage tolerance. Figure 3-3 shows the minimum margins of safety for the side quadrant, illustrating the "over-designed" regions. These zones have ADLs and CDTs larger than the rest of the

fuselage section. Zoned ADL and CDT information should prove useful to airlines desiring minimum maintenance costs.

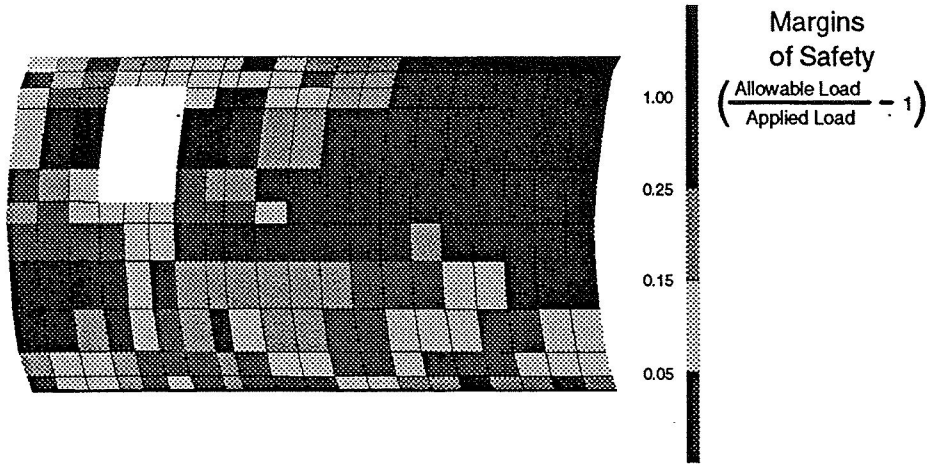

Figure 3-3: Strength Margin of Safety Distribution for the Side Quadrant Subjected to Ultimate loads

The understanding derived from residual strength analyses and tests will also ultimately lead to DBT cost and weight trades that affect nearly all of the total direct operating costs (DOC). Small increases in manufacturing cost and structural weight may be traded against increased damage tolerance to reduce maintenance costs. Decisions may be required to balance the ADL and CDT. For example, test results for laminate tension notch sensitivity showed an inverse relationship between small and large notch strength [4, 5]. Under such circumstances it may be desirable to have some ADL capability to avoid having to repair small damages but not at the expense of CDTs that allow sufficiently long inspection intervals and satisfactory failsafe behavior.

Returning to Figure 3-2, another requirement for maintainable composite structure is the establishment of nondestructive inspection (NDI) and evaluation (NDE) procedures for practical damage location and quantitative assessment, respectively, during scheduled maintenance. The latter, which may require ultrasonic methods, should only be required to assess the effects of damage found by more easily performed procedures (e.g., visual).

When damage is found, efficient repair procedures are needed which the airlines can accomplish with available resources (tooling, equipment, etc.) and with a minimum amount of airplane down time. In order to develop repair concepts for a broad range of damage scenarios, the repair design philosophy is focusing on more generic repairs which are not damage-specific. This approach will be beneficial because generic designs and corresponding repair "kits" can be developed for various levels of damage which are, within certain limits, independent of specific damages. This is intended to greatly reduce the need to develop repairs for each damage event as it occurs, providing a higher level of maintainability. Initially, three damage levels have been defined and are shown in Table 3-1 as they apply to a skin/stringer configuration.

Table 3-1: Damage Level Definitions

Designation	Damage Description	Repair
Level 0	Skin delamination or disbond from stiffening elements	Fastener restraint or wet resin repair
Level 1	Critical damage to a single structural element (skin or stiffener)	Mechanically fastened patch and/or splice
Level 2 (and higher)	Multiple occurrences of Level 1 damage	Same as Level 1

Designs will address repair in a building-block approach in that each bay is looked upon as a unit, or building block. Restoration of that unit (frame, stringer, and/or skin) will be designed so that larger multiple-bay damages can be handled with less effort. Structural units are less easily defined for sandwich structure; however, the same general philosophy applies. The strategy behind this approach is to address the repair scenarios for a large range of damage at the beginning of the design process to ease the maintenance burden.

Another aspect of the approach is to provide airlines with multiple options for a given repair situation. Options might include temporary vs. permanent repair, bonded vs. bolted, or which specific repair material/processing combination to employ. An airline's choice might depend on the severity of the damage, the time available to perform the repair, the airline's facilities and capabilities, inspection/overhaul schedules, and/or current field environmental conditions.

3.2 Skin/Stringer Repair Concepts

3.2.1 Scope

The ATCAS tension-load-dominated fuselage crown panel is a stiffened skin design with cocured hat stringers and cobonded J frames (Figure 3-4). Only mechanically fastened repair concepts were considered for the crown. Repair design variables were first investigated on building-block coupons with Level 1 damage. Subsequently, a repair was designed for a large aft crown panel with Level 3 damage (i.e., a through-penetration, longitudinally oriented, severing two skin bays and a central circumferential frame). These efforts focused on an early crown-quadrant design which included a skin laminate which was much stiffer in the hoop than the axial direction.

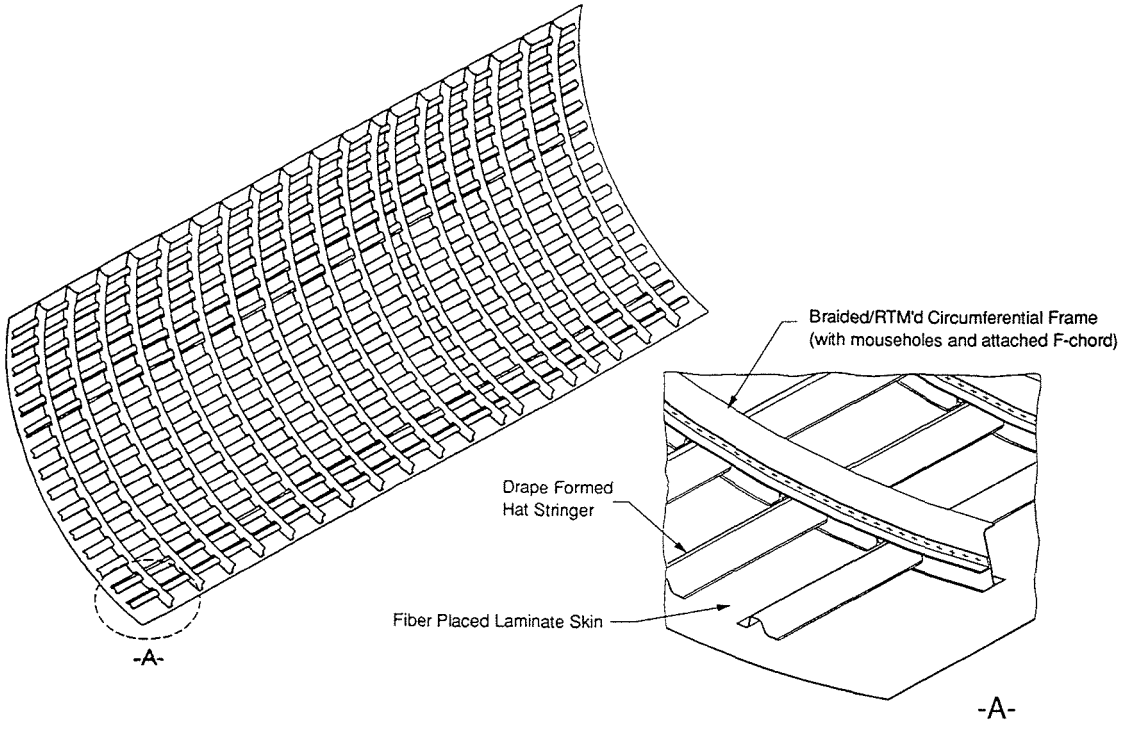

Figure 3-4: Baseline ATCAS Crown Panel.

3.2.2 Issues

Crown repair concepts are focusing on mechanically fastened external skin patches and nested frame splice angles. Mechanically fastened repairs require care and accuracy in the drilling of holes and the alignment of parts during assembly. Fastener hole breakout is a characteristic problem, commonly solved by using a layer of fabric as the outermost ply for all laminates. Typically, even though there may be other methods to avoid fastener hole breakout, there are numerous situations in the real world that challenge a good mechanic's ability to consistently drill high quality holes. Provisions to locate the position of the drilled holes in the structure include alignment marks and templates. Also, sealant must be applied both on faying surfaces and at each fastener location to ensure pressure containment. Because of these issues, a repair that contains a large number of fasteners, though sometimes unavoidable, is also less desirable.

Typical issues associated with external patches include weight, surface profile, and load path eccentricities. The added patch material, in addition to increasing weight, can locally increase the stiffness so as to create a hard spot, which can affect load distributions in the area of the repair. Concerns over external patches projecting into the airstream are similar to those for metal repairs. Eccentric load paths, although contributing to bending stresses, are less of an issue in the crown quadrant where compression loads are less critical than tension loads, and concerns over stability are therefore low.

Another question is whether patch stiffness should be tailored to a specific damage site, or be made more generic (e.g., all quasi-isotropic) for more general applicability. An airline's

inventory of materials can be reduced through standardization of the supplies needed for repairs, such as fasteners, specialized repair materials, tools, and equipment.

Inspection methods must be sufficient to identify the damage area for removal. The choice of methods for inspecting the repaired structure may depend on the type of repair. A one-sided repair can be easier to install, but is limited to one-sided NDE techniques and requires the use of blind fasteners, which are difficult to inspect and have less consistent strength. A two-sided repair is less convenient to perform, but can make use of more common fasteners and a wider array of inspection methods.

3.2.3 Concepts

The repair concept chosen for demonstration on the large crown panel is shown in Figure 3-5. A predetermined cutout is used to simulate a failed frame and two bays of skin, assuming that the damage did not interact with the stringer. If stringer damage had occurred, it would also have to be repaired. The predetermined cutout does not reflect any anticipation of damage type, shape, or orientation, but rather is generalized. This approach lets the design of the repair cover a large range of damage scenarios.

The crown repair design includes a two-layer external skin patch for commonality with the smaller damage. Based on this design, parts of the skin patch can be used for a Level 1 skin repair. The larger Level 3 damage requires a much thicker patch for ultimate load capability, hence two layers are used. The Level 3 skin patch design utilizes a stack of two 0.08" skin patch laminates, with the outer patch being shorter than the inner patch to allow the first row of fasteners to only interact with one patch, thereby locally reducing the intensity of the load introduction in the longitudinal direction. The longer skin patch includes holes at the corners to alleviate the severe load introduction at those locations. Skin patches are quasi-isotropic layups of fiberglass/epoxy fabric which are precured and bolted to the base structure. Splice members for the severed frame are precured angles made of graphite/epoxy fabric, bolted to the frame web and caps.

Analysis efforts described in Section 4.2.1 identified two additional configurations which provide improved structural performance relative to the above baseline. The second configuration utilizes E-glass/epoxy tape instead of fabric in the skin patches to achieve anisotropic properties and better match the stiffnesses of the base structure. Similarly, the frame splice material was changed to graphite/epoxy tape, with a laminate equal to the skin. Although this concept was shown to enhance structural performance, its generality to repair of the entire fuselage, where stiffness requirements would vary, is questionable.

The third repair configuration (Figure 3-6) was developed for a more recent version of the crown design, which was generated to satisfy an increased axial damage tolerance design goal. The redesign included updated strain allowables and increased axial stiffness characteristics for the crown skin and stringers. These changes allowed a simpler, one-layer, mechanically fastened, graphite/epoxy patch design than was possible with the softer skin and stiffeners of the earlier concept. The modified design also includes a narrower skin patch, a slightly altered frame splice (also incorporated on the second repair configuration), and a modified fastener pattern.

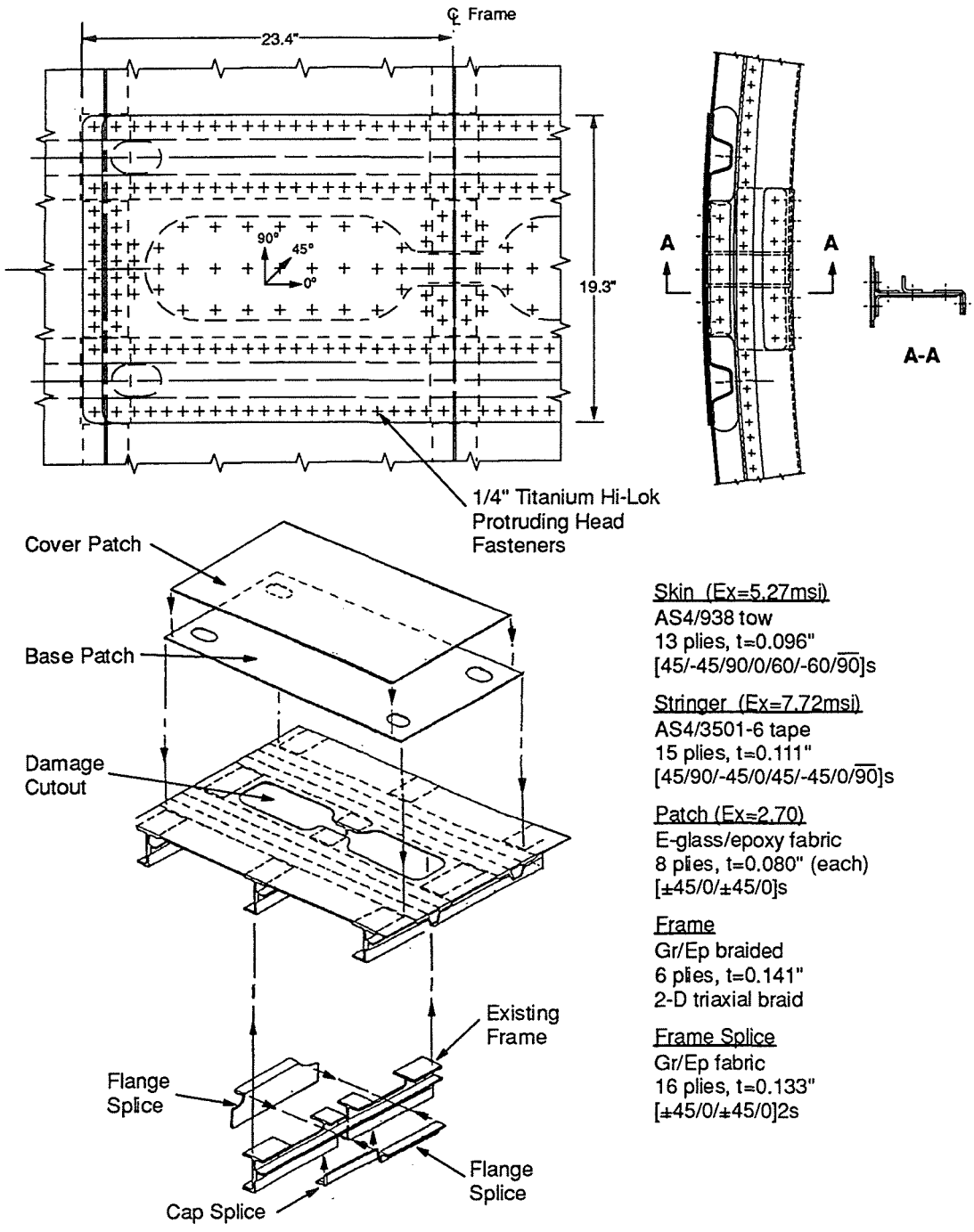

Figure 3-5: Demonstrated Crown Panel Repair Concept.

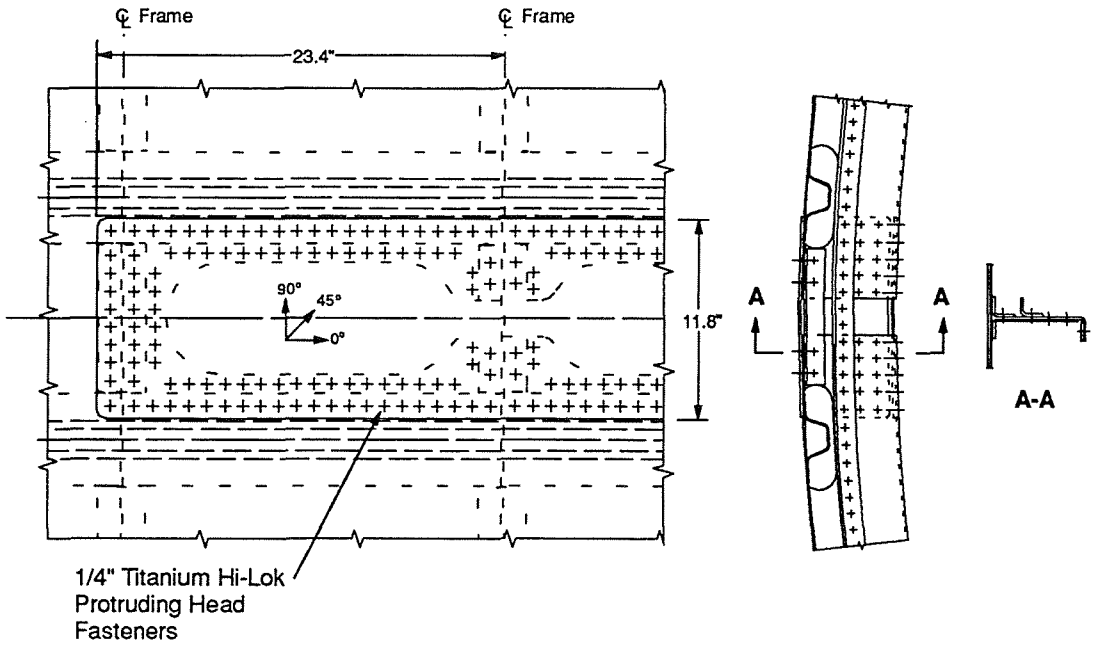

Skin (Ex=10.8msi)
AS4/938 tow
16 plies, t=0.118"
[45/-45/90/0/30/0/0/-30]s

Patch (Ex=8.92msi)
AS4/938
13 plies, t=0.096"
[-45/45/0/90/-30/30/0]s

Frame Splice
Gr/Ep fabric
16 plies, t=0.133"
[45/-45/90/0/60/-60/90]s

Stringer (Ex=12.4msi)
AS4/3501-6 tape
15 plies, t=0.111"
[45/0/-45/0/90/0/15/0/-15]s

Frame
Gr/Ep braided
6 plies, t=0.141"
2-D triaxial braid

Figure 3-6: Alternative Crown Repair.

3.3 Sandwich Repair Concepts

3.3.1 Scope

The configuration of the compression-dominated fuselage keel structure is driven by load concentrations at the forward end due to the large cutouts for the wing center section and wheel well [1,3]. The resulting baseline keel design features a thick solid laminate at the forward end which transitions via ply drops and tapered core to an equally thick sandwich structure with relatively thin (12 ply) facesheets at the aft end (Figure 3-7). The current study addresses the repair of sandwich structure in the mid keel area where the facesheets are 30 plies and the honeycomb core thickness is 0.637". The damage scenario under consideration is a 2" diameter penetration of the outer facesheet, and corresponding core damage. For the Phase B study, all design, analysis, manufacturing trials, and test activities were tied to this damage state. The emphasis was on permanent bonded repairs, while a parallel effort to investigate temporary repair options was also conducted.

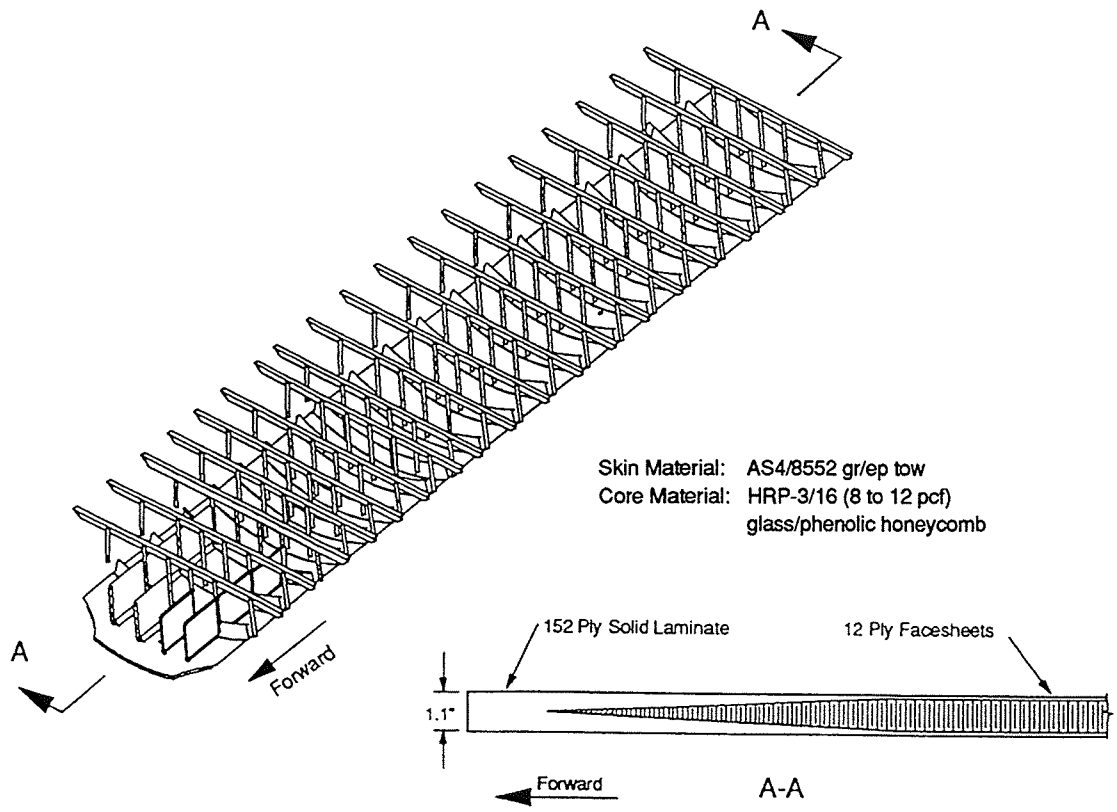

Figure 3-7: Baseline ATCAS keel panel.

3.3.2 Issues

Conventionally, sandwich structure is repaired with in-situ processed bonded scarf patches. With the thick facesheets in the keel panel, however, scarf repairs with traditional shallow taper ratios (e.g., 20:1) result in very large patch sizes and the removal of a large amount of undamaged material. Also, thick facesheets require thick patches, which may require special processing to achieve proper consolidation. Patch and bondline porosity are of particular concern with normal field processing, which is accomplished with vacuum pressure and heat blankets. Lower temperature cures are generally preferred due to concerns over causing additional damage via vaporization of water which has infiltrated the core. Also, the surrounding structure may act as a heat sink, making it difficult to achieve and control the higher temperatures with heat blankets, and may contribute to thermal gradients which can result in warpage or degradation of the surrounding structure. Still, the shorter processing times generally associated with higher temperature cures are very attractive in terms of minimizing the out-of-service time for a damaged airplane.

Patch materials may have to differ from the base structure to achieve the desired properties within the constraints of the processing environment. Some airlines prefer wet layup material systems for their ability to cure at lower temperatures, and to avoid freezer storage of prepregs; however, there is concern about the quality of wet layup repairs on

thick primary structural parts. The current study is focused on prepreg materials, which can be easier to work with, but which require freezer storage. Precured patches are considered for bolted repair concepts. Core material options include replacing damaged honeycomb by bonding in a plug of the same material, or by some alternative such as in-situ foam.

Repair concepts must address the effects of moisture in the core — both by minimizing the degree of moisture ingression, and by determining what its presence does to the performance of the structure. A drying cycle is typically performed prior to the accomplishment of any bonded repair. Lastly, the completed repair must be inspectable to ensure its structural integrity.

3.3.3 Concepts

A DBT was formed to conceptualize and evaluate repair designs for the keel sandwich structure. Input was solicited from internal Boeing repair specialists and airline personnel. A number of basic repair concepts were identified, and are shown schematically in Figure 3-8. There are a number of options within each basic concept including various scarf angles, patch shapes, sizes, materials, core plug vs. foaming core, etc.

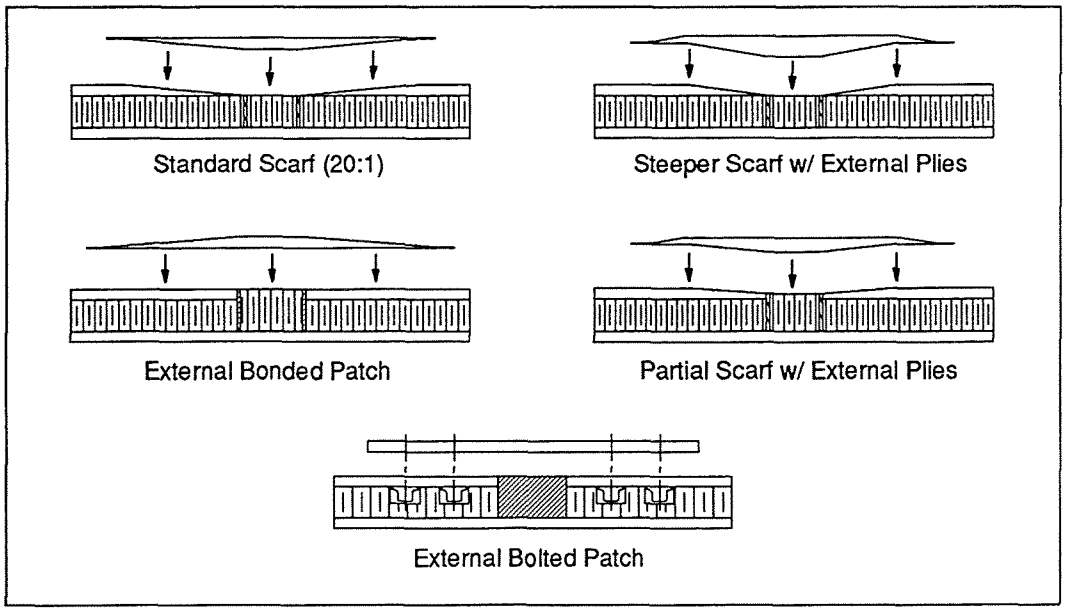

Figure 3-8: Sandwich Repair Concepts

Bonded scarf patches have the advantages of being lightweight and low profile, but result in the removal of a large amount of undamaged material, particularly in the thick facesheets of the mid and forward keel. *External bonded patches* add weight, have a higher surface profile, and represent a load eccentricity, but require only the damaged facesheet material to be removed. As a compromise between the fully scarfed or fully external concepts, *partial scarf* and *steep scarf* bonded patches compensate for reduced-capability scarfs with the addition of a few external plies. *External bolted patches*, like their bonded counterparts, have the advantage of removing only minimal facesheet

material, and the disadvantages of high surface profile, weight, and load eccentricities. Achieving more than one row of fasteners with these concepts would probably require the use of blind fasteners. Another option is to fasten through the full sandwich thickness, but this would require the addition of potting or some other means to provide support for fastener clamp-up. Mechanically fastening precured patches has the potential of representing a quickly accomplished repair.

Variations on the above concepts were explored which included, for instance, rings of reinforcement to provide an alternate load path around the damage, or elliptical shaped patches with variable scarf angles (i.e., steeper scarf angles in the direction of lesser load). The added complexity of these refinements was found to be too labor intensive, overshadowing any potential gains in structural efficiency. Later efforts were therefore concentrated on simple patch geometries.

3.3.4 Temporary Repair Options

In keeping with the goal to provide airlines with multiple options to repair damage, temporary repairs of sandwich structure were also investigated. Such repairs are characterized by simple, rapid installation, but potentially reduced durability. They would be applied to small damages which do not take the structure below ultimate load capability. The intent is to seal the sandwich core from the environment until a major aircraft check or overhaul is made, when time can be spent to permanently repair the structure, or the continued integrity of the repair can be verified.

Typical temporary repair designs have focused on thin precured patches which can be cut to size and adhered with two-part epoxies or other quick-setting adhesives (Figure 3-9). The patches themselves could be gr/ep, fiberglass, or even metal. Each material/processing combination considered will have its own characteristics in terms of installation time, performance, and inspection requirements. The goal is to provide the airlines with a range of options for a given repair scenario where, for instance, when only a short time is available prior to airplane departure, a very quick but perhaps less durable repair could be performed. Other times, when an airplane is grounded for a longer period of time, a less quick but more structurally robust repair could be accomplished which would last longer and/or require fewer intermediate inspections. Current field environmental conditions may also play a role in determining which repair option to pursue. The temporary repairs could even become permanent repairs if the associated inspection burdens are acceptable to the operator.

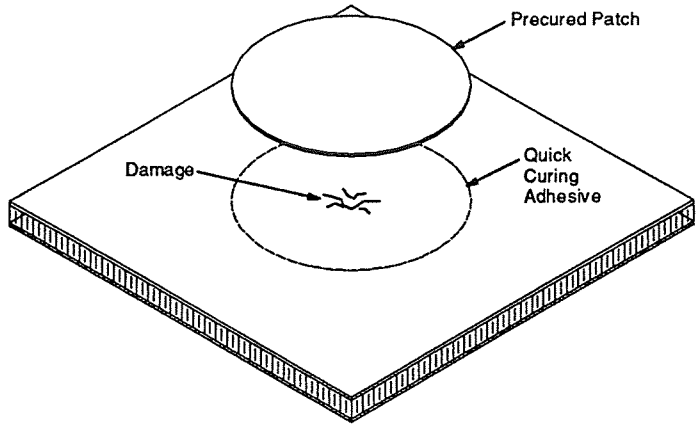

Figure 3-9: Temporary Repair Designs

4.0 STRUCTURAL ANALYSIS SUPPORTING MAINTENANCE

Analysis methods are needed to support the design of both the original and repaired structures. By determining the effects of damage on a structure's residual strength, informed design decisions can be made when faced with the normally competing goals of minimum structural weight and improved damage tolerance to reduce maintenance costs. Furthermore, the analysis can determine repair requirements and ensure repair designs are sufficient to restore the required structural capability.

4.1 Effects of Defects

Current standard repairs for composite structures are generally inadequate for the range of damages seen in service, thereby causing airlines to frequently perform special repairs that require input from the manufacturers. A preferred alternative is to determine at the beginning of the design process what the flight restrictions of the likely damages are. For example, when damage is detected, it is often desirable for the airline to perform a quick temporary repair (such as speed tape) and delay a permanent repair until the next scheduled maintenance. Since the repair design must satisfy an ultimate load requirement, it is important to understand the damage tolerance capabilities of the structure in advance to be able to quickly respond to this type of in-service inquiry. To understand the effect of that damage on the residual strength of the structure is to have an answer to the question, "Do we really need to repair it?"

The most common damage threats for composite structure include impacts caused by accidental collision or foreign objects (e.g., runway debris, service vehicles, hail, tool drop), overheated surfaces, lightning strike, and other environmental effects (e.g., UV exposure, moisture uptake, or thermal cycles) which may degrade existing damage [6]. Significant research has been performed to understand the effects of impact on composites. Unfortunately, most efforts have been focused on understanding the fundamentals of composite material impact resistance and tolerance in controlled laboratory experiments for ideal impact scenarios. Although providing some support to the development of impact resistant and damage tolerant structural designs, most studies have not supported the maintenance of composite structures in service.

Preliminary impact studies have been performed for structural design details in all ATCAS quadrant concepts to understand critical damage characteristics (i.e., those which are least visible, while having the strongest effect on residual strength) and suitable NDE procedures. The most complete study was a designed experiment performed for stiffened structure with skin gages typical of the ATCAS baseline crown design [7]. Destructive and nondestructive evaluation of impact damage identified complex combinations of matrix cracks, fiber failure, and delaminations. The extent of damage and visibility was found to depend on numerous impact, material, and laminate variables. Matrix damage size for minimum skin gages was found to be independent of matrix toughness. The least

visible, yet most serious damage (significant areas of fiber failure) was found to occur due to high energy and large diameter impactors.

Residual strength as a function of damage size can be determined through a combination of test and analysis. Nonlinear, progressive damage analysis methods developed under ATCAS have successfully scaled laminate coupon test results to predict structural residual strength [8]. In addition to achieving the desired accuracy for structural analysis, these methods could potentially be combined with quantitative NDE to create residual strength charts and tables suitable for practical assessment of damage found in service. This includes the establishment of the ADLs and CDTs discussed earlier.

4.2 Analysis and Test of Repaired Structure

4.2.1 Skin/stringer

Initial analysis and test of skin/stringer crown repairs were focused on gaining an understanding of the critical variables affecting structural performance. A series of experiments were performed on notched coupons of graphite/epoxy laminate with various repair patch configurations, materials, and load conditions. Both uniaxial and biaxial loading tests were conducted. The uniaxial tests indicated a large patch with multiple rows of titanium bolts was more effective at restoring strength than a small patch with a single row of bolts around its periphery. Additionally, titanium fasteners were found to be more effective than thermoplastic rivets at load transfer into the patches.

Finite element models were constructed at Oregon State University (OSU) for each test case, and the experimental results were compared to the theoretical predictions. In general it was found that strains in repaired composites could be predicted with reasonable accuracy, provided that geometric nonlinearities (large deflections) were taken into account. Likewise large deflection analysis better modeled the nonlinear evolution of the repair's in-plane stiffness. Generally, strain predictions outside of the repair area were in excellent agreement with test data; whereas within the repair region less correlation was achieved, especially for biaxial load conditions. The fact that strains within the repair area were greater than predicted for both specimen and patch suggests the influence of friction coupling between patch and specimen. No such part contact nonlinearities were modeled.

Agreement between predicted and measured failure loads was not as good as that obtained for strains. Generally, the finite element analysis predicted failure loads that were lower than those measured (Table 4-1). This was apparently due to the fact that the bolt loads in the fasteners connecting the patch to the coupon were more uniformly distributed than predicted because of nonlinear material response at the fastener holes. No material nonlinearities were included in the finite element analysis.

Table 4-1: Predicted vs. Test Failure Loads for Flat Laminate Repair Coupons

Coupon No.	Predicted Failure Load (kips)	Test Failure Load (kips)
1b	41.4	44.4
2a, 2b	42.2	54.8 (1)
3a, 3b	42.2	51.1 (1)
4a, 4b	43.4	50.0 (1)
5	43.4	40.4
6	44.9	43.5
7	42.3	40.1
9	43.0	47.7
10	43.1	56.0
11	42.8	45.4
12	43.0	41.5
22	42.6	48.7
23	41.3	51.4
24a, 24b	48.4	53.7 (1)
26a, 26b	20.1	26.9 (1)

(1) Average of two tests

An additional finite element model was developed by OSU to represent Panel 11a, the large aft crown repair test panel described in Section 3.2.3. Overall panel size was dictated by test machine constraints, leading to a configuration with three frames (22" spacing) and four stringers (14" spacing). Four design ultimate load conditions for the aft crown panel were examined in the repair analysis (Table 4-2). A fifth condition was also analyzed to represent a flight condition which combines fuselage bending-induced crown compression with cabin pressure.

The analysis modeled two external patch layers (see Figure 3-5) — a base patch and a shorter cover patch — effectively stepping the patch thickness, and reducing the peak fastener shear loads at the axial leading edge of the repair. The closed-cell geometry of the hat-section stringers made it undesirable to locate fasteners between the stringer flanges, thereby causing overload of the flange fasteners. The large elongated cutouts in the corners of the base patch serve to reduce the base patch axial stiffness locally and redistribute loads away from the flange fasteners. These design details were incorporated into the repair demonstration on configured crown panel 11a. The repaired panel is scheduled for testing at NASA-LaRC in early 1996.

Table 4-2: Design Ultimate Load Conditions - Aft Crown

Load Case	Description	Nx Axial (lb/in)	Ny Hoop (lb/in)	Nxy Shear (lb/in)	Pressure (psi)
1	Maximum Pressure (acting alone)	1110	2220	0	18.2
2	Maximum Axial Tension (2.5 g Maneuver)	5000	1665	0	13.65
3	Maximum Shear	833	1665	773	13.65
4	Maximum Axial Compression	-1690	0	0	0
5*	Axial Compression + Pressure	0	1665	0	13.65

* This analysis load case is a test condition in the pressure box test machine. Since the machine can only apply tension loads, $N_x = 0$ represents induced crown compression of 833 #/in which balances the bulkhead pressure.

The analysis of the Panel 11a repair shows that ultimate strength is approached but not fully recovered; however, load carrying capacity demonstrated by test would likely exceed the prediction, as indicated by the trend toward underprediction of building block test results. Table 4-3 is a brief summary of the resulting margins of safety for the most critical elements of the test panel repair (a). As the table indicates, despite the efforts to reduce peak fastener loads, bearing/bypass is the controlling criteria. Permissible loads on the fasteners were limited by the allowable bearing/bypass strains, a direct result of originally sizing the panel to have little or no margin of safety. Further evaluation of the repair design and verification of the corresponding analysis will be performed with the test of Panel 11a at NASA-LaRC.

Two additional repair configurations, both described in Section 3.2.3, are included in Table 4-3. The first alternate configuration (b) was analyzed to assess the potential benefits of tailoring the patch stiffness to better match that of the cut-out fuselage structure. This configuration produces an increase in strength over the first design, but still falls just short of ultimate load capability.

The second alternative repair configuration (c) was developed for a more recent crown design. The new skin and stringer stiffnesses associated with this design, combined with the aspect ratio of the damage cut-out, better matched what was feasible in a repair patch. Also, as part of the redesign, repair strength objectives were considered from the outset by increasing the margin between nominal (no damage/no repair) strains and allowable strains — a margin which was previously too narrow for effective repair. Repair of complex structure entails some degree of perturbation to the developed strain field and a repairable fuselage must include a minimal strain margin to account for this. These modifications allowed the development of a simplified repair for the redesigned crown for which analysis predicted a full return of ultimate strength (see Table 4-3).

Table 4-3: Margin of Safety Summary for Aft Crown Repair Test Panel

	Criterion	Test Panel Repair (a)	Alternate Test Panel Repair (b)	Alternate Fuselage Repair (c)
Graphite/Epoxy	Bearing/Bypass	- 0.02	- 0.01	+ 0.10
	Buckling	Stable	Stable	Stable
E-Glass/Epoxy	Bearing - Ultimate	- 0.18	+ 0.23	---
	Bearing - Yield (1.15 x Design Limit Load)	- 0.30	---	---

The repair of a frame alone was demonstrated and tested on Panel 14, a five-stringer/four-frame crown compression test article [9]. Following initial tests of the panel undamaged and with impact damage, a portion of the frame web and flange were removed from the center of the panel as indicated in Figure 4-1a. Removing this portion of the frame effectively extended the frame cutout over two adjacent stringers. The panel was tested again with this damaged-frame configuration prior to being repaired. To accomplish the repair, a section was cut from a spare crown panel frame and attached to the panel by metal fasteners through both flanges and through the web (Figure 4-1b). A layer of adhesive was also used between the frame flanges and the crown panel skin.

Experimental results for Panel 14 indicate the frame repair was effective in restoring the test article to its original, undamaged state. The response of the panel with the repaired frame was nearly identical to that of the undamaged panel, and the failure did not occur through the repair.

4.2.2 Sandwich

Initial analyses related to the repair of keel sandwich structure were conducted, with the goal of understanding the effects of repair design variables on load paths and structural integrity. As with the skin/stringer crown repair analysis, a finite element approach was used to evaluate candidate repair designs. This method permits the inclusion of material nonlinearities (both in adhesive response and facesheet failure progression), and geometric nonlinearities (due to load path eccentricities through external patches, peel stresses). Nonlinear analysis techniques similar to those used in ATCAS damage tolerance studies [4, 5, 8] were employed. ABAQUS [10] finite element models were developed for the single baseline damage scenario described in Section 3.3.1, but for a range of repair configurations. The models were used to evaluate (1) the influence of a repair on the overall load carrying capability of the panel, (2) the stress distribution in the vicinity of the repair, and (3) the effects of design details (i.e., patch sizes, scarf depths, materials, etc.) on load paths and the overall panel strength.

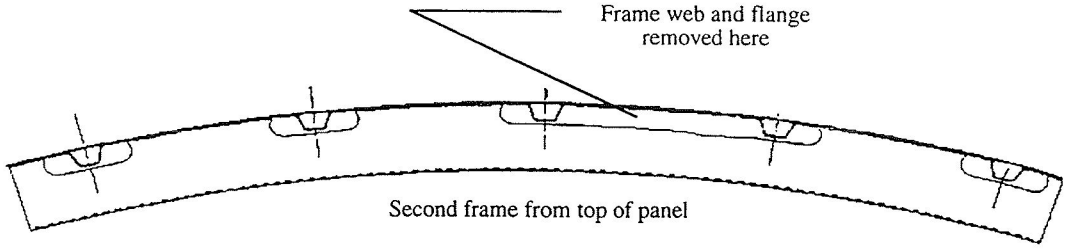

(a) Frame Damage

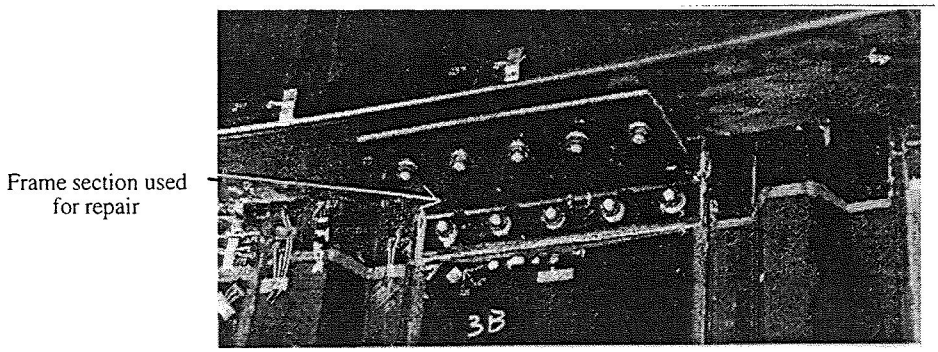

(b) Frame Repair

Figure 4-1: Crown Compression Test Panel -Frame Damage and Repair

The desire to capture possible interactions between the repair and the overall structural behavior required a large section of the fuselage to be modeled. Thus a 66" x 88" mid keel section with four frames was chosen as the reference structure. This size corresponds to the test panel dimensions and is close to the full keel width between splices. A quarter finite element model was generated with the repair located at the center of the structure on the tool (outer) side. To reduce the size of the model, the structure was idealized with shell elements except in the vicinity of the repair. There the structure was modeled with solid elements to provide accurate through-the-thickness stress distributions. The quarter model is shown in Figure 4-1 and a detail of the repair area is shown in Figure 4-3. The model included approximately 2500 elements and 10,800 degrees of freedom.

Two basic failure mechanisms were considered — buckling and material failure. In the detailed area near the repair, the core material was modeled as orthotropic with an elasto-plastic behavior. The yield stress was assumed to simulate the core crushing strength. The facesheets here were modeled as shells with smeared orthotropic properties. Laminate failure was modeled by a strain softening law established from previous testing and analysis [11]. The strongly nonlinear behavior evident in the stress-strain relationship of the repair adhesive was modeled as elastic-plastic. The adhesive material law was strongly dependent on the temperature and humidity.

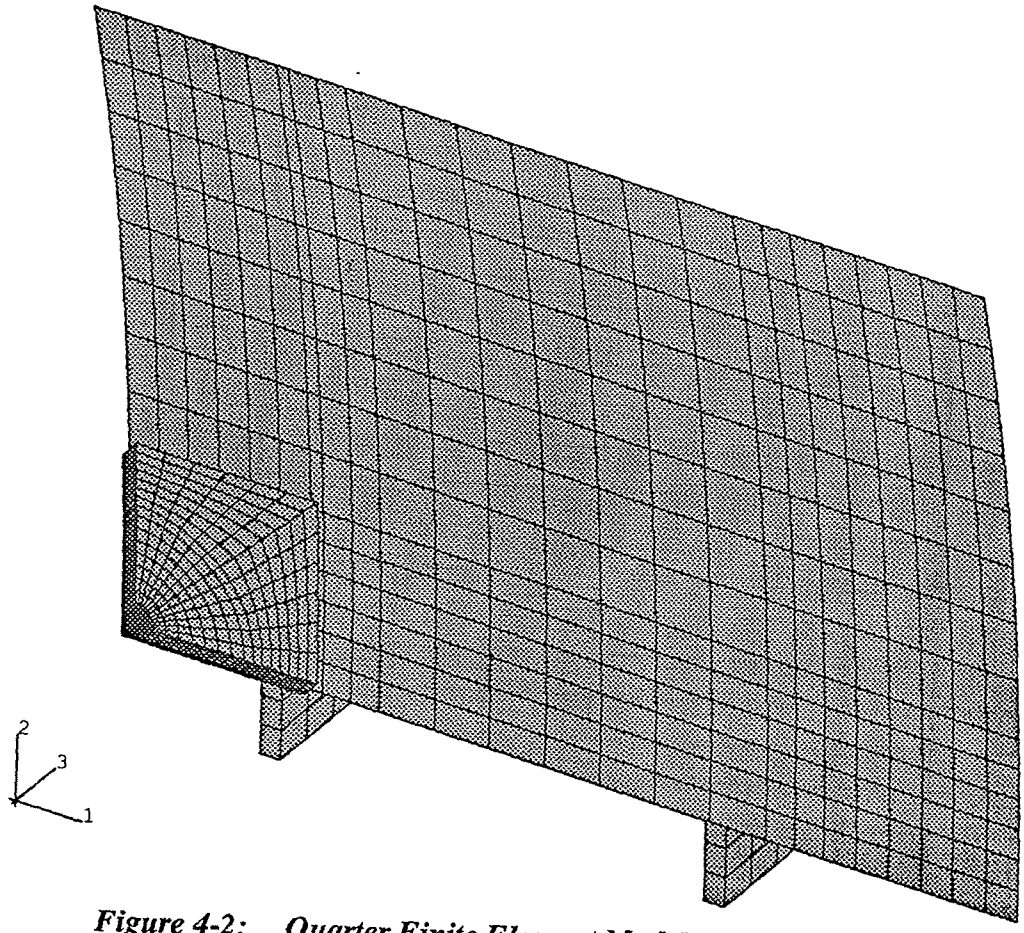

Figure 4-2: Quarter Finite Element Model of Repair Panel

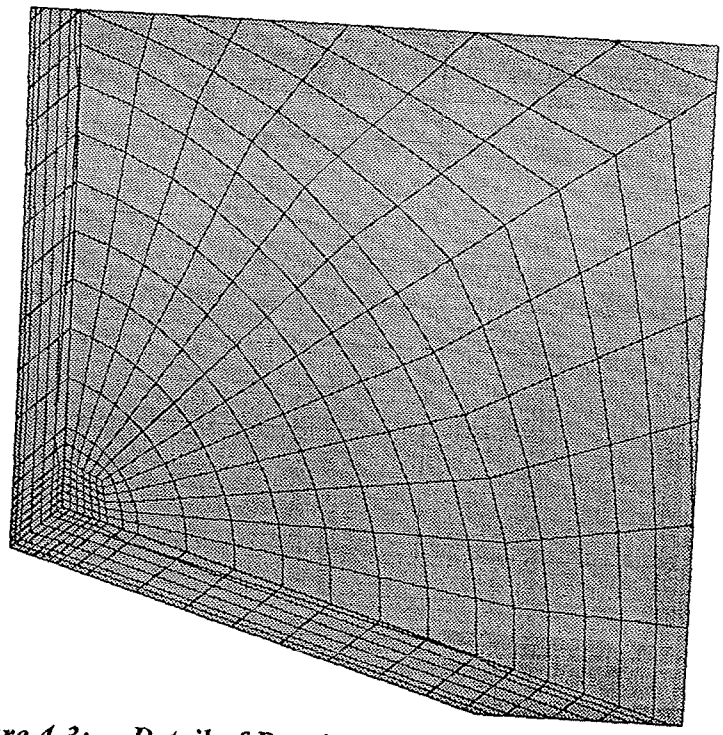

Figure 4-3: Detail of Repair Area in Finite Element Model

Boundary conditions and external loads were used to approximate the influence of the remaining fuselage on the component response. Radial movement was restrained at the loaded ends and simple supports were applied along the sides (near the longitudinal splice locations). The frames were allowed to move freely. These conditions also represent a typical test panel configuration.

Two reference points were analyzed prior to evaluating individual repairs: the undamaged system and a damaged but unrepaired component . The latter included an upper bound on the assumed baseline damage scenario comprising a 2" diameter hole in both the outer facesheet and the core. Both axial tension and compression load cases were considered. The compression load is dominant in the keel, but tension can determine some key elements of the repair such as the patch size, thickness, and scarf angle.

Three types of bonded repairs were modeled: scarfed, externally bonded, and combinations of the two methods. Tension load strength predictions are presented in Figure 4-4 for a basic repair of each type. Many variations to the basic design were modeled, including increased bond areas, reduced patch thicknesses, modified material properties, etc. The strengths of several of these variations are shown in the figure. The undamaged, damaged but unrepaired, and applied loads are also plotted for reference. Note that the applied tension loads for the mid keel area modeled are low enough such that even the unrepaired damaged panel has sufficient load carrying capability. The design details (e.g., bond area, patch thickness, etc.) are shown to have greater effect on the performance than the general type of repair (e.g., scarf vs. external patch).

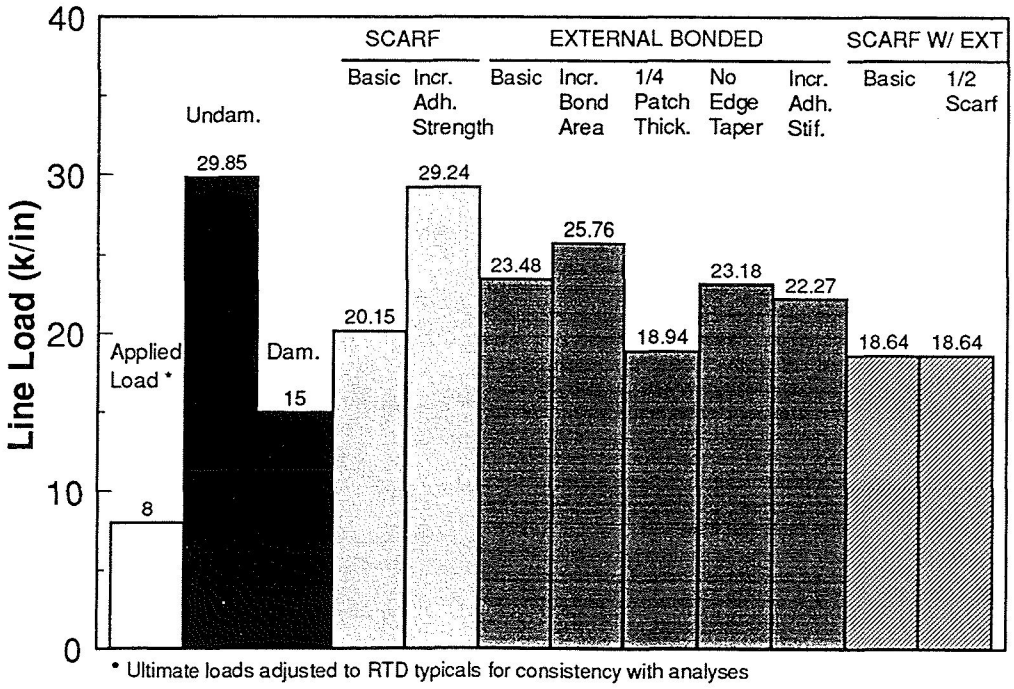

Figure 4-4: Analysis Predictions of Tension Strengths for Sandwich Repair Designs

Tension loads produce a stress concentration adjacent to the hole in the unrepaired structure and material failure is initiated at this location. The addition of a patch provides a second load path around the damage and reduces, but does not eliminate, the stress concentration at the edge of the hole. In a scarf repair, the highest laminate stress is at this location where the thickness of the original structure has been reduced to almost zero. Nevertheless, in all tension cases modeled, the overall strength was driven by the adhesive, which entered its plastic regime and could not, therefore, increase its load carrying capacity.

For compression cases, the failure mechanisms are quite different because of interaction with the stability failure modes. The adhesive enters its nonlinear range, but the total bond surface does not fail. Still, it reduces the stiffness sufficiently to force a buckling failure. Because of this response, there is little variation in the strength predictions for the various repair schemes, as shown in Figure 4-5. Again, even the damaged but unrepaired structure is seen to have sufficient capability. This is similar to previous findings from the analysis of an aft keel compression damage tolerance panel [4], wherein a tool side impact was found to cause only a minimum strength reduction. The tool side damage was less critical than the bag side damage due to the superposition of bending stresses from global panel deformation.

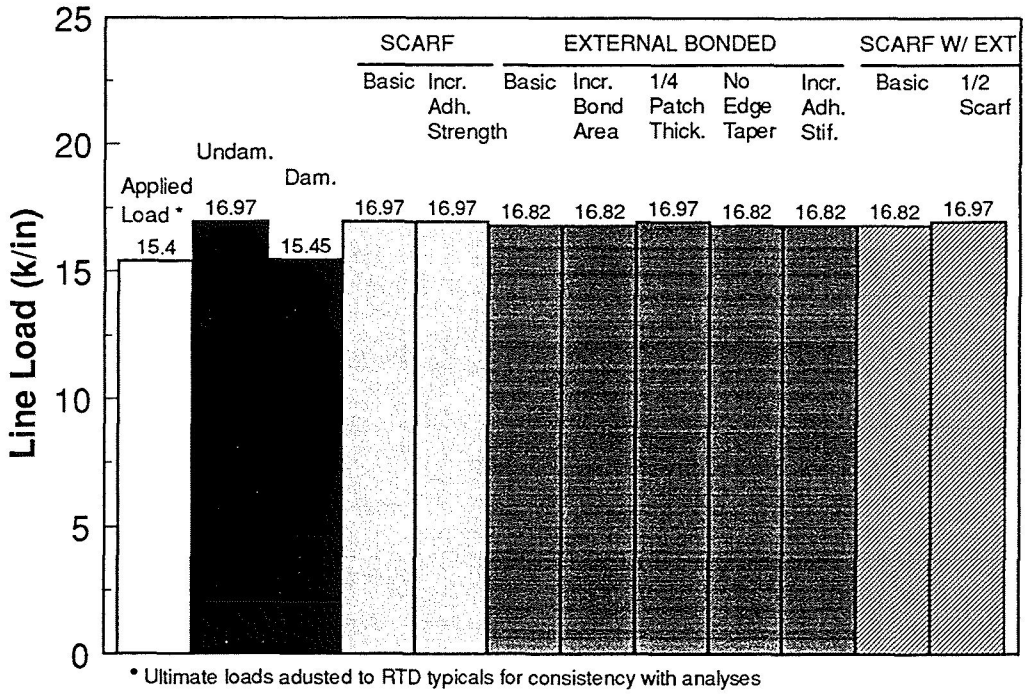

Figure 4-5: Analysis Predictions of Compression Strengths for Sandwich Repair Designs

The above analysis was tied to the same baseline damage scenario as the manufacturing process trials and repair test activities. The size of the manufacturing and test articles were limited, and therefore so were the damage and repair sizes. Unfortunately, the small size of the damage analyzed did not result in a great amount of load being transferred into

the repair patch. This prevented the full effects of the repair design variables from becoming evident. Still, some trends were discerned from these analyses. The tension cases point toward the importance of patch bond area, patch thickness, and adhesive strength. Also, scarfing through the full thickness may not be necessary, and in fact may even degrade the overall strength because of the reduced material thickness at the area of greatest stress concentration. Given the stiff bending section of the mid keel sandwich structure, the load eccentricities associated with external patch plies do not appear to be an issue.

These analysis methods were used to predict the response of three permanent repairs applied to the large mid keel demonstration panel (MK1), described in the next section. This panel was tested in uniaxial compression in the 1M lb test frame at NASA-LaRC. Extensive instrumentation was provided for evaluation of load paths around the repairs. The panel failed away from the repairs at 99% of ultimate load (after adjusting to account for room temperature dry test conditions) away from the repairs. Test setup, fixturing, and/or manufacturing anomalies may have contributed to the early failure at the edge of a frame flange [4]; however, the performance of the repairs appeared to be very good. At the time of this writing, test strain and displacement data was being assembled for comparison to predictions and validation of the analysis. In the subsequent Phase C effort, the remaining panel may be cut into quadrants for additional tests of individual repairs. These might include additional structural tests or evaluations of moisture ingression. Subsequent cross-sectioning may provide insight into the quality of the repairs and verification of previously conducted nondestructive examinations.

5.0 REPAIR FABRICATION

Repair fabrication developments conducted under ATCAS have focused on mechanically fastened concepts for the crown panel design (skin/stringer) and bonded concepts for the keel panel design (sandwich). Repair materials and processes were evaluated with consideration given to the capabilities of airline repair facilities and the constraints of a typical field processing environment. The goal is to achieve a quality repair which restores the necessary structural capability, with a minimum amount of time and effort required of the airline. The developments and demonstrations discussed below were coordinated with the design and analysis activities, and subject to the same limitations (e.g., types of structures and damage states considered).

5.1 Skin/Stringer Bolted Repair Developments and Demonstrations

The mechanically fastened repair concepts investigated for crown structure offer several advantages including: compatibility with hat-stiffened structure; repair configuration flexibility to restore structural integrity to large panel areas; and proven low-cost, inspectable installation techniques. Repair manufacturing activities included fabrication of coupon and element test specimens, limited manufacturing trials, and repair by American Airlines personnel of a fully configured 63" x 72" crown pressure-box test panel, designated Panel 11a. Extensive manufacturing development of crown repair techniques was unnecessary due to the fairly straightforward approach of using precured elements and mechanical fastening. Still, lessons learned from coupon fabrication and manufacturing trials were incorporated into the repair demonstration on Panel 11a.

5.1.1 Large Crown Panel Repair Demonstration

The precured, pretrimmed repair pieces for Panel 11a (Figure 3-5) were fabricated at Boeing. A readily available fiberglass/epoxy fabric material was chosen for the skin patches in order to standardize the overall repair design approach. The two patch layers were stacked on the same 122"-radius cure tool (separated by a slip sheet) and cured simultaneously. Damage cleanup was also accomplished at Boeing using a hand held router, followed by deburring of the edges.

Graphite/epoxy fabric material (standard modulus, untoughened resin) was chosen for the frame splice application based on the material's availability and its compatibility with the drape forming process. Unidirectional material forms (e.g., tow-placed laminate charges) are much more difficult to drape-form to shapes with complex curvature. Titanium was also considered as a viable option, but was not used due to the difficulty of fabricating a complex curvature with that material within schedule constraints. Also, use of titanium would likely constrain the frame splice elements to be provided by Boeing, given the cost and difficulty for the airlines of procuring, storing, and machining titanium parts.

Assembly of the mechanically-fastened repair of Panel 11a was completed by American Airlines personnel at their Composite Repair Center in Tulsa, OK. The two skin patches

were held in place using jigs, and all bolt holes were drilled. All drilling and reaming was accomplished with a sacrificial backup tool in place to minimize fiber breakout around the exit of the hole. Carbide drills and reamers were used. After cleaning all bolt holes, the skin patches were installed with pressure sealant between the skin and the base patch. Sealant was applied using a roller applicator. Lastly, the frame splice members were mechanically fastened in place. Titanium lockbolts were installed where access was adequate for the fastener installation tool; titanium Hi-Loks were used where access was limited, since the collars for these fasteners can be wrench-torqued.

5.1.2 Airline Comments

Consistent with the objective of involving the airlines in the development of repair processes and design concepts, American Airlines personnel were requested to provide their comments on relevant repair design and assembly activities. They were generally receptive to mechanically attached stock elements used in the crown repair approach. Their only concerns related to drilling fastener holes in laminates, high costs for small quantities of composite fasteners, and a desire to produce stock patches themselves for future applications (as opposed to a commitment for purchasing specialty repair parts from Boeing).

During the repair assembly of Panel 11a, American Airlines created a logbook and entered pertinent remarks, difficulties experienced and steps taken to resolve them, design improvement suggestions, etc. The logbook was defined as a "tell it like it is" record to be produced by those doing the assembly work. The following excerpts from this record are offered with only slight editing:

> *"The structure itself, as supplied by Boeing, is fabulous — what a work of carbon art! All repair materials supplied were very well done, from the pre-cured skin patches to the doublers for the frames. All parts were manufactured, cut and prefit quite well.*
>
> *Not having any engineering background, it is my opinion that the size and quantity of fasteners is quite sufficient to fasten a Sherman tank to the side of a Space Shuttle. There is no doubt in my mind that this repair will simply not fall off.*
>
> *It is also my opinion that a much stronger, aerodynamically smoother repair can be bonded more quickly by composite personnel than the repair done by us. First of all, bolt-on scab patches need to be done by structures guys that know how to lay out a fastener pattern ... if you want this kind of repair to be done quickly. Let's face it, most bonders can't drill a round hole!*
>
> *Like the bolt-on scab patch, a bonded repair would also require all repair materials to be of the pre-cured nature. The outer repair patch could be made of carbon (not glass), and only a single thickness (not double) would be sufficient. All plies on the patch would be tapered off, making for a*

much more aerodynamically smooth repair. Inside, a stacked carbon ply would fill the damage cutout, and a doubler bonded between the stringers over the repair would complete the skin repair. I would, however, do a 'riveted' repair to the frame, as was done in the repair we did."

5.2 Sandwich Bonded Repair Developments and Demonstrations

Development of repair manufacturing techniques for mid keel sandwich structure progressed from small-scale trials to full-scale demonstrations. These efforts were undertaken concurrently with design and analysis activities to help focus the manufacturing developments toward the most promising materials and design concepts. The scope of this effort was consistent with that described in Section 3.3.1; i.e., the focus was on a specific damage state and a specific area of the keel sandwich structure. The emphasis was on permanent bonded repairs, although a parallel effort to investigate temporary repair options was also conducted.

5.2.1 Subscale Process Trials

Initially, an effort was undertaken to understand the cure kinetics and mechanical properties of candidate patch materials. Laminates representative of patches were cured under vacuum to evaluate different prepreg materials and determine the effects of processing on patch quality. As a means of assessing patch quality, cross-sections were taken and porosity was either measured or estimated. Patch porosity raises concerns about loss of strength and the potential for moisture ingression. Strength was assessed with open hole compression (OHC) tests.

Two materials were evaluated: AS4/8552, the baseline system for the keel; and HTA/M-20 (formerly known as HTA/DLS1194). Both of these prepreg systems are typically cured in an autoclave at 40 to 80 psig. The M-20 is an epoxy normally cured at 250°F, while the 8552 is normally a 350°F cure epoxy. The laminates were evaluated for OHC under room temperature dry (RTD) and hot/wet (H/W) conditions. Little difference was found between the OHC strengths of HTA/M-20 and AS4/8552, whether cured at 250°F, 300°F, or 350°F. An extended 250°F cure cycle produced essentially the same hot/wet properties as higher temperature processes (Figure 5-1). Furthermore, laminates cured at the lower temperatures for longer times produced lower porosity than those cured at higher temperatures for shorter times (0% vs. 1% for HTA/M-20, 1% vs. 3% for AS4/8552).

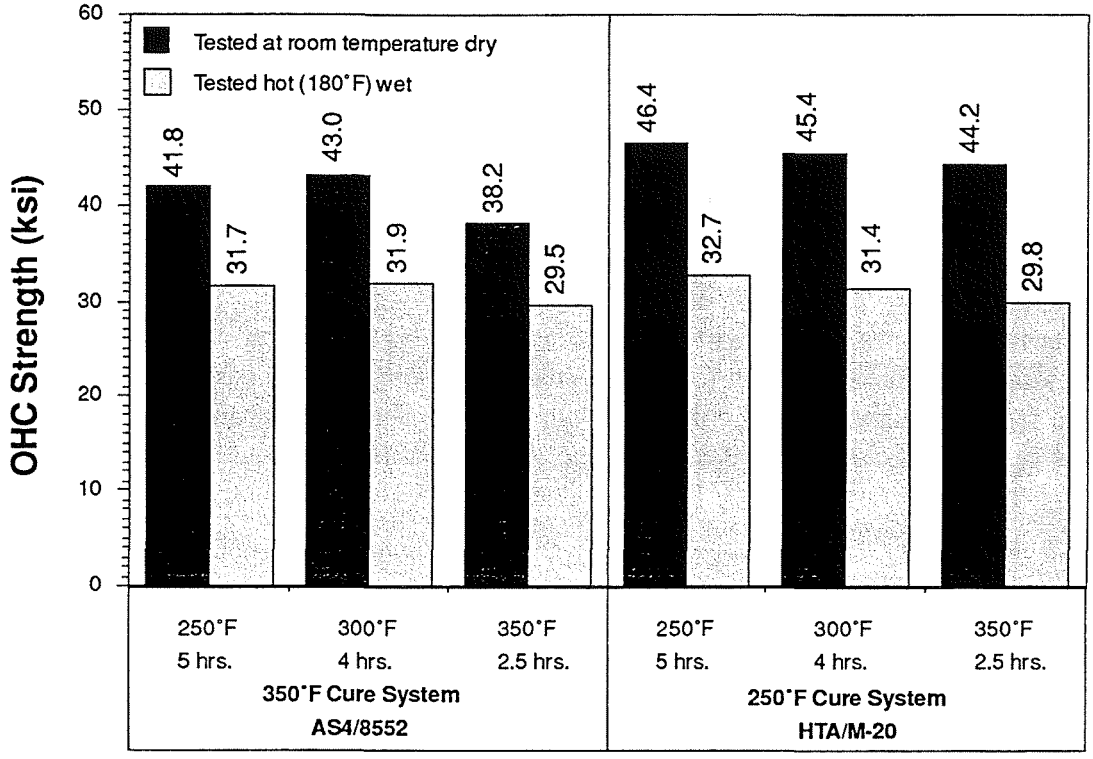

Figure 5-1: Open Hole Compression Strengths of Patch Laminates

Patch configuration and thickness were also found to affect laminate porosity. Several laminates, rather than having squared-off edges, were laid up in an inverted pyramid, effectively sealing the edges, much as in a scarfed-out repair (Figure 5-2). All such laminates had at least some porosity, while some of those with squared off edges had essentially none. Using the inverted pyramid configuration, three patches made from HTA/M-20 were cured at 250°F, and varied in thickness from 4 to 12 plies. Five patches made from the standard-grade AS4/8552 prepreg were cured at 350°F, and varied in thickness from 8 to 30 plies, including some which were staged in 8- or 12-ply increments. Porosity measurements were taken of the cured laminates; results are presented in Table 5-1. (Note that maximum porosities of 2% to 3% are generally considered acceptable.) The lowest porosity was measured in a patch consisting of a 4-ply stack of HTA/M-20, which had a nominal porosity of 1.4%. Porosity increased with increasing patch thickness. The 30-ply AS4/8552 patch had 4.55% porosity. Patches staged at 8 to 12 plies at a time generally had levels of porosity between 2% and 3%.

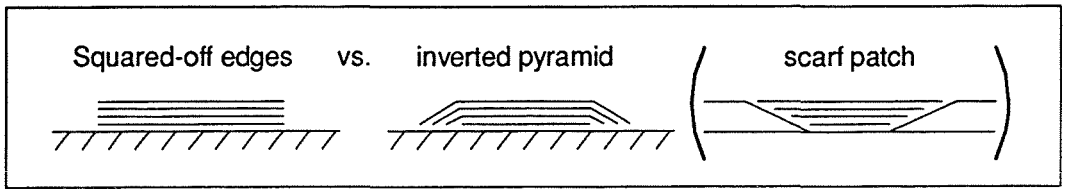

Figure 5-2: Patch Laminate Configurations

Table 5-1: Porosity measurements.

Material	Total plies	Plies per stage	Porosity (%)
HTA/M-20	4	4	1.40
	8	8	2.49
	12	12	2.10
AS4/8552	24	8*	2.54
	12	12	2.90
	24	12*	3.15
	24	24	4.22
	30	30	4.55

* Intermediate stages at 225F for 1 hour

As in the first set of subscale trials (with squared-off edges), HTA/M-20 patches generally had lower porosity than comparable AS4/8552 patches. The standard-grade AS4/8552 prepreg was expected to yield lower porosity than the automated tape layup (ATL) grade prepreg used in the first set of trials, which has limited flow. The data did not conclusively show this result; however, the standard-grade 8552 prepreg was old, and the affect of prepreg aging on porosity is not well characterized.

Development of repair manufacturing techniques for mid keel sandwich structure progressed from small-scale trials to full-scale demonstrations. These efforts were undertaken concurrently with design and analysis activities to help focus the manufacturing developments toward the most promising materials and design concepts.

5.2.2 Full-Scale Process Trials

The subscale investigations were expanded in the full-scale trials to represent an array of design variables including scarf and patch geometry, patch material, adhesive, core replacement, ply staging, damage cleanup, bagging, and cure cycle. The repairs, performed on a number of previously fabricated keel sandwich panels, were conducted both at the Boeing B-2 repair shop and at American Airlines. Some of the attempted repair concepts reflect the ideas of the technicians performing the work. Each completed repair underwent a number of inspection procedures, including TTU, pulse-echo, sectioning, photomicroscopy, low frequency bondtester, and/or degree-of-cure analysis. Comments from the repair technicians were also solicited to assist in the evaluation of the various repair concepts. Figures 3a and 3b presents the matrix of variables investigated through the full-scale trials, as well as a summary of the results.

Process Trial Number [1]	Summary Description	Patch Matl.	Scarf Patch Plies			External Patch Plies			Total No. of Plies	Patch Adhesive			Core Plug			
			type	no. of plies	taper	type [2] [3] [4]	no. of plies	edge taper		type	thickness (@ f.s.)	thickness (@ core)	type	adhesive (to core)	adhesive to back f.s. type	adhesive to back f.s. thickness
AK24-2	Circular Scarf, 250 cure	AS4/8552	full	13	20:1	cover	2	n/a	15	EA9628 (BMS 5-129)	0.009	0.009	h/c	BMS 5-90 foam	350 F cure (BMS 8-245)	0.009
AK24-3	Circular Scarf w/ Ext. Plies, 250 cure	HTA/M-20 (DLS1194C)	full	13	10:1	standard	19	20:1	32	EA9628 (BMS 5-129)	0.010	0.010	h/c	BMS 5-90 foam	EA9628 (BMS 5-129)	0.010
AK24-4	Oval Scarf, 250 one step core bond/patch cure	HTA/M-20 (DLS1194C)	full, oval	13	10:1 to 20:1	cover	2	n/a	15	EA9628 (BMS 5-129)	0.010	0.010	h/c	BMS 5-90 foam	EA9628 (BMS 5-129)	0.010
AK24-5	Circular External Bond, reverse scarf, 300 cure, potted core	AS4/8552	-	-	-	standard	15	10:1	15	EA9628 (BMS 5-129)	0.010	0.010	potting compound	n/a	n/a	n/a
AK24-6	Ring External Bonded, 250 cure	AS4/8552	-	-	-	ring reinforced [7]	32	20:01	32	EA9628 (BMS 5-129)	0.010	0.010	h/c	BMS 5-90 foam	EA9628 (BMS 5-129)	0.010
AK24-7	Circular External Bolted, precured patch, blind bolts	AS4/8552	-	-	-	precured (bolted)	15	square	15	n/a	n/a	n/a	potting compound	n/a	n/a	n/a
AK24-8	Circular Scarf, B2 cure cycle, repair over frame	AS4/8552	full	13	30:1	cover	2	n/a	15	350 F cure (BMS 8-245)	0.008	0.008	h/c	BMS 5-90 foam	EA9628 (BMS 5-129)	0.010
AK24-9	Precured External Bonded, room temp. bond, over frame, not all core removed	AS4/8552	-	-	-	precured (r.t. bond)	15	square	15	sealant	n/a	n/a	potting compound	n/a	n/a	n/a
AK24-10	Filler Plug, B2 cure cycle, over frame	AS4/8552	filler	13	square	cover	2	n/a	15	350 F cure (BMS 8-245)	0.008	0.008	potting compound	n/a	n/a	n/a
AK24-11	Precured External Bonded, 250 hot bond, over frame	AS4/8552	-	-	-	precured (hot bond)	15	20:1	15	EA9628 (BMS 5-129)	0.010	0.010	none	n/a	n/a	n/a
B-MK1	Partial Scarf w/ External Plies, 4-ply staging, 250 cure, 3M adh., alum caul	HTA/M-20 (DLS1194C)	partial	15	10:1	inverted pyramid	10	20:1	25	AF3113-5	0.005	0.020	h/c	BMS 5-90 foam	AF3113-5	0.020
B-AK22-1	Full Scarf w/ External Plies, 4-ply staging, 250 cure, 3M & Hysol adh.	HTA/M-20 (DLS1194C)	full	12	10:1	inverted pyramid	10	20:1	22	AF3113-5, EA9628 [5]	0.005	0.020	h/c	synspand [6]	AF3113-5, EA9628 [5]	0.020
AA1 (AK23-2)	Full Scarf w/ External Plies, 250 Cure	HTA/M-20 (DLS1194C)	full	12	20:1	inverted pyramid	10	20:1	22	EA9628 (BMS 5-129)	0.005	0.020	h/c	synspand [6]	EA9628	0.020
AA2 (AK23-2)	Full Scarf w/ External Plies, 4-ply staging w/ flex bag, 250 cure	HTA/M-20 (DLS1194C)	full	12	20:1	inverted pyramid	10	20:1	22	EA9628	0.005	0.020	h/c	synspand [6]	EA9628	0.020
AA3 (AK22-2)	Full Scarf w/ External Plies, string breather, 250 cure	HTA/M-20 (DLS1194C)	full	12	20:1	inverted pyramid	10	20:1	22	EA9628	0.005	0.020	h/c	synspand [6]	EA9628	0.020
B-AK23-1	Full Scarf w/ External Plies, string breather, 250 cure	HTA/M-20 (DLS1194C)	full	12	20:1	inverted pyramid	10	20:1	22	EA9628	0.005	0.020	h/c	synspand [6]	EA9628	0.020

Notes: [1] Base panels are as follows:
- AK24: T300/F584 12 ply facesheets, 0.75" thick HRP-3/16-8.0 core (large aft keel demo panel)
- MK1: AS4/8552 30 ply facesheets, 0.638" thick HRP-3/16-12.0 core (scrap area of mid keel panel used for trial)
- AK22: AS4/8552 12 ply facesheets, 0.75" thick HRP-3/16-8.0 core (failed aft keel test specimen)
- AK23: AS4/8552 12 ply facesheets, 0.75" thick HRP-3/16-8.0 core (failed aft keel test specimen)

[2] "Standard" implies larger diameter plies are against facesheet, outer plies are progressively smaller
[3] "Inverted pyramid" implies smaller diameter plies are against facesheet, outer plies are progressively larger
[4] All cobonded patches include two "cover" plies of fabric
[5] Each half of bond area used different adhesive
[6] Synspand is a syntactic foaming adhesive
[7] Includes 10 continuous plies, remainder constitute ring reinforcement; Taper inside of ring was 10:1

Figure 5-3a: Full-Scale Process Trials - Geometry and Materials.

Process Trial Number [1]	Core Plug Cure			Patch Ply Staging or Precure		Repair Cure				
	process [2] [3]	core/back f.s. bondline results	core/core bondline results	type [5]	process	bagging, cauls, etc.	cure temp (F)	heat rate (deg/min)	patch porosity [8]	results
AK24-2	standard	poor - disbond (up to 60 deg colder)	good	-	-	standard [6]	250	3 - 5	2-4%	porosity in patch and bondline
AK24-3	standard	poor - disbond	good	-	-	standard	250	3 - 5	2-4%	small area of bondline porosity
AK24-4	cured w/patch	poor - disbond	good	-	-	standard	250	3 - 5	2-4%	core plug disbond to back f.s.
AK24-5	cured in place	n/a	good	-	-	standard	300	3 - 5	2-4%	porosity in adhesive layer
AK24-6	standard	average	good	-	-	standard	250	3 - 5	2-4%	porosity in adhesive layer
AK24-7	cured in place	n/a	good	precured	autoclave at 350 F	-	-	-	~0%	good bondline, good patch
AK24-8	standard	good	good	-	-	standard	330 +20, -30	3 - 5	2-4%	disbonded patch
AK24-9	cured in place	n/a	good	precured	autoclave at 350 F	standard	room temp	n/a	~0%	good bondline, good patch
AK24-10	cured in place	n/a	good	-	-	standard	330 +20, -30	3 - 5	2-4%	gap around filler plies
AK24-11	n/a	n/a	n/a	precured	cured on part w/ heat blanket, vacuum	standard	250	3 - 5	2-4%	porosity in laminate, bondline
B-MK1	standard	average	poor [4]	stage	standard	alum caul	250	3 - 5	1.18%	poor core plug bondlines, gross bondline porosity
B-AK22-1	standard	good	good	stage	standard	standard	250	3 - 5	3.47%	good core plug bondlines, gross bondline porosity (EA9628 side)
AA1 (AK23-2)	standard	good	good	-	-	standard	250	2	3.39%	gross bondline porosity
AA2 (AK23-2)	standard	good	good	stage	heat lamps, flexible bag	standard	250	2	3.62%	small area of bondline porosity
AA3 (AK22-2)	standard	good	good	-	-	string breather [7]	250	2	2.21%	excellent
B-AK23-1	standard	good	good	-	-	string breather	250	2	2.18%	excellent

Notes: [1] Base panels are as follows:
AK24: T300/F584 12 ply facesheets, 0.75" thick HRP-3/16-8.0 core (large aft keel demo panel)
MK1: AS4/8552 30 ply facesheets, 0.638" thick HRP-3/16-12.0 core (scrap area of mid keel panel used for trial)
AK22: AS4/8552 12 ply facesheets, 0.75" thick HRP-3/16-8.0 core (failed aft keel test specimen)
AK23: AS4/8552 12 ply facesheets, 0.75" thick HRP-3/16-8.0 core (failed aft keel test specimen)
[2] "Standard" implies a separate cure cycle for core bond
[3] Potting compound was cured prior to patch layup
[4] Poor foaming, repaired with potting compound
[5] Staged patches included 15 min, 150F debulk cycles every 4 plies
[6] Nonperforated FEP was used
[7] Envelope bag needed due to impact penetration of panel
[8] Ranges are estimates, specific values were measured

Figure 5-3b: Full-Scale Process Trials - Processes and Results.

The first ten repairs were completed on a large section of aft keel sandwich panel AK24. The bolted repair (AK24-7) was successfully achieved, and with relative ease. This type of repair is limited in applicability, however, to those areas with sufficient core thickness to accommodate the blind ends of the fasteners. There are also concerns about the difficulty of thoroughly removing the core so as to allow proper seating of the bolts. Additionally, fastener holes present potential moisture paths into the core. Subsequent damage to a previously repaired area would probably require the difficult step of drilling out these bolts.

Repairs with complex patch ply geometries, such as the oval scarf (AK24-4) and ring reinforced external patch (AK24-6), were found to be too labor intensive. The ring patch also suffers from a poor surface profile. The filler plug (AK24-10) offers no reliable structural load path. Simple scarf, externally bonded, and scarf/external hybrid designs were found to offer the best balance of manufacturing ease, surface profile, weight, and structural performance.

As Figure 5-3 indicates, many of the repairs had a significant amount of porosity in the patch and adhesive. Furthermore, the repaired core was not adequately bonded to the back facesheet in several cases. Additional full-scale trials were conducted to resolve these issues prior to repair demonstrations on the large mid keel test panel. All of the additional trials incorporated simple, circular patches with full or partial scarfs plus external plies. All used a separate honeycomb core plug bond operation, HTA/M-20 prepreg material, Hysol EA9628 film adhesive, vacuum compaction of each ply, and a 250°F cure.

The core-plug-to-back-facesheet bondline was improved by increasing the adhesive thickness and raising the temperature of heat application to account for a thermal gradient through the thickness of 40-60°F. The inclusion of a 15 minute, 150°F debulk cycle every 4 plies did not consistently result in reduced patch porosity as it had in the subscale trials. There were also persistent problems with gross bondline porosity between the patch and scarfed facesheet (e.g., Figures 5-4 and 5-5).

One potential contributor to the gross bondline porosity was thought to be bridging of the prepreg during successive debulk cycles, caused by a stiff heating pad, breather and vacuum bag system. This possibility was investigated in trial AA2 by employing a special elastic vacuum bag, a stretchable breather (Airweave), and a heat lamp (instead of a heat blanket). Debulking in this manner tended to reduce the amount of gross bondline porosity, although not to an acceptable level.

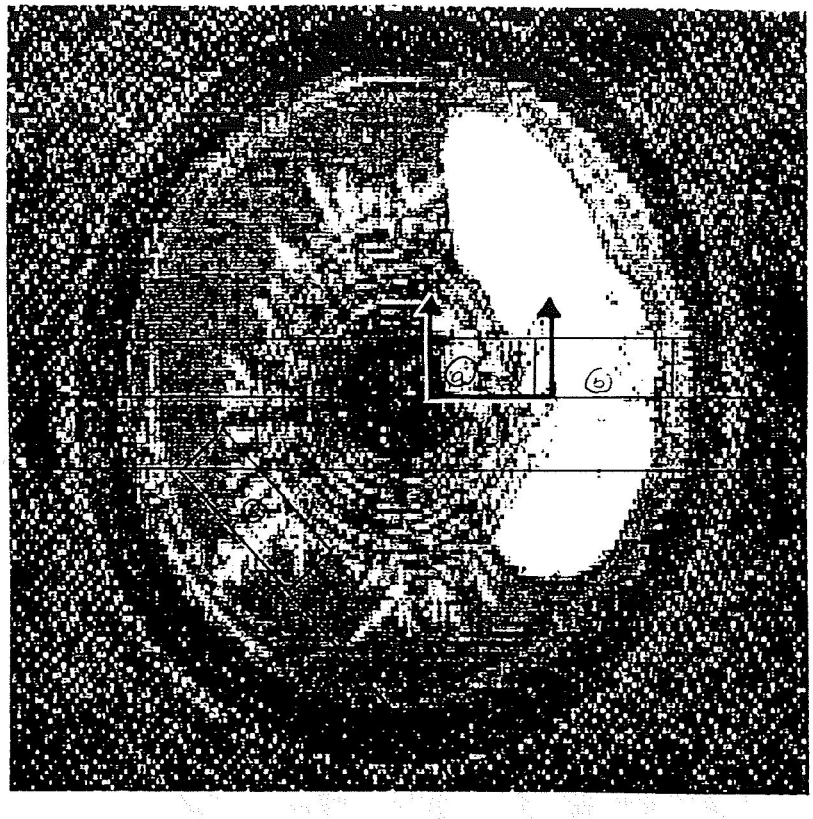

Figure 5-4: Pulse-Echo Ultrasonic Inspection of Repair Trial AA1 (3.5 MHz, White Areas are Regions of High Porosity or Disbonds)

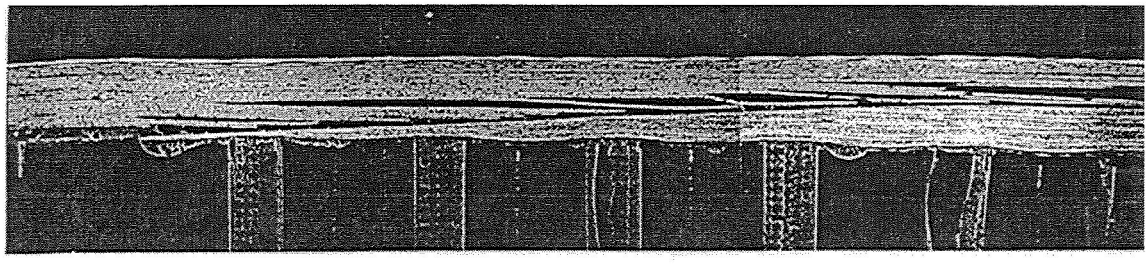

Figure 5-5: Cross-Section Photomicrograph (Shown 3X) of Repair Trial AA1

Another possible contributor was that the escape path for air under the patch could be getting sealed off, thus preventing sufficient pressure from forming to seat the patch onto the scarf area. This problem is exacerbated in repairs with thick facesheets and small exposed core areas, such as were used in this study. Since entrapped air must be vented from the core plug across the patch-to-facesheet bond area, an advantage is given to thinner facesheets (shorter radial distance for the vent path) and larger core plug areas (greater volume-to-perimeter ratio, and therefore greater force to open a vent path). The

gross bondline porosity was solved by inserting two small glass string-breathers under the adhesive layer to evacuate the core during the vacuum-bag cure. The string breather is closed off during the cure process by infiltrating adhesive.

This string breather process was successfully demonstrated on full-scale trial AA3 at American Airlines, and later confirmed at Boeing with trial B-AK23-1. The patches were well consolidated and the repairs had no areas of gross bondline porosity. The overall quality of the repairs appeared to be very good, as illustrated in the ultrasonic inspection results (Figure 5-6) and photomicrographs (Figure 5-7). The glass string breather was completely infiltrated with resin and sealed from the environment, as observed in the photomicrographs. Patch porosity measurements were lower (~2.2%) in repairs using the string breather also, despite the fact that no debulk cycles were used.

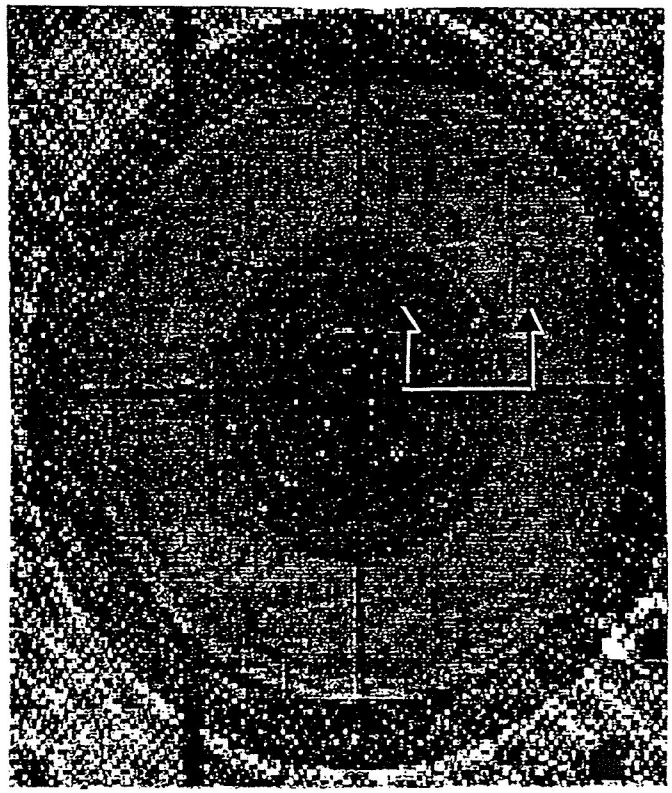

Figure 5-6: Pulse-Echo Ultrasonic Inspection of Repair Trial AA2 (3.5 MHz)

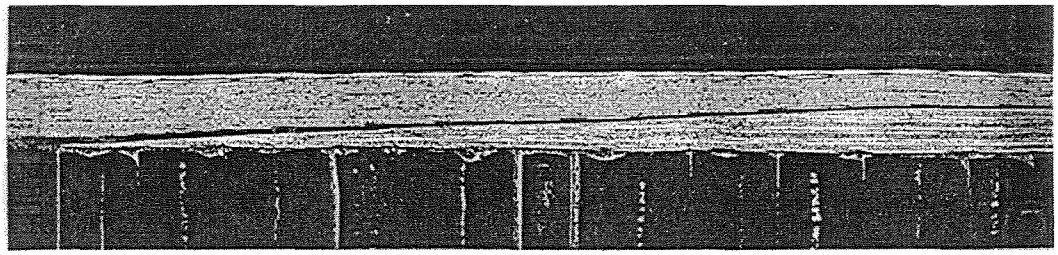

Figure 5-7: Cross-Section Photomicrograph (Shown 3X) of Repair Trial AA2

5.2.3 Demonstrations

Results from the subscale and full-scale process trials were used to select repair designs, materials, and processes for demonstration on large mid keel panel MK1. The panel was a curved composite sandwich structure with 30-ply facesheets and cobonded J frames (Figure 5-8), originally built to the dimensions 79.5" x 118", but later cut down to 66" x 88" for test. Three permanent bonded repairs were performed by American Airlines at their repair facility. The repairs included a full scarf, external patch, and partial scarf, and are shown in Figures 5-9 through 5-11, respectively. As in the most recent full-scale trials, the 250°F cure Ciba Geigy HTA/M-20 prepreg and Hysol EA9628 film adhesive were again used.

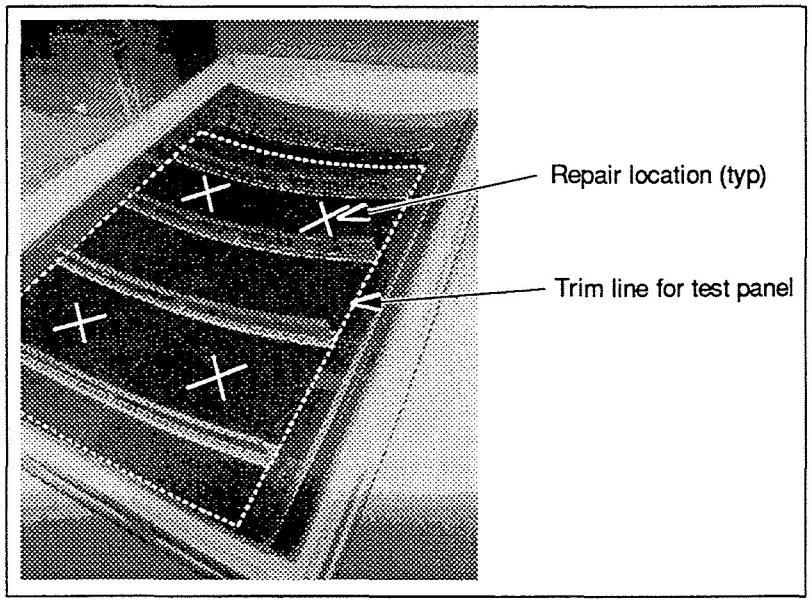

Figure 5-8: Mid Keel Repair Panel MK1

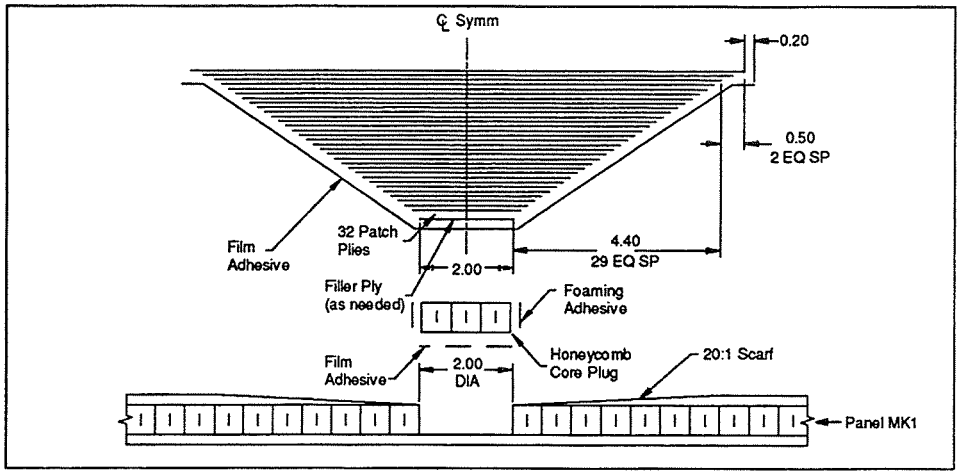

Figure 5-9: Full Scarf Bonded Repair - Panel MK1

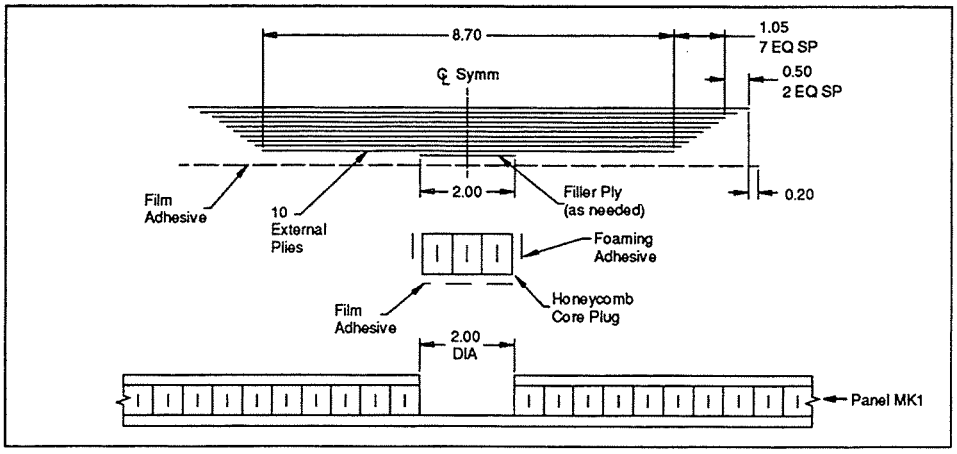

Figure 5-10: External Bonded Patch Repair - Panel MK1

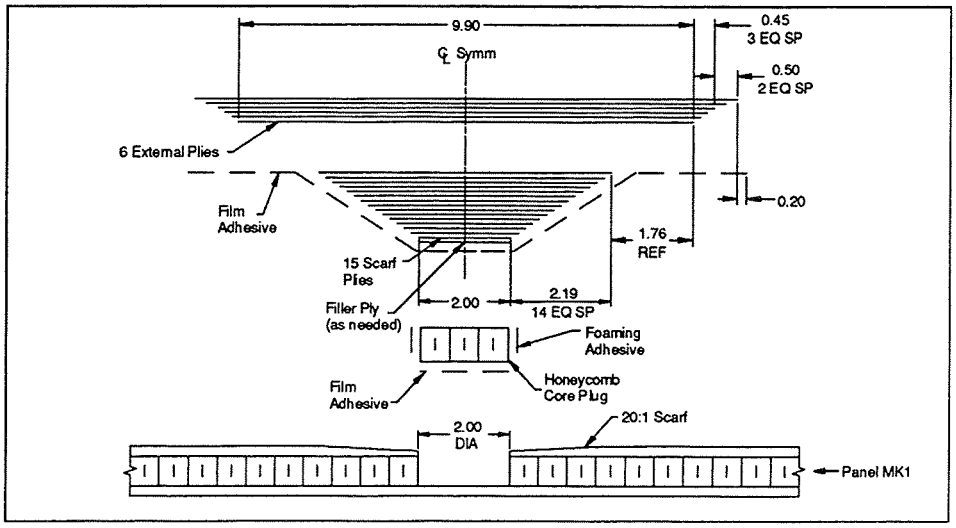

Figure 5-11: Partial Scarf Bonded Repair - Panel MK1

Each repair was intended to restore a penetration of the outer (tool side) facesheet and corresponding core damage. The simulated damage was removed by grinding a 2 inch diameter area from the outer facesheet down through the core, leaving the backside facesheet intact. The back facesheet adhesive layer was abraded but not completely removed. Material was ground-away using a hand-held, pneumatic grinding wheel and a router. Facesheets were scarfed in a similar manner, giving a taper ratio of 20:1.

Prior to laying up the patch, the damaged core was replaced using a separate cure cycle. (This can also serve as a drying cycle to remove moisture which may have entered through the damage). A core plug, made from the same type of honeycomb as was removed (HRP-3/16-12.0), was cut to size and bonded in place with a thick layer of film adhesive (0.020 inch, 4 plies of grade 5) against the back facesheet. Foaming adhesive (Synspand) was used to bond the sides of the core plug to the pre-existing honeycomb core. Since the patch was not yet in place, a thermocouple could be inserted inside the core, touching the adhesive layer, to control the adhesive temperature. The adhesive was cured at 250°F for 2 hours with a vacuum bag and a heat blanket. Because the repair was treated as "one-sided", heat was only applied to the outer (tool-side) facesheet which typically heats 40-60°F hotter than the adhesive layer because of the thermal gradient through the core. The temperature gradient has no affect on the foaming adhesive which can be cured between 250-350°F. After the cure, the thermocouple was removed and the core plug was ground down level with the edge of the scarf or, in the case of the external patch, flush with the facesheet surface.

Patch bonding was always done to an abraded, solvent-wiped surface. The bonding surface was roughened in all areas, including those intended for external plies where no scarfing was done. The solvent wipe, accomplished just prior to the patch lay-up, removed all oils and dirt. String breathers were laid down first. The film adhesive was then laid down over the string breathers, followed by a vacuum debulk cycle. Debulking was done with a vinyl vacuum bag and no heat. Next, the pre-cut prepreg was laid-up, with each patch ply matching the orientation of the scarfed ply it was replacing. External plies were also added as required. Each patch ply was debulked.

Bagging of the patch is illustrated in Figure 5-12. Liberal amounts of breather were placed both above and below the heating pad to ensure good compaction and removal of volatiles. The string breathers were placed in physical contact with the breather system. Caul plates, such as 0.020" thick aluminum, are sometimes used to smooth the patch surface. However, in patches with external plies and tapered edges, it is believed that a caul plate would not be able to sufficiently conform to the patch contour, creating bridging and leaving areas of high porosity or disbonds. For this reason, caul plates were not used in the repairs assembled at American Airlines.

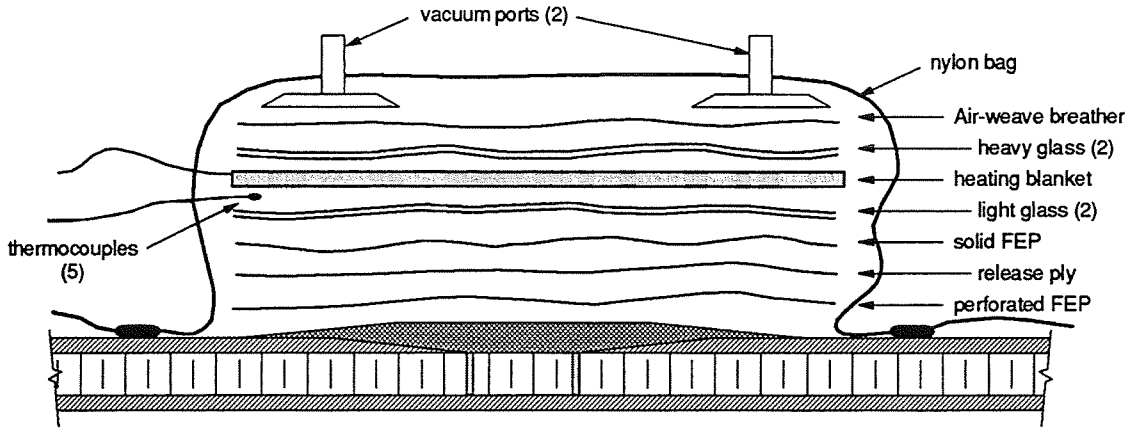

Figure 5-12: Bagging Procedure

The patch was cured for 2 hours at 250°F with full vacuum. A slow heating rate (2°F/min) was chosen to promote removal of volatiles and entrained water before the resin gels. Four to six thermocouples were placed around the perimeter, but were not allowed to touch the patch so as to prevent mark-off. Although heating blankets were placed only on the outer facesheet due to the one-sided nature of the repair, insulation blankets were used in some cases to provide more even heat distribution.

5.2.4 Temporary Repair Trials

A limited number of temporary repair trials have also been conducted as part of this activity. As described earlier, the intent of such repairs is to provide a moisture seal for sandwich structure with small damage, typically through the use of small precured patches and quick-setting adhesives. Efforts have focused on patch configuration, adhesives, surface preparation, bond cure, and surface finish.

Without any significant structural requirements, the precured patches can be quite thin. This allows them to be cured flat but still conform to the fuselage curvature. Still, there must be sufficient plies for the patch to serve as a moisture barrier. As a goal the patches should be easily sized without the use of power tools or expensive tooling aids. It is also desirable to produce patch material without excessive warpage or distortion.

Several thin precured patches were fabricated in thickness increments of one to five plies. Materials included graphite/epoxy tape and fabric, fiberglass fabric, and primed aluminum (0.016" thick). Ply stacking was such that patches were as close to quasi-isotropic as possible. The precured patches were visually inspected for warpage and possible moisture paths prior to being bonded to a panel. It was found that 3-ply fabric patch laminates exhibited minimal warpage, were conformable to curvature, and could be easily cut to size with hand shears. The addition of an exterior layer of Tedlar (polyvinyl fluoride) aids in providing an additional moisture barrier. (Although not included in this study, paint alone might also provide sufficient additional moisture resistance.) The fiberglass patch appears to be the least expensive approach; it can be precured at 250°F and has good adhesion properties.

A variety of adhesives are available for temporary repairs. The goal is to offer a large number of adhesives that vary in cure time, cure temperature, viscosity, pot life, and shelf life. Naturally, each adhesive will have different material storage and processing requirements. Furthermore, each may exhibit different mechanical properties and carry inspection and repair life requirements that directly relate to its expected performance. Depending on the specific repair situation, an airline would be able to choose an adhesive with its associated processing time and inspection schedule that best suits its need.

Three different types of epoxy adhesives were used in the trials: a two-part fast-setting room temperature cure, a two-part higher-strength room temperature cure (which can also be cured more quickly at elevated temperatures), and a 250°F cure film adhesive. The film adhesive is easiest to apply but requires freezer storage and a bagged cure. The two part systems can be stored at room temperature and cured without a vacuum bag, but require more time to mix and apply. Destructive inspections revealed the film adhesive to provide a qualitatively better bondline, while the two-part epoxies tended to produce small air pockets.

Three different methods of bond surface preparation were investigated for use with the temporary repairs: sanding, peel ply, and grit blasting. Sanding has the most practical application for in-field use. The basic process steps were to mask off the area, sand with 150 grit paper, and then solvent wipe. Grit blasting uses a similar process, however care must be exercised in not dwelling too long in one area, and in preventing grit from penetrating or becoming lodged in the local damage area. Grit blasting also would require specialized tooling and equipment. Both of these methods were used on the patch and the repaired structure. The peel ply method can make surface preparation a very quick and easy process with no tools involved, but can only be used on the patch material (either sanding or grit blasting would still have to be used for the base material). The peel ply must be cured into the patch and requires an extra step during lay-up.

Several cure cycles were evaluated for the temporary repairs depending on the resin system and the ambient conditions. The fast-setting epoxy system was cured at room temperature both with and without vacuum for 20 minutes. One of these cures was accomplished at an ambient temperature of 47°F, using a heat gun to apply heat locally. The remaining fast-setting epoxy patches were cured at 70°F. The higher strength two-part epoxies were cured with vacuum and a heat blanket at 200°F for one hour, and at 300°F for 15 minutes. The film adhesives were also cured using vacuum and a heat blanket at 250°F for one hour. The use of vacuum during cure on the two part resin systems improved the flow and distribution of the resin around the patch but is not necessary.

Some of the variables investigated in the temporary repair trials were intended to improve the surface finish. The inclusion of an outer layer of Tedlar, in addition to improving the moisture resistance of the patch, provides a visually appealing surface that may not require paint to match the aircraft color. In some cases, dry peel ply was placed against the exterior patch surface during the bonding operation to act as a breather and a flash

breaker. The dry peel ply would impregnate with excess resin and, when removed, provide a smooth faired-in surface without the need for a post-bond sanding operation.

6.0 INSPECTION METHODS

When damage is found in service, there is often little or no detailed information on the event that caused the damage (e.g., impactor geometry, energy levels, time since occurrence). Reliable nondestructive inspection (NDI) and evaluation (NDE) methods are needed to locate damage, quantify the extent of the damage, assess its effect on residual strength, and verify the integrity of the completed repair. Such methods can be used to avoid overly-conservative maintenance procedures, thus gaining airline acceptance of composite structures.

6.1 Inspection of Skin/Stringer Structure

Evaluation of mechanically fastened repairs of skin/stringer crown structure can be accomplished with standard NDI methods: TTU to evaluate precured patch laminates, visual inspections and physical measurements to verify sealant and fastener installation. This study has therefore focused on innovative methods to detect damage and evaluate its effect on residual strength.

6.1.1 Simulation of Warpage Due to Damage

When analyzing the window belt panels associated with the side quadrants, it was observed that a significant change in a panel contour was induced by machining the window cutouts. Similar changes in contour might result from impact damage. Simulations of this effect were conducted to evaluate its use as a damage detection and quantification method. Specifically, deformations of a flat five stringer crown panel was predicted for two specific damage scenarios described in Figure 6-1.

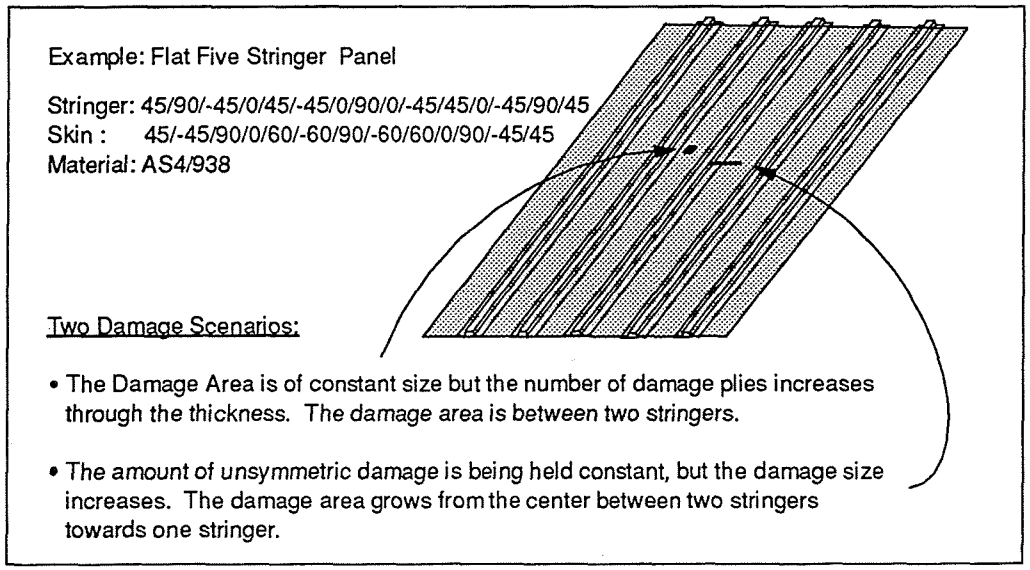

Figure 6-1: Warpage Due to Damage - A Simulation Approach

The first investigation assumed damage of constant size centered between two stringers. Levels of damage were simulated by degrading the fiber and matrix stiffness by three orders of magnitude for various numbers of plies. Results given in Figure 6-2 indicate that the damage induces out-of-plane deformation. For low damage severities, large deformation changes were observed. However, as damage levels increased, deformations become less severe; with all plies damaged, deformations differed only slightly from the undamaged panel. This deformation reversal is likely the result of increasing damage symmetry. Small changes in the deformation contours shown in Figure 6-2 for the fully damaged panel are due to overall load redistribution. A more refined mesh surrounding the damage would help quantify some additional local effects The results indicate that visual techniques have limitations relative to detecting and quantifying damage. Changes in panel contour indicate the presence of damage. However, a lack of contour change does not guarantee that no significant damage exists.

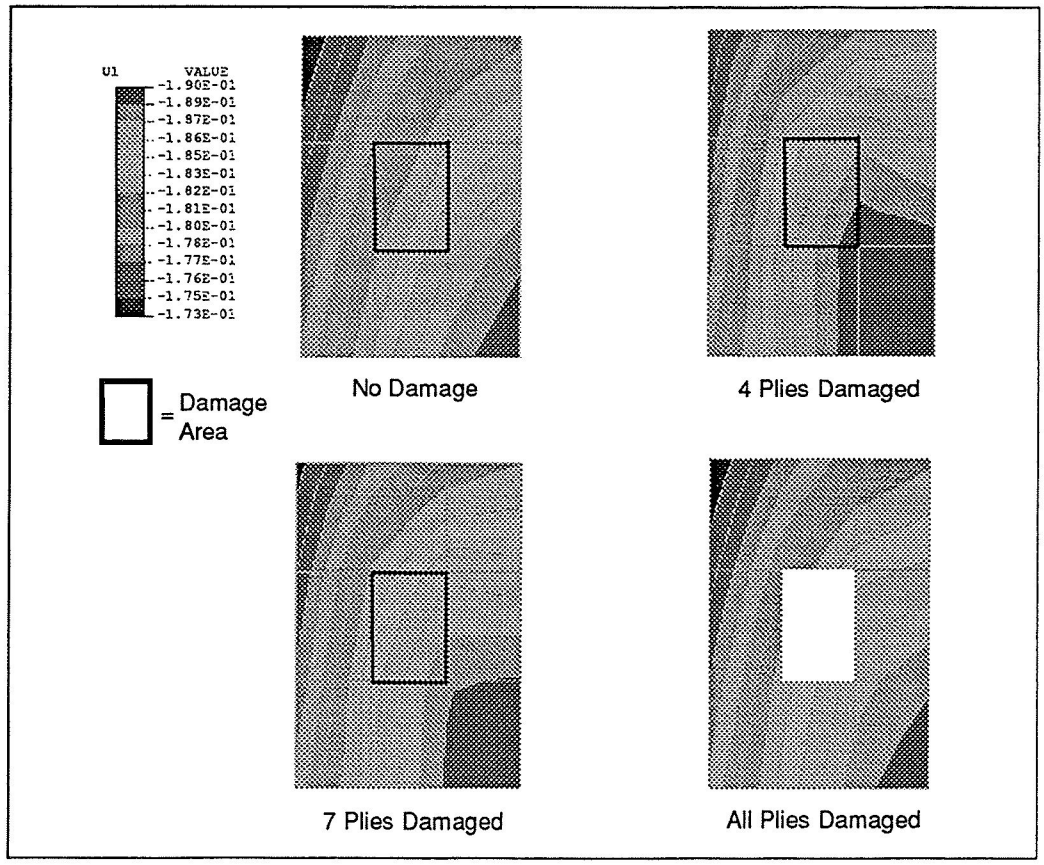

Figure 6-2: Increasing Out-Of-Plane Deformation Due to Increased Damage Through the Thickness

In the second investigation, the amount of through-the-thickness damage was held constant. The damage was limited to the inner four plies. The damage size was increased from no damage to a 1.5" x 2.5" size damage. Results, shown in Figure 6-3, again indicate that the damage induces changes in the out-of-plane deformation contours. The magnitude of out-of-plane deformation initially is very large with the onset of damage, but appears to converge to a maximum value as damage size increases. This provides further

evidence that the magnitude of panel deformations cannot be used to easily assess damage extent.

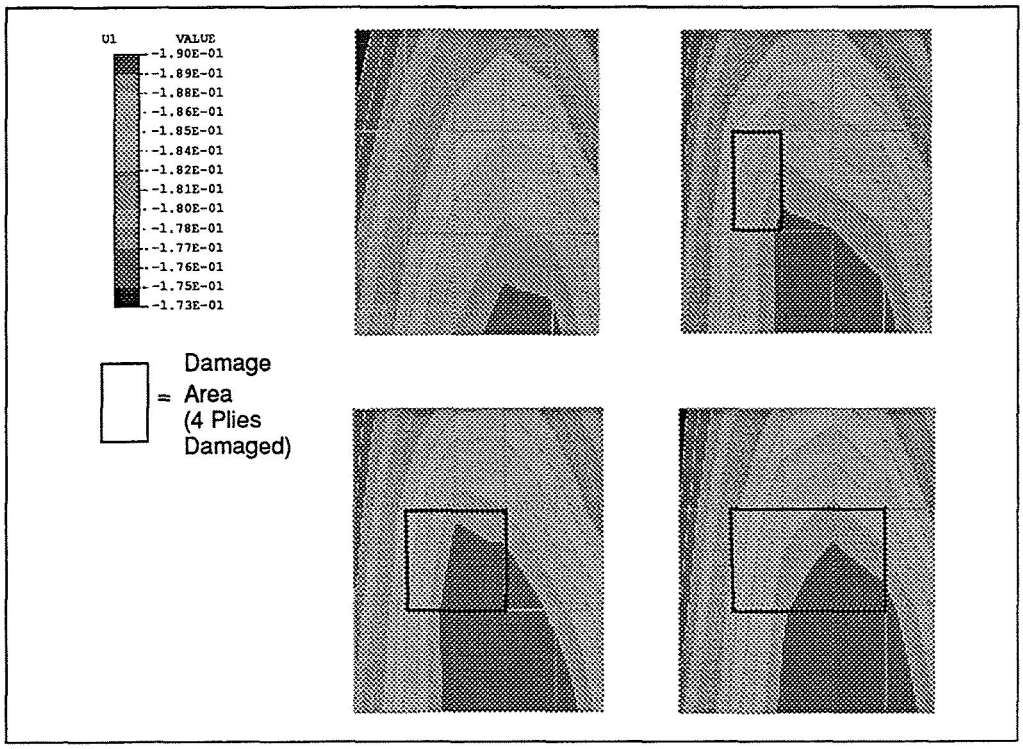

Figure 6-3: Increasing Out-Of-Plane Deformation Due to Increased Partial Damage Area

Figure 6-4 summarizes the ability of the method to relate out-of-plane deformation changes to panel residual strength, which in turn relates directly to repair requirements. Since the relationship between damage size/severity and panel out-of-plane deformation is not unique, the relationship between residual strength and out-of-plane deformation is also not unique. This indicates that the out-of-plane deformation cannot be used to determine residual strength.

6.1.2 Enhanced Optical Schemes

Most airlines use a detailed visual inspection, supplemented with both mechanical (i.e. coin taps) and electronic NDI methods to locate damage. Advanced NDI methods that have recently been considered for in-service application include enhanced optical schemes and thermography. Such procedures have the potential to inspect large surface areas of structure with minimum costs. The technique shown in Figure 6-5 [12, 13] has the resolution to locate the local thermal distortions considered in analyses described in [8]. Any advanced procedures will need to gain airline acceptance as being practical and reliable, and resulting in lower total inspection costs (including the combined costs of labor, equipment acquisition, and down time).

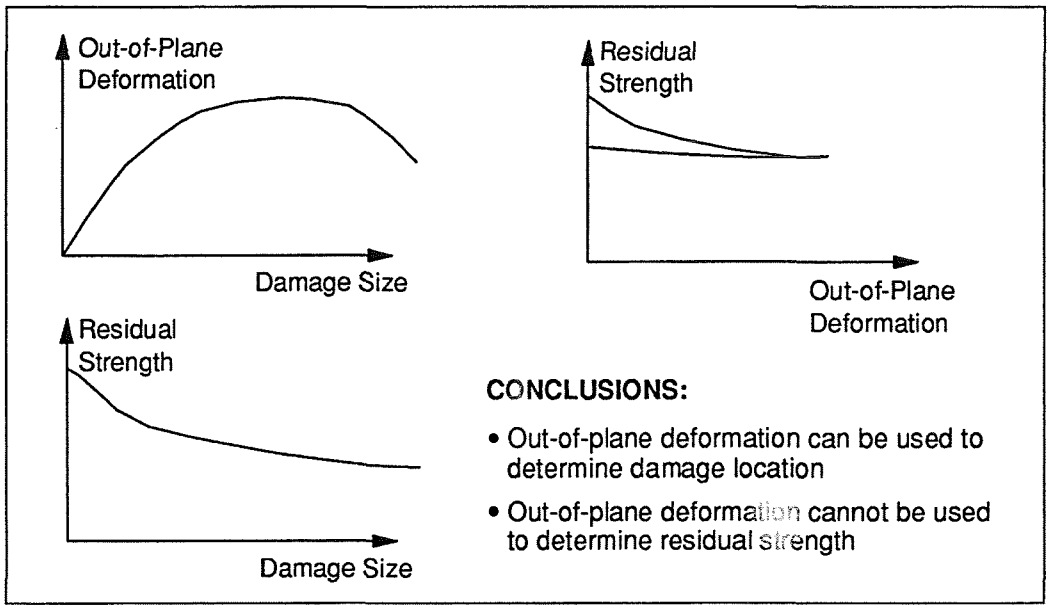

Figure 6-4: Residual Strength and Out-of-Plane Deformation

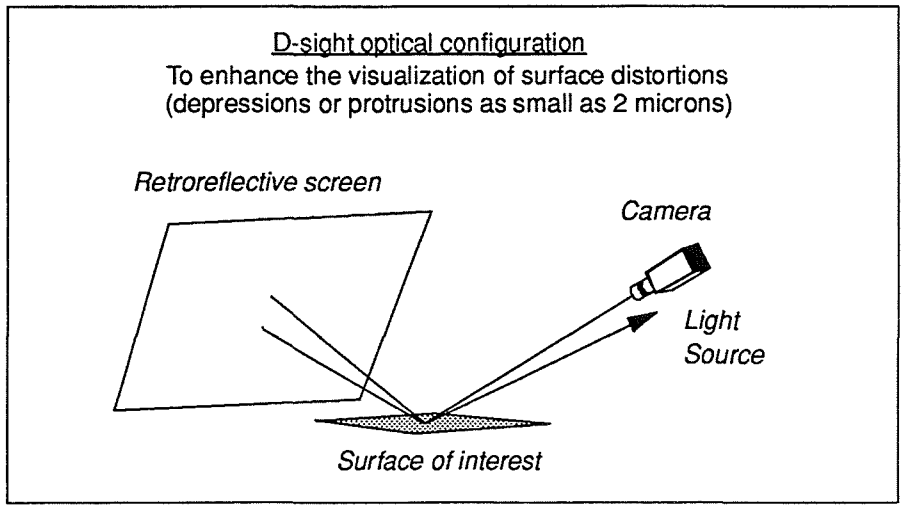

Figure 6-5: Enhanced Optical Schemes to Inspect Large Surface Areas for Visible Indications of Damage

6.1.3 Lamb Wave Propagation

As discussed above, visible schemes may provide sufficient resolution for locating damage; however, they do not provide quantitative data to predict the effects of damage on structural residual strength. Figure 6-6 shows the most reliable NDE method pursued in ATCAS for quantifying the effects of impact damage. This technique utilizes experimental data from Lamb wave propagation (one-sided gated pulse/catch) and analysis based on long wavelength dispersion relationships for laminated plates [14, 15]. Back calculations of reduced plate bending and transverse shear stiffnesses provide an estimate of the effect

of damage in degrading local load paths [16]. Good correlations have been found between reduced local stiffnesses experimentally measured by Lamb wave dispersion and out-of-plane mechanical loading devices in the impact designed experiment discussed earlier [7]. Other methods evaluated in these experiments, including visible dent depth, pulse-echo damage area, and other one-sided inspection procedures were found to have little or no correlation with the mechanical load measurements.

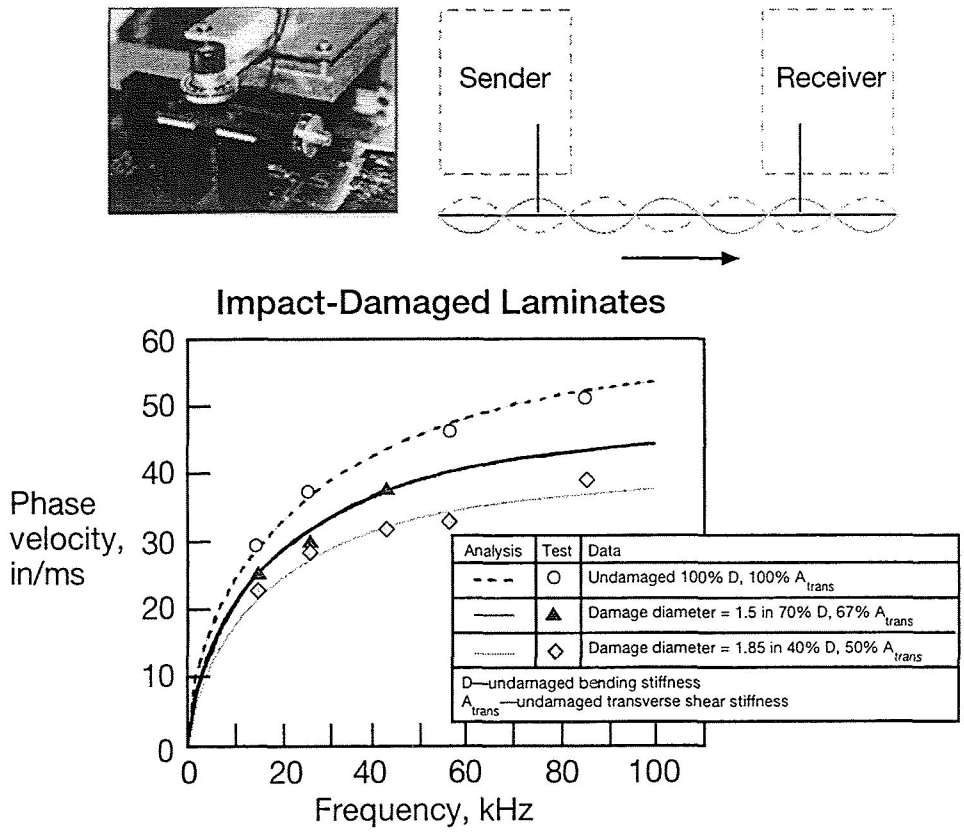

Figure 6-6: Development of Reliable Lamb Wave Dispersion NDE Methods

6.2 Inspection of Sandwich Structure

The full-scale process trials and repair demonstrations discussed in Section 5.3 were inspected using a number of nondestructive techniques including pulse-echo ultrasonics, through-transmission ultrasonics (TTU), and low-frequency bondtesting. The capabilities of different methods are compared and contrasted in light of the special limitations of a repair environment.

6.2.1 Pulse Echo Ultrasonics

Pulse echo inspection, using a 3.5 MHz focused transducer and a bubbler arrangement, gave high resolution (characteristically 0.010 inch) images of the skin and doubler areas on

the repaired side. Disbonds and concentrations of porosity could be identified in some panels, while in others the path of migrating gas could be discerned. Core anomalies can not be imaged with this technique. Furthermore, porosity and adhesive bondlines can prevent detection of anomalies at deeper levels of the repair. The technique was chosen to provide high-definition data of each repair skin.

6.2.2 Through-Transmission Ultrasonics (TTU)

Through-transmission inspection was performed at 1 MHz with tone-burst excitation and a 100 dB dynamic range. The equipment was Boeing-developed. The TTU inspection passes sound through the part thickness so that anomalies in the core and both skins are detected. The technique requires access to both sides of the part, a condition not normally existing on an in-service airplane. The technique was chosen to provide an accurate baseline for comparing other methods, as well as to characterize the patch quality. TTU located the same disbonds and regions of high porosity in the patches as did the pulse-echo technique. No core-related defects were identified by TTU.

6.2.3 Low Frequency (Dry-Coupled) Bondtesting

A Sondicator S9 and a Staveley Bondmaster, at frequencies of 14 to 40 kHz, were used as a third inspection method. Both instruments employ a pitch-catch arrangement wherein an acoustic wavetrain is generated by one probe tip and measured by the receiving probe tip. The application of this same technique to skin/stringer configurations was described in Section 6.1.3. Sondicator results are interpreted in terms of the wave propagation speeds. Fast speeds indicate a relatively stiff structure; slow speeds indicate a soft structure associated with damage or defects. The technique requires access to only one side of the part.

Sondicator inspections were performed on several of the full scale process trials. The sondicator was able to detect a disbond in one case, although the indications were not as strong as desired. In other cases, laminate and bondline porosity was not detected. However, the method successfully located a 1-inch diameter impacted area (outside of the repair) on the far side of one repair panel. Images of a frame flange lying on the far surface were also visible, indicating complete penetration of the part.

Low frequency bondtesting is currently the best choice for an in-service technique that can detect flaws in the core. Computerized data-acquisition greatly enhances the usefulness of this method. Boeing is currently using bondtester C-scan techniques in production and is extending these techniques to field applications.

6.2.4 Inspection At Field Bases

The American Airlines repair shop employs pulse-echo ultrasonics using commercially available portable C-scan equipment. This inspection equipment represents the leading edge of conventional technology. Even though several airlines have purchased such systems, most still rely on interpretation of real-time data from hand held probes, or simple tap tests conducted with a coin or tapping hammer.

The large disbond of trial AA1 (Figure 5-4) was first discovered by American Airlines using a tap test, and later confirmed with pulse-echo. The pulse-echo scans conducted at the airline's facility had a lower resolution when compared to those conducted at Boeing, and the color scale had fewer gradations. Although the equipment was capable of detecting a large area disbond close to the surface, it was incapable of detecting a smaller disbond deeper in the patch (trial AA2). The tap test could also not detect this smaller disbond.

Improvements would be needed before the portable pulse-echo method as used by American Airlines would be acceptable as a field inspection technique. Use of a focused transducer setup, with distance-amplitude correction and appropriate gating, might improve the results. Additional C-scanning with a bondtester would still be necessary to detect defects in the core.

7.0 CONCLUDING REMARKS

The design of composite fuselage structure must incorporate maintainability and repairability considerations to satisfy customer requirements and reduce total direct operating costs. Maintenance concerns should be addressed early in the design cycle to ensure realistic designs and easier supportability in the field. This may include providing operators with multiple repair options for a given level of damage, or "generic" repairs which can be applied over a broad range of damage scenarios. Airline participation is encouraged in the design process to ensure the customers' needs are met.

Design decisions are supported by analysis techniques for assessing the "effects of defects", i.e., the residual strength characteristics of the structure in the presence of damage. In this way, trade-offs can be made between structural weight, damage tolerance (repair frequency), and inspection burdens. The analysis methods must also be capable of evaluating specific repair design details, and determining the resulting strength of the repaired structure.

Repair materials and processes must be consistent with the capabilities of the airline repair facilities, and practically applied within the constraints of the typical field processing environment. Given the wide range of airline capabilities and environments, this reiterates the importance of providing multiple repair options. In all cases, however, the goal is to minimize the effort needed by the airline to return the damaged aircraft to full service. Inspection methods must be developed which can both assess the damage state (to help determine the need for repair) and verify the integrity of the completed repair.

These maintenance issues were addressed throughout the ATCAS program through the design of skin/stringer crown and sandwich keel structure. Panel design details such as skin layup were found to have a significant impact on the complexity of mechanically fastened crown repair designs. Keel repair designs focused on bonded concepts with simple patch geometries which were found to offer the best balance of manufacturing ease, surface profile, weight, and structural performance. In the case of both crown and keel, tradeoffs were possible between highly tailored repair designs with improved structural performance and simpler, more generic designs with less manufacturing complexity and/or greater applicability to other areas of the fuselage.

Analysis methods were developed to aid in the design of both the original and the repaired structure. Nonlinear, progressive damage analysis techniques developed in the ATCAS program have successfully scaled laminate coupon test results to predict structural residual strength. These methods, in conjunction with quantitative NDE, have the potential to create the tools necessary for practical assessment of damage found in service. Use of the methods to evaluate repair design details and predict coupon test results revealed the importance of including both material and geometric nonlinearities in the analysis. Post-processing of data from a recent large keel panel test and an upcoming large crown panel test will further validate the analytical techniques.

Repair materials and processes were successfully developed for both crown and keel, initially in small-scale trials, then demonstrated on large panels. Extensive manufacturing development of crown repair techniques was unnecessary due to the fairly straightforward approach of using precured elements and mechanical fastening. In-situ processing of bonded repairs for keel sandwich structure was more difficult. Persistent problems with gross bondline porosity were eventually solved by the addition of two small glass string-breathers under the adhesive layer to evacuate the core during the 250°F vacuum-bag cure. This string breather process also produced well consolidated patches, without the addition of any incremental heated debulk cycles. Subcontracts were established with American Airlines to perform the major repair demonstrations and some of the process trials at their repair facility. Feedback from this interaction was invaluable.

A limited investigation of temporary repair options found 3-ply precured fiberglass patches to be easily fabricated and applied with fast-setting epoxy adhesives at room temperature. More robust adhesives can be substituted with the addition of a short heat/vacuum cycle. Sanding and peel ply were found to be the most practical methods for surface preparation. The addition of an outer layer of Tedlar improves the moisture resistance of the patch.

New NDI and NDE techniques have been pursued under ATCAS to find damage and evaluate its effect on residual strength. Advanced optical surface mapping can rapidly and efficiently characterize geometric changes due to damage. This, in conjunction with out-of-plane deformation simulations can be employed to estimate the location of damage. Besides providing a large-scale, rapid inspection procedure, difficult to inspect areas can be evaluated without disassembly. Lamb wave propagation techniques were not as successful as pulse-echo and TTU at detecting disbonds and regions of high porosity in repair patches; however, this method did provide good estimates of the effects of impact damage in degrading local load paths.

Further development of maintenance/repair technology will be performed as part of the Phase C contract: Technology Verification of Composite Primary Fuselage Structures for Commercial Aircraft (NAS1-20553). Consideration may be given to a wider range of damage scenarios (different locations, different damage sizes and types) and load conditions (combined load, environment, and fatigue). Associated detailed design and analysis would allow the refinement of repair design variables such as patch layups, scarf angles, scarf depths, bond areas, and edge tapers. Alternative prepregs and adhesives may be explored, as may a wet layup repair option. Processing parameters would necessarily evolve with design and material changes (e.g., a different adhesive eliminating the need for string breathers in sandwich bonded repairs). Low-cost temporary repairs may also be further investigated.

Developed repair designs and processes would be evaluated through extensive demonstrations, inspections, and tests. The evaluations would be supported by the development of inspection methodologies which are more quantitative, useful, and practical for field application. Inspection intervals could be established for specific repair types as a function of their durability, determined in part through analysis and test.

8.0 REFERENCES

1. Ilcewicz, L., et al: "Advanced Technology Composite Fuselage - Program Overview," NASA CR-4734, 1997.

2. Ilcewicz, L., et al: "Application of a Design-Build Team Approach to Low Cost and Weight Composite Fuselage Structure," NASA CR-4418, December 1991.

3. Hanson, C., et al: "Design Integration of a Composite Aft Fuselage Barrel Section," *Sixth NASA/DoD Advanced Composite Technology Conference*, NASA CP-3326, 1995.

4. Walker, T., et al: "Advanced Technology Composite Fuselage - Structural Performance," NASA CR-4732, 1997.

5. Walker, T., et al: "Damage Tolerance of Composite Fuselage Structures," *Sixth NASA Advanced Composite Technology Conference*, NASA CP-3326, 1995.

6. Harris, C.: "Assessment of Practices in Supporting Composite Structures in the Current Fleet," *Fourth NASA/DoD Advanced Composites Technology Conference*, NASA CP-3229, 1993, pp. 21-35.

7. Dost, E., et al: "Impact Damage Resistance of Composite Fuselage Structure", NASA CR-4658, 1997.

8. Dopker, B., et al: "Composite Structural Analysis Supporting Affordable Manufacturing and Maintenance," *Sixth NASA Advanced Composite Technology Conference*, NASA CP-3326, 1995.

9. McGowan, D., et al: "Compression Tests and Nonlinear Analyses of a Stringer- and Frame-Stiffened Graphite-Epoxy Fuselage Crown Panel," *Fifth NASA Advanced Composite Technology Conference*, NASA CP-3294, 1994, pp. 321-350.

10. Hibbitt, Karlsson & Sorensen, Inc.

11. Avery, W., et al: "Design and Structural Development of a Composite Fuselage Keel Panel," *Fifth NASA Advanced Composite Technology Conference*, NASA CP-3294, 1994, pp. 463-495.

12. Komorowski, J., et al: "Inspection of Aircraft Structures Using *D* Sight," *39th International SAMPE*, 1994.

13. Reynolds, R., et al: "Theory and Applications of a Surface Inspection Technique Using Double Pass Retroreflection," *Optical Engineering*, 32 (9), 1993, pp. 2122-2129.

14. Lamb, H.: "On Waves in an Elastic Plate", *Proc. of the Royal Society of London, Series A*, 1917.

15. Tang, B., et al: "Low Frequency Flexural Wave Propagation in Laminated Composite Plates", *Acousto-Ultrasonics: Theory and Application (edited by J.C. Duke, Jr.)*, 1988, pp. 45-65.

16. Dost, E., et al: "Experimental Investigations Into Composite Fuselage Impact Damage Resistance and Post-Impact Compression Behavior," *37th International SAMPE Symposium & Exhibition, Soc. for Adv. of Material and Process Eng.*, 1992.

APPENDIX A

Subcontractor Final Report:

"Evaluation of Repair Concepts for Composite Fuselage Shell Structures"
Oregon State University

EVALUATION OF REPAIR CONCEPTS FOR COMPOSITE FUSELAGE SHELL STRUCTURES

by

Timothy C. Kennedy and Matthew F. Nahan

Department of Mechanical Engineering

Oregon State University

Corvallis, OR 97331

June, 1994

SUMMARY

The objective of this project was the development of cost-effective repair techniques for aircraft fuselage made of composite materials. The primary focus was on a damage scenario consisting of a 22-inch, through-penetration notch in the aft crown section of the fuselage of a wide-bodied commercial airplane. The notch ran parallel to the central axis of the fuselage and included the severing of a circumferential frame member. Only mechanically fastened repair concepts were considered. These concepts were evaluated through finite element analysis.

To help gain an understanding of the critical variables that affect the performance of a repair design, a series of experiments was performed on notched coupons of graphite/epoxy laminate with various repair patches. Both uniaxial and biaxial loading tests were conducted. Finite element models were constructed for each case, and the experimental results were compared to the theoretical predictions. The strain response predicted by the finite element analysis was generally in good agreement with the strain gage output provided that geometric nonlinearities (large deflections) were taken into account. Likewise, large deflection analysis better modeled the nonlinear stiffness evolution of the repair and its effect on surrounding structure. Generally, strain predictions outside of the repair area were in excellent agreement with test data; whereas within the repair region less correlation was achieved, especially for biaxial load conditions. Agreement between predicted and measured failure loads was not as good as that obtained for strains. Generally, the finite element analysis predicted failure loads that were lower than those measured. This was apparently due to the fact that the bolt loads in the fasteners connecting the patch to the coupon were more uniformly distributed than predicted because of materially nonlinear response at the fastener holes. No material nonlinearities were modeled in the finite element analysis.

A final repair design was developed which addressed the 22-inch axial notch in the fuselage aft-crown panel. Cut-out of the damaged skin and frame took on an hour-glass shape and reflected removal of damaged structural units rather than being specific to the 22-inch notch. The skin was patched externally in a bi-level configuration using stock composite laminate of E-glass/epoxy fabric. The frame was spliced using multiple angle brackets of graphite/epoxy. Analysis of the final repair showed that return of the fuselage to ultimate strength was not possible. However, true load carrying capacity would likely be greater than predicted as indicated in the coupon tests described above.

An alternate repair design was developed which differed from that of the final design by incorporating stiffness anisotropy in the stock patch laminate. This trait was achieved using a tailored ply layup of E-glass/epoxy tape. Analysis demonstrated a strength increase over the final design. Although this concept was shown to enhance structural performance, its generality to repair of the entire fuselage, where stiffness requirements would vary, is questionable.

In developing the repair design, it became clear that fuselage design development should include repair strength objectives and costs in determining an optimal configuration. In the present case the margin between fuselage strain and the various allowable strain limits was allowed to be too narrow for effective repair. Repair of complex structure entails some degree of perturbation to the developed strain field and a repairable fuselage must include a minimal strain margin for this reason.

Taking repair performance and costs into consideration, an alternate (modified) fuselage design was proposed. A repair design was developed for which analysis predicted a return of ultimate strength. The repair differed from those presented above in its use of a significantly reduced patch size, of only one layer, and composed of graphite/epoxy. The alternate fuselage differed from the nominal design in providing a larger margin between operational strain and allowables. In addition, its skin stiffness anisotropy and damage cut-out aspect ratio combined to allow for improved repair stiffness matching.

TABLE OF CONTENTS

A1.0 INTRODUCTION

A1.1 Background and Objective

During the past 2.5 years Oregon State University (OSU) has been a participant in the Advanced Technology Composite Aircraft Structures (ATCAS) program under subcontract to the Boeing Commercial Airplane Company. The primary objective of this program is the development of cost- and weight-efficient structural design concepts for commercial transport fuselages made of composite materials. OSU's involvement in this program has focused on the development of cost-effective repair techniques for damaged skin/stringer fuselage configurations.

During the service life of an aircraft structure composed of composite materials, damage of various types may develop. This includes delaminations caused by small impacts, delaminations combined with broken fibers caused by larger impacts, and large through-cracks caused by penetration impacts or handling damage. Cost-effective methods for repair of such damage will be necessary to meet regulatory requirements and insure that life-cycle costs are competitive with current metallic structure.

The primary effort in this project has focused on a damage scenario consisting of a 22-inch, through penetration notch in the aft crown section of the fuselage. The penetration includes the severing of a frame member as shown in Figure A1-1. Only mechanically fastened repair concepts were considered in this investigation because of the advantages that they offer over bonded repairs including: (a) installation is low cost (neither special equipment nor extensive surface preparation is required), (b) material handling and storage problems are minimized, (c) sophisticated nondestructive evaluation equipment is not needed for inspection, (d) they are compatible with hat-stiffened structure, and (e) there is flexibility to restore structural integrity to large panel areas.

This report documents the work performed at OSU in investigating the structural integrity of repair concepts for damaged composite fuselage panels. The remainder of this section gives a review of the relevant literature in the field of composite repair. Section A2 describes the results of tests on damaged coupons with repair patches and a comparison of the results with finite element analysis predictions. Section A3 presents the development of repair designs for the 22-inch notch in a crown panel described earlier. Section A4 presents the conclusions drawn from this research project.

A1.2 Literature Review of Repair Procedures for Composite Aircraft Structures

Although the primary focus of this research is on mechanically fastened repair, this literature review will consider bonded repairs as well. A number of repair procedures have been proposed and those relevant to composite repair needed for the ATCAS

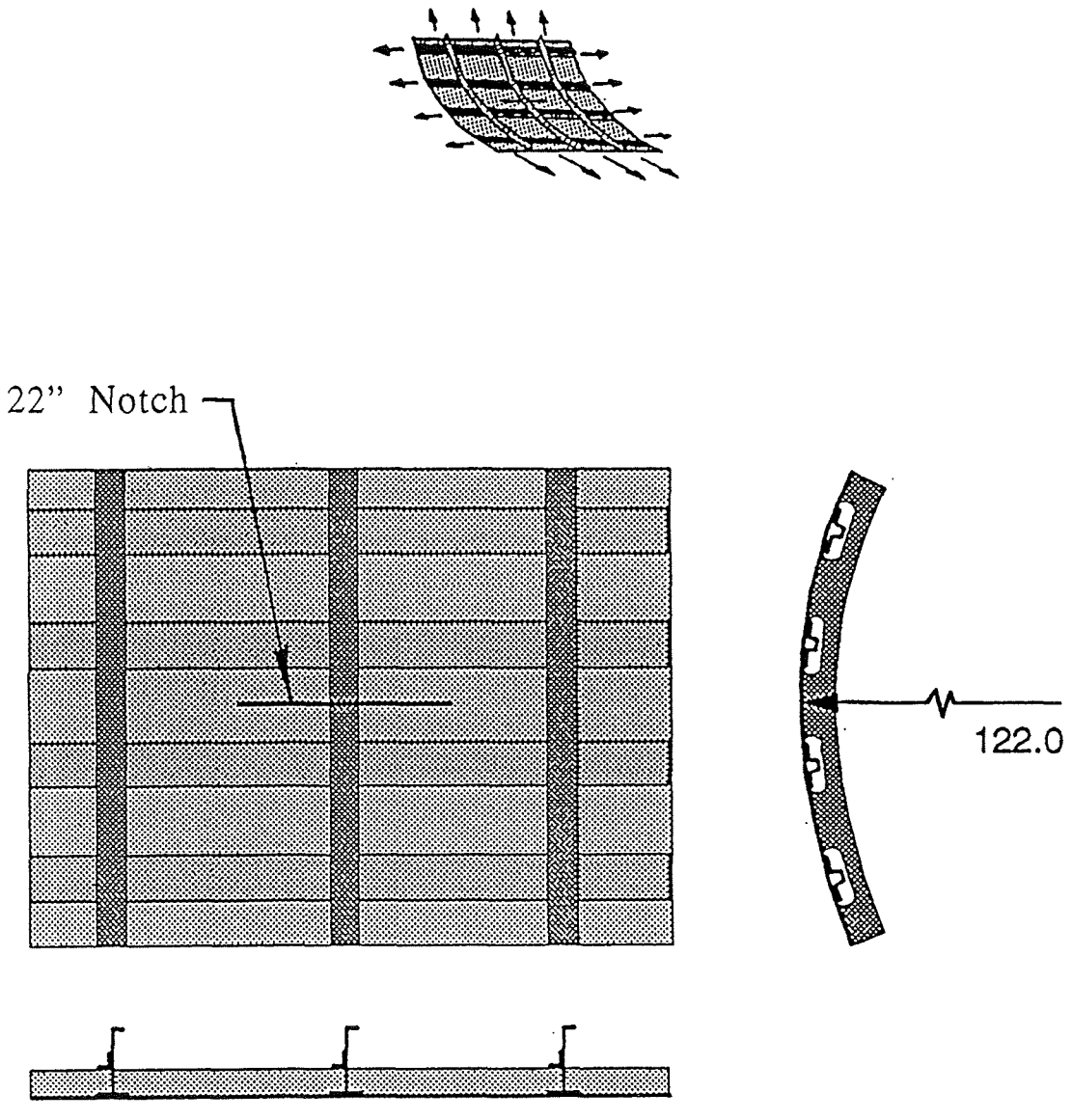

Figure A1-1: Damaged Fuselage Panel

program will be examined here. The majority of repair procedures involve removing the damaged material by cutting a circular or oval hole around the damaged area. The hole is then covered with a patch that is either bonded flush with the parent laminate or attached externally to it by adhesive bonding or mechanical fasteners. A general discussion of these procedures can be found in a review article by Baker (1986b) that describes damage assessment, common repair procedures (including surface preparation, adhesives, and curing), and some simplified analysis techniques for calculating adhesive stresses. Trabacco et al (1988) also present a review article on composite aircraft repair describing repair materials, the advantages and disadvantages of bolted repairs vs. bonded repairs, the effects of moisture on bonded repairs, and several examples of successful repairs. We will examine the work that has been done on three different categories of repair procedures: flush patches, adhesively bonded external patches, and mechanically fastened external patches.

A1.2.1 Flush Patches

Flush patches are used when a smooth surface is required for aerodynamic reasons, and the load eccentricity produced by external patches must be avoided. Flush patches are normally mated to the parent laminate along a scarf joint. The scarf taper ratio is normally 20:1 or higher in order to minimize stress in the joint. The patch ply layup usually matches that of the surrounding laminate. Both precured and cocured patches have been used in flush repairs. Although the precured patch is easier to install, it is usually more difficult to match the scarf angle with this type of patch. This problem can be reduced somewhat with a stepped joint rather than a smooth scarf joint. The repaired area is usually covered with several additional plies that extend over the surrounding laminate. Although these repairs produce the maximum joint efficiency, they tend to be the most difficult and time-consuming to produce. An analysis of the stress in a scarf joint was presented by Adkins and Pipes (1985). They showed that joints with small scarf angles are very sensitive to stiffness mismatch between adherends and to adherend tip bluntness. Reasonable agreement was found between experimental data and theoretical predictions.

Flush patch repairs have been the subject of a number of theoretical and experimental investigations. Myhre and Kiger (1980) tested four repaired panels of graphite/epoxy laminates with oval holes. In each case a scarf joint was used and the original material was replaced with a cocured patch with a layup similar to the removed material plus several additional plies. In each case the panel was restored to its original strength. Labor and Myhre (1979b) presented the results of a testing program to evaluate adhesively bonded repairs of graphite/epoxy laminates. Both flush repairs employing scarf joints and external patch repairs were evaluated. Test results generally showed that the repairs restored over 80 percent of the parent laminate ultimate allowable fiber failure strength. Labor and Myhre (1979a) also presented detailed step-by-step procedures for making repairs developed during the testing program just described.

Labor (1981) studied concepts for repair of monolithic skin panels, full-depth honeycomb sandwich structure, and sine-wave substructure. For the monolithic skin panels, two

concepts were described for flush repairs with outside access only. The first concept consisted of laying down a thin precured laminate over a scarf joint followed by cocured replacement plies and cocured surface plies. The second concept was similar but used precured replacement plies. For honeycomb sandwich structure the repair was similar to the first one described above with a core plug inserted to replace damaged honeycomb. For sine-wave substructure two repair concepts were studied. The first replaced the damaged web with an aluminum honeycomb sandwich element fabricated separately and bonded to the undamaged web. The second used a precured sine-wave web segment held in place with precured splice doublers.

Dehm and Wurzel (1989) performed an experimental study of laminates with damage consisting of a 51-mm hole. The repair consisted of a flush patch bonded to the laminate on a scarf joint with additional surface plies. The panels were loaded in torsion, compression, and combined torsion and compression. The failure loads of the patched material were higher than the undamaged material, apparently because of the extra overlapping plies. Mahon and Candello (1981) studied the repair of a 15-cm diameter hole in the skin of a boron/epoxy skin with honeycomb core sandwich plate. A stepped joint was prepared around the hole, and then a flush boron/epoxy internal patch was cocured in place. An external stepped cover was also bonded onto the outside of the laminate. The repair was tested and failed at 139% of the design ultimate load.

Bair et al. (1991) analyzed a laminate consisting of a boron/epoxy laminate with a 15-cm diameter hole under tension. The repair consisted of internal and external adhesively bonded stepped patches. Strains calculated from a finite element analysis were found to be in reasonable agreement with experimental results. Maman (1989) presented a methodology for evaluating the reliability of a repaired structure using a probabilistic failure criterion. He performed a sample analysis for the case of a laminated plate under tension with damage represented by a circular hole. The repair consisted of a flush patch filling the hole. More development is needed to make this method practical for large, complex structures.

Lin and Wang (1988) analyzed a novel repair concept developed by Boeing. In their work they evaluated both theoretically and experimentally three different repairs of a circular hole in a laminate. The first repair consisted of a laminate patch attached to the parent material along a scarf joint with overlay patches on the top and bottom surfaces. The second repair consisted of an aluminum bow-tie splice across the hole and an overlay patch. The end of the bow-tie had a triangular shape. The third repair was similar to the second but with the end of the bow-tie having a circular shape. The circular-shaped bow-tie splice was found to produce a smaller stress concentration near the edge of the bearing surface than the triangular-shaped bow-tie splice. Analysis of the shear stress in the scarf joint indicated the importance of the patch material having properties similar to those in the parent material.

Siener (1992) performed a finite element analysis on single lap scarf joints. He considered several patch thicknesses but with the section modulus of the patch material kept constant

in the direction of loading. This was accomplished by reorienting the plies in the patch. The purpose of this was to increase the load transfer efficiency of the joint. Experimental results were found to be in qualitative agreement with the finite element predictions. It was concluded that more detailed models would be required to accomplish quantitative agreement.

A1.2.2 Adhesively Bonded External Patches

In an adhesively bonded external patch repair, the repair area is covered with a composite patch that is bonded to the top or bottom surface of the parent laminate. Baker (1986b) discussed several options for this type of patch: it may have a ply layup similar to the parent laminate; it may be a quasi-isotropic layup that is thicker than the parent laminate; or it may be made of layers of titanium foil adhesively bonded together. The primary drawback to this type of patch is that it consists of a lap joint with an eccentric load path that can result in bending in the patch and the development of peel stress in the adhesive. It can also lead to stability problems in compression. Renton and Vinson (1977) have presented a stress analysis for this type of joint. In a review article on joining composites, Baker (1986a) discussed some of the problems associated with the joints. The load carrying capacity of the joint increases in proportion to the square root of the thickness of the adhesive. For most practical joints the adhesive layer thickness is in the range 0.13 to 0.26 mm. Peel stresses under tension loading arise at the outer edges of the adherends as a result of the tendency of the outer adherend to bend away from the inner adherend under the moment produced by the shear stress. These joints can be improved by tapering the ends to reduce the peel stresses. Rivets are also occasionally used at the ends of these joints to reduce these stresses. Unfortunately, the presence of fastener holes allows moisture to enter into a high stress area and can lead to environmentally induced bond failure.

Despite these drawbacks, the ease of installation of this type of patch as compared to a flush patch has made it a commonly used repair concept and the subject of several investigations. Labor and Myhre (1979a,b) studied it extensively and compared it to flush patch repair. However, they recommend a flush patch over an external patch because of the superiority in strength, aerodynamic smoothness, weight, stiffness (i.e., avoiding a "hard spot"), and uniformity of load distribution.

Hunter (1990) considered a graphite/epoxy laminate with a circular hole repaired by an adhesively bonded external patch. They performed a finite element analysis of the specimen using spring elements to model the adhesive layer between the panel and the patch. Experiments were also performed. Experimental and finite element analysis results were compared and reasonable agreement was found. Cripps (1984) performed a series of experiments on damaged kevlar/epoxy cloth mini-sandwich panels with cellular foam core. The damage consisted of a hole, and the repair consisted of a plug and an adhesively bonded external patch of either kevlar/epoxy or fiberglass. The fiberglass patch was found to make an effective repair and was easier to apply than the kevlar/epoxy. Paul and Jones (1989) considered the case of damage consisting of a delaminated region around a circular

hole (e.g., a bolt hole). They made a 3-D finite element model of the delaminated panel. The repair consisted of a bonded external patch. They concluded that the resulting increase in residual strength was proportional to the reduction in net section stress. Myhre (1981) presented a simplified repair where the damaged material was left in place, a low viscosity resin was injected into the damaged area, and an external patch was cocured in place.

For adhesively bonded external patch repair of metal structures, several investigators considered the situation where the damaged area is not removed but allowed to remain as a crack through the parent material. Jones and Callinan (1979) considered a crack in a metal sheet under tension that was repaired by adhesively bonded strips of composite. Through a finite element analysis, they found that the optimum location of the strip was at a point centered near the crack tip. They also found that if the patch was made too thick, the reduction in stress intensity factor was more than offset by a significant increase in the adhesive shear stress. Jones and Callinan (1981) also analyzed the repair of a centrally-cracked aluminum plate by adhesively bonded boron/epoxy patches on one or both sides of the plate. Through finite element analysis, they found that the most effective patches were those on both sides of the plate and having a variable thickness from a maximum in the center to a minimum on the edges. Chandra and Subramanian (1989) studied the influence of patch parameters (stiffness, width, and length) on the stress intensity factor in a plate with a central crack using transmission photoelasticity. They found that there was a critical value of patch length beyond which there was no further reduction in stress intensity factor. They also found that a symmetric patch was more effective than an unsymmetric one.

A1.2.3 Mechanically Fastened External Patches

A mechanically fastened external patch is similar to an adhesively bonded external patch except for the method of attachment (bolts or rivets rather than adhesive) and for the greater variety of materials used (aluminum, steel, or titanium as well as composites). Baker (1986b) recommends bolted patches for thick laminates (8-15 mm) where high shear stress exceeds the capability of the adhesive. In mechanically fastened joints most of the shear load is transmitted through individual fasteners, and the shear loads in the fasteners are transmitted to the joint members as bearing loads on the faces of the fastener holes. Load transfer between the joint members by interfacial friction does not usually constitute a large portion of the shear load because friction transfer usually cannot be maintained at a high level during prolonged service due to the loss of clamping pressure resulting from vibration and wear. The stress concentration that develops at a fastener hole in a composite cannot be ignored (as is often done for metals) because general yielding is not possible. Bearing failures at the holes in the composite must also be considered as these are usually the result of local buckling and kinking of the fibers and the subsequent crushing of the matrix.

These types of repairs have been the subject of a number of theoretical and experimental investigations. Manno (1981) studied two repair concepts for 10-cm diameter holes in

laminates with skin thicknesses ranging from 4.8 to 12.7 mm. The first repair consisted of a titanium plate bolted to the laminate. The second consisted of an external cocured patch formed by stacking graphite/epoxy discs on a disc of fiberglass epoxy prepreg. A quasi-isotropic patch was formed with a 25 to 1 taper ratio. These two concepts were tested and were found to exceed design requirements. Bohlman et al. (1981) presented an analysis of the repair of a circular hole in graphite/epoxy wing skins (4.8 to 12.7 mm thick) by means of a bolted titanium patch. They have developed a computer program, BREPAIR, that takes into account bolt clearance and flexibility. Allowables for edge of hole strains, tension/bearing interaction, and fastener shear were determined from experiments. Correlations between code predictions and test results were good. Bohlman et al. (1986) extended the BREPAIR program to include the capability of handling biaxial and shear loading as well as uniaxial tension. They used this program to analyze a carbon/epoxy laminate with a titanium patch. Hoehn and Ramsey (1986) have also made enhancements to the BREPAIR program. They performed tests and analysis of carbon/epoxy panels (5.3 mm thick) under uniaxial and biaxial load. Damage consisted of holes of various sizes and shapes. Repairs consisted of sheets of stainless steel bolted to the laminate. Good correlation was found between predicted and measured strains.

Shyprykevich (1986) used finite elements to analyze a wing cover featuring compliant skin (6.6 to 7.8 mm thick) between I-stiffeners. Three damage scenarios were considered. The first consisted of a 10-cm diameter hole in the skin only. This was repaired by an aluminum plate bolted to the skin. The second damage consisted of a 10-cm diameter hole in the skin with part of the hole through the top and bottom flanges on one side of the stiffener. The skin was patched with an aluminum plate. The flanges on the stiffeners were patched with titanium straps. The third damage consisted of a 10-cm diameter hole through the skin and stiffener. The skin was patched with a titanium plate and the stiffener was patched with titanium angles and straps. Shyprykevich et al (1991) conducted a testing program to evaluate the repair concepts analyzed previously using finite elements. Good correlation was found between the strains predicted by finite element analysis and those measured in the tests.

Russel et al (1991) presented an analysis procedure applicable to unrepaired and repaired damaged composites. The unrepaired analyses used either empirical relations or elasticity solutions. The repaired analysis procedure used the Rayleigh-Ritz method. They applied the latter technique to the bolted-patch repair of a circular hole and compared their results to a similar analysis using a boundary element program. Busch and Dompka (1991) described the evolution of a repair design for damage of a lower wing skin plank and stringer on the V-22 aircraft. The initial repair design consisted of carbon/epoxy plates bolted to the skin and carbon/epoxy C-channels bolted to the stringer. Through a finite element analysis, they were able to optimize their design and bring strain levels to within specified allowables. Reisdorfer (1992) also developed a similar design for a wing skin plank and stringer on the V-22 aircraft. Bolted joints used in the repair design were investigated through static and fatigue tests on coupons and were found to be adequate.

Four different repair methods for a 9.5-cm diameter hole were evaluated experimentally by Deaton (1991). The first consisted of a bolted external aluminum plate with supplemental adhesive. The hole was filled with the circular piece obtained from the hole forming operation and epoxy. The second method consisted of a precured bonded external graphite/epoxy patch with the patch having four more plies than the original laminate and a slightly different layup. The third method consisted of a cured-in-place external graphite/epoxy patch with the patch having four more plies than the original laminate and a slightly different layup. The fourth method consisted of a cured-in-place flush graphite/epoxy patch with a scarf joint matching the original laminate plus additional plies covering the top and bottom surfaces. After seven years of outdoor exposure plus 1.75 lifetimes of fatigue, only the fourth repair method did not show a loss in residual strength.

A1.2.4 Conclusion

The steps needed for the development of a composite structures repair methodology have been presented by Hall et al (1989). First, mechanical properties of the basic materials as well as data on mechanical and adhesive joints are determined. Next, tests of repair concepts are performed on simple coupons and the results compared with theoretical predictions. The final phase proceeds on to testing and analysis of complex built-up structures. Dodd and Sandow (1991) recommend that this process be capped off with the development of an expert system to guide technicians in the selection of a repair procedure. The system that they described was for battle-damaged aircraft structures. It used existing software for the analysis of adhesively bonded or mechanically fastened joints and for the calculation of stresses around the damaged area. The system also contains rules, developed from interviews with experts in the field of repair design, that assess the adequacy of the repair.

A2.0 REPAIRED COUPON TESTS AND ANALYSIS

To help gain an understanding of the critical variables that affect the performance of a repair design, a series of experiments was performed on notched coupons with various repair patches. Both uniaxial and biaxial loading tests were conducted. A finite element analysis was performed on each repair, and the theoretical predictions of response were compared with the experimental results. Details are given below.

A2.1 Uniaxial Loading Tests and Analysis

Uniaxial loading tests were conducted to determine the effectiveness of repair patches under simple loading conditions. This also provided a means to evaluate the validity of finite element models used in the analysis.

A2.1.1 Repaired Coupon Test Specimens

A list of the tests on repaired coupons is given in Table A2-1. The coupons were 10" x 30" laminates with 2.5"-long line notches (representing damage) at the center, as shown in Figure A2-1. For all but two cases the coupon material was a 13-ply graphite/epoxy laminate (0.074" ply thickness) with a [45/-45/90/0/60/-60/90/-60/60/0/90/-45/45] layup, which is representative of fuselage skin material. Three of these coupons also had a 2.5"-wide tear strap running down the center consisting of a 0.0765"-thick graphite fabric composite. The remaining two coupons consisted of 15-ply graphite/epoxy laminates with [-45/45/0/90/-30/30/-75/0/75/30/-30/90/0/45/-45] layups. These two coupons also had the notches aligned parallel to the load direction. Three different patch sizes (6.66" x 4.02", 7.60" x 2.77", and 7.60" x 5.27") were examined. The patch materials that were considered consisted of 13-ply graphite/epoxy laminate (identical to fuselage skin), a 24-ply glass fabric in epoxy laminate (0.0045" ply thickness) with alternating 0° and 45° layers, a 12-ply graphite/epoxy laminate with a [-45/90/45/90/0/90]s layup, and a 0.1"-thick titanium plate. The elastic properties for each ply of these materials is given in Table A2-2. The fasteners that were considered consisted of 3/16"-diameter titanium bolts, 1/4"-diameter titanium bolts, and 1/4"-diameter thermoplastic rivets. Sketches of the various repairs that were tested are shown in Figures A2-2 through A2-9. For Case 17 there is an additional 2.60" x 5.27" patch on the tear strap side of the coupon consisting of the graphite fabric composite described earlier. The coupons were instrumented with strain gages and tested to failure under tension by Intec (Polland and Swanson, 1993).

A2.1.2 Finite element Analysis of Repaired Coupons

A finite element model was constructed for each of the test coupons listed in Table A2-1 using the general purpose finite element program COSMOS/M. Four-node quadrilateral and three-node triangle, layered shell elements were used to model the coupons and patches. Beam elements were used to model the fasteners. The length of the beam

Table A2-1: Predicted and Measured Failure Loads for Coupon Test Specimens

Case	Coupon Material	Patch Material	Patch Size	Bolt Type	Crack Orientation	Predicted Failure Load (lb)	Measured Failure Load (lb)
1	13-ply GR/EP	24-ply GL/EP	6.66"×4.02"	3/16" Ti	Horz.	41,400 (B)	44,400 (N)
2	13-ply GR/EP	13-ply GR/EP	6.66"×4.02"	3/16" Ti	Horz.	42,200 (B)	54,840 (N)
3	13-ply GR/EP	12-ply GR/EP	6.66"×4.02"	3/16" Ti	Horz.	42,200 (B)	51,075 (N)
4	13-ply GR/EP	1/10" Ti	6.66"×4.02"	3/16" Ti	Horz.	43,400 (B)	50,000 (B)
5	13-ply GR/EP	24-ply GL/EP	7.60"×2.77"	1/4" Ti	Horz.	43,400 (N)	40,410 (N)
6	13-ply GR/EP	13-ply GR/EP	7.60"×2.77"	1/4" Ti	Horz.	44,900 (B)	43,510 (N)
7	13-ply GR/EP	24-ply GL/EP	7.60"×2.77"	1/4" T.P.	Horz.	42,300 (N)	40,090 (N)
8	13-ply GR/EP	13-ply GR/EP	7.60"×2.77"	1/4" T.P.	Horz.	44,100 (N)	31,850 (N)
9	13-ply GR/EP	24-ply GL/EP	7.60"×5.27"	1/4" Ti	Horz.	43,000 (B)	47,690 (N)
10	13-ply GR/EP	13-ply GR/EP	7.60"×5.27"	1/4" Ti	Horz.	43,100 (B)	55,980 (B)
11	13-ply GR/EP	24-ply GL/EP	7.60"×5.27"	1/4" T.P.	Horz.	42,800 (B)	45,400 (N)
12	13-ply GR/EP	13-ply GR/EP	7.60"×5.27"	1/4" T.P.	Horz.	43,000 (B)	41,460 (N)
13	15-ply GR/EP	13-ply GR/EP	5.27"×7.60"	1/4" Ti	Vert.	42,600 (B)	48,720 (B)
14	15-ply GR/EP	13-ply GR/EP	2.77"×7.60"	1/4" Ti	Vert.	41,300 (B)	51,400 (B)
15	13-ply GR/EP with severed tear strap	none			Horz.	20,100 (N)	26,875 (N)
16	13-ply GR/EP with intact tear strap	none			Horz.	59,100 (N)	39,270 (N)
17	13-ply GR/EP with severed tear strap	13-ply GR/EP and 9-ply fabric	7.60"×5.27" and 2.60"×5.27"	1/4" Ti	Horz.	48,400 (N)	53,730 (N)

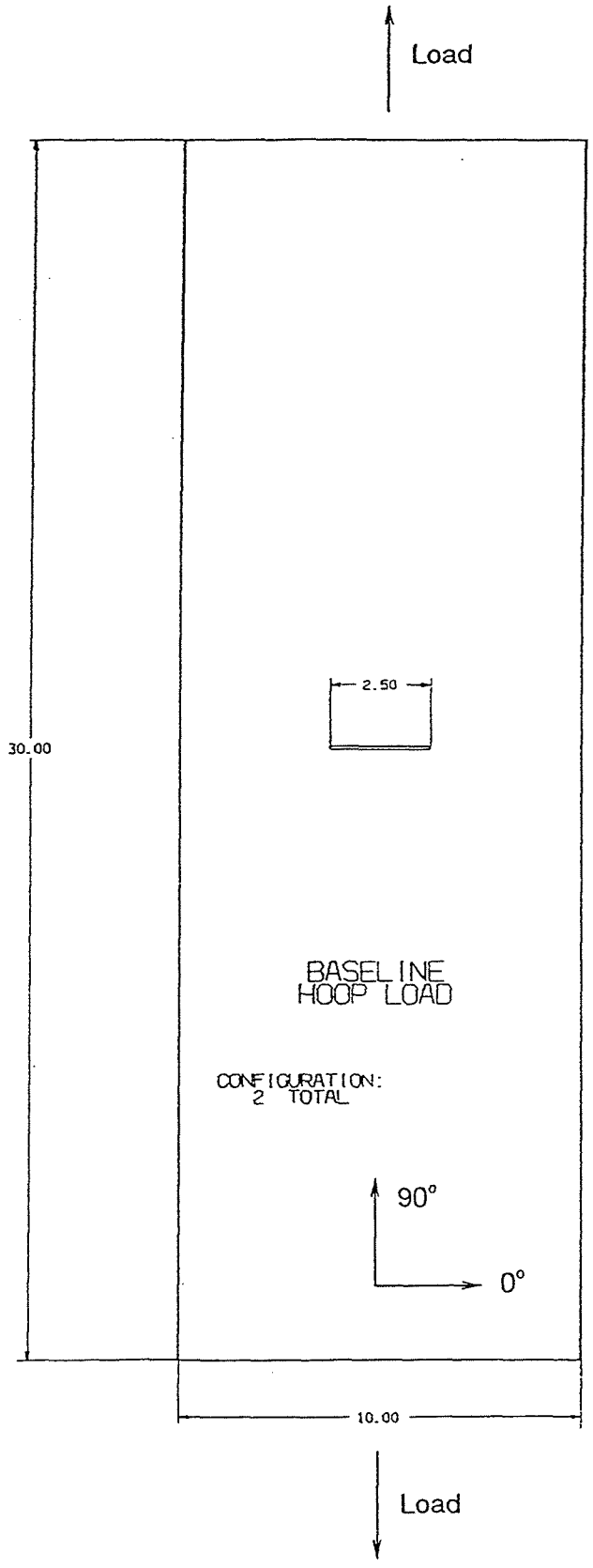

Figure A2-1: Test Coupon with No Repair

Table A2-2: Elastic Properties of Patch Materials

Material	E_1 (psi)	E_2 (psi)	G_{12} (psi)	ν_{12}
GR/EP	19.2×10^6	1.36×10^6	0.72×10^6	0.32
GL/EP	3.5×10^6	3.2×10^6	0.80×10^6	0.20
Titanium	16.5×10^6	16.5x106	6.99×10^6	0.18

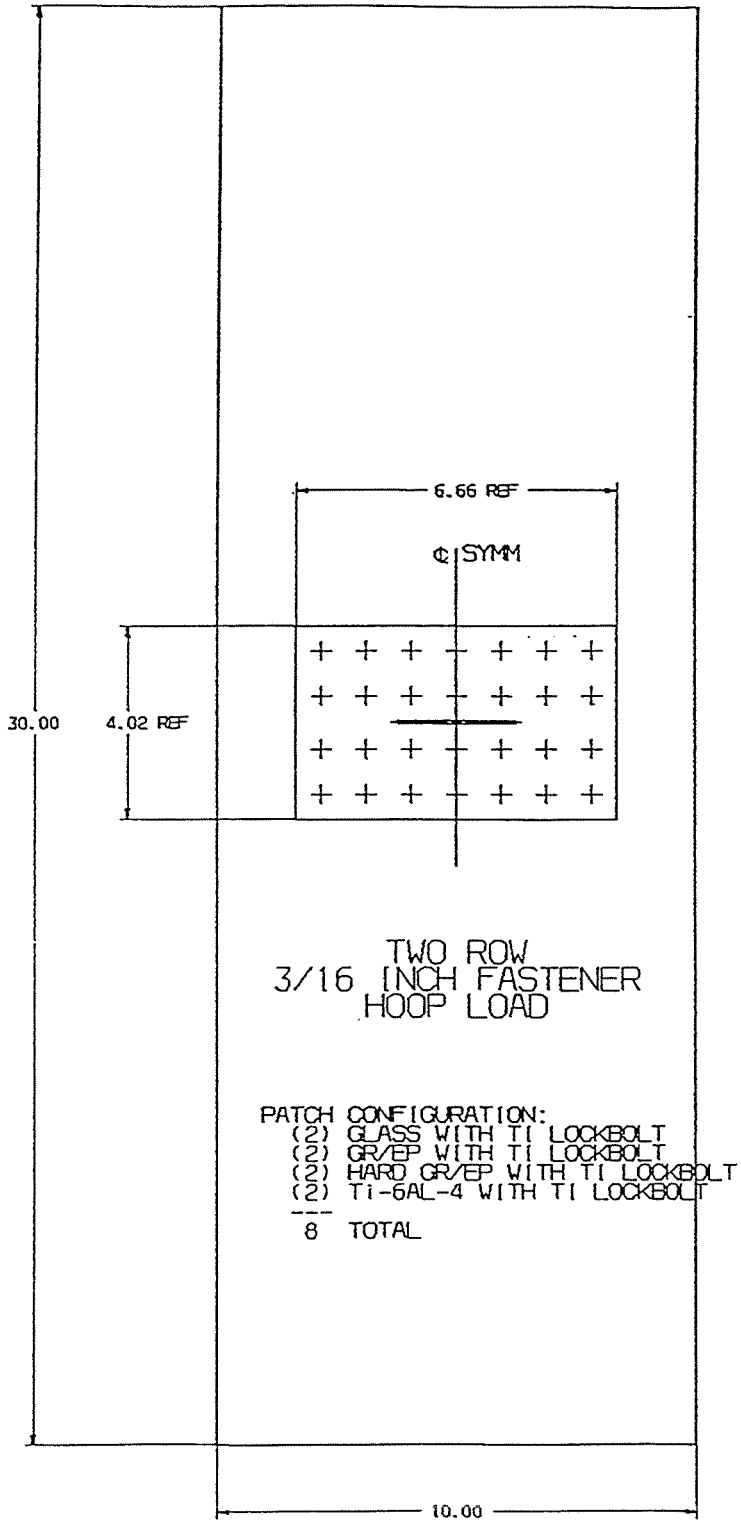

Figure A2-2: Repaired Coupon Cases 1 through 4

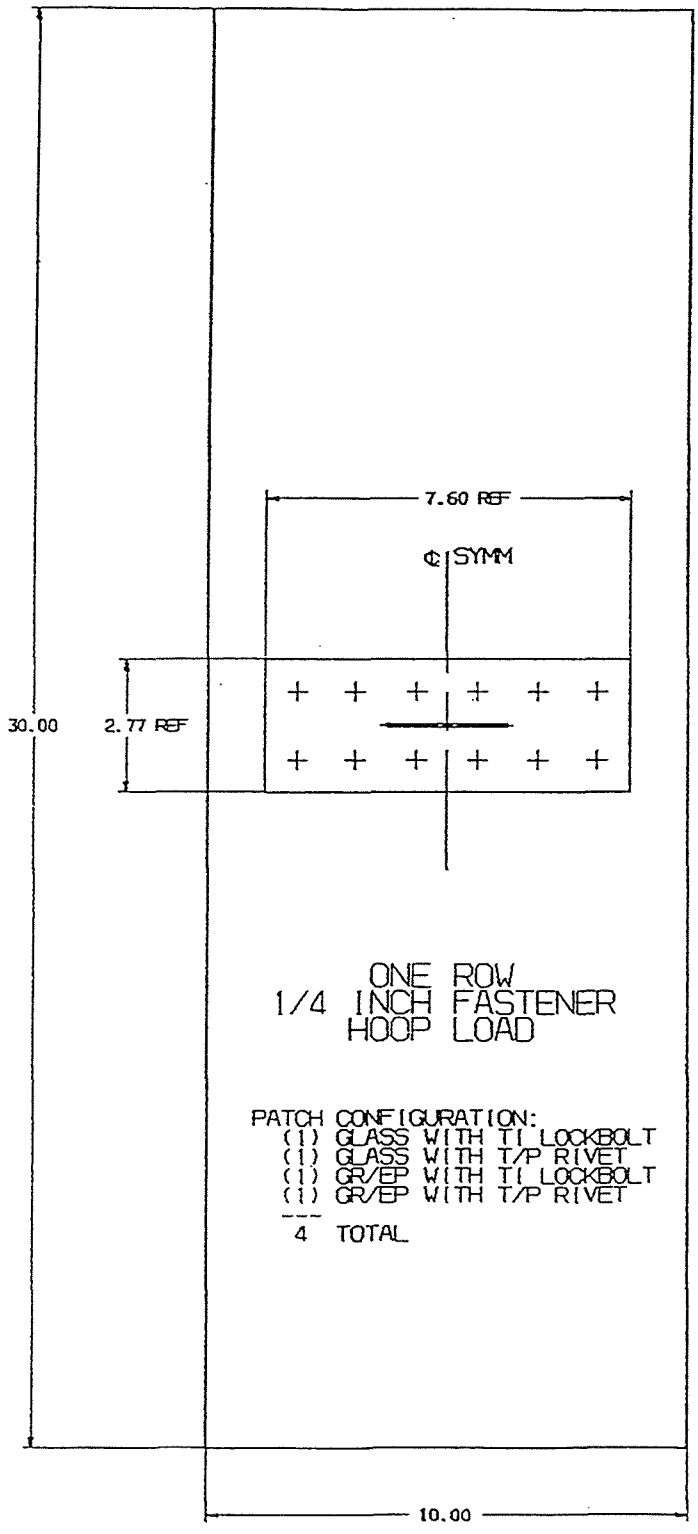

Figure A2-3: Repaired Coupon Cases 5 through 8

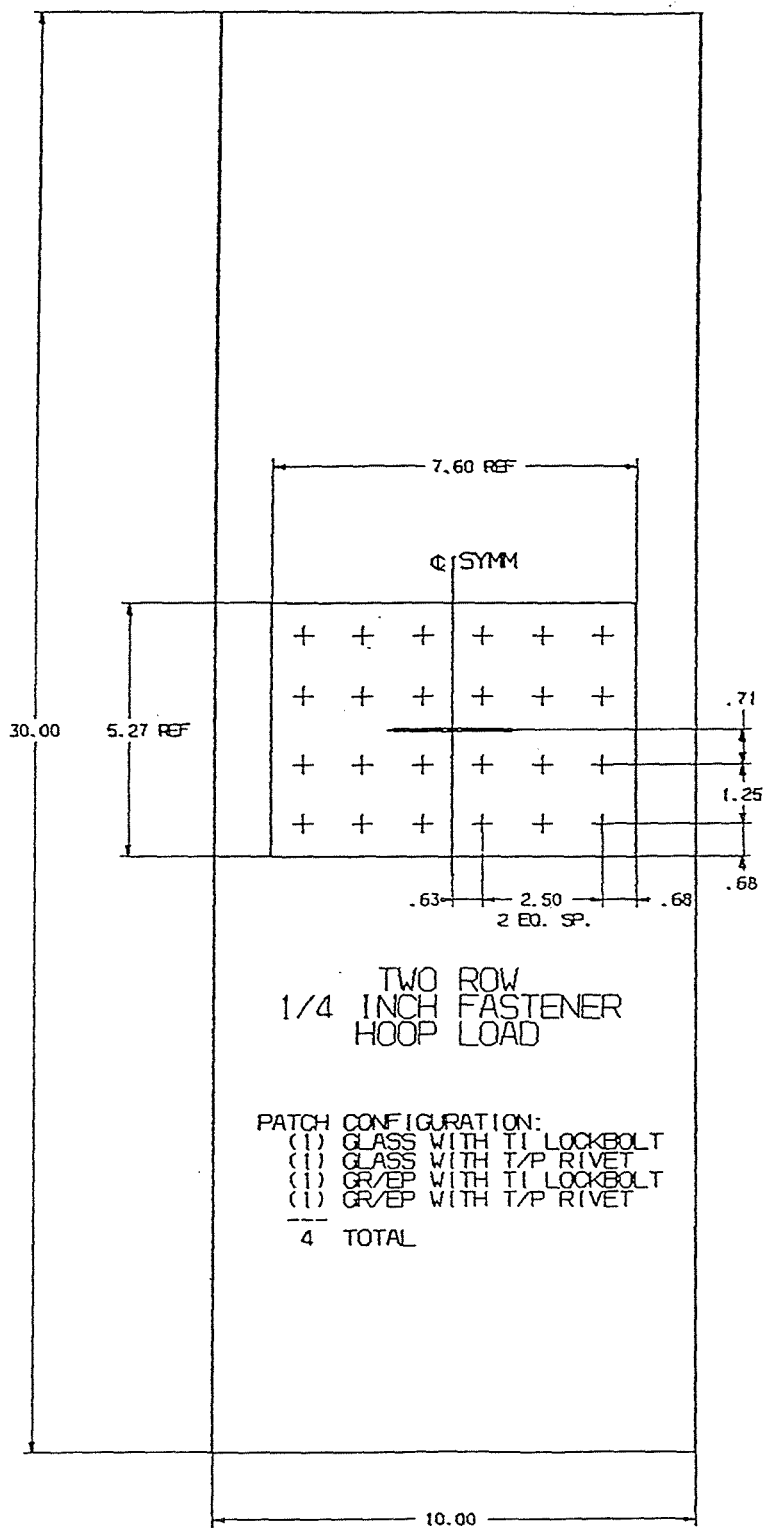

Figure A2-4: Repaired Coupon Cases 9 through 12

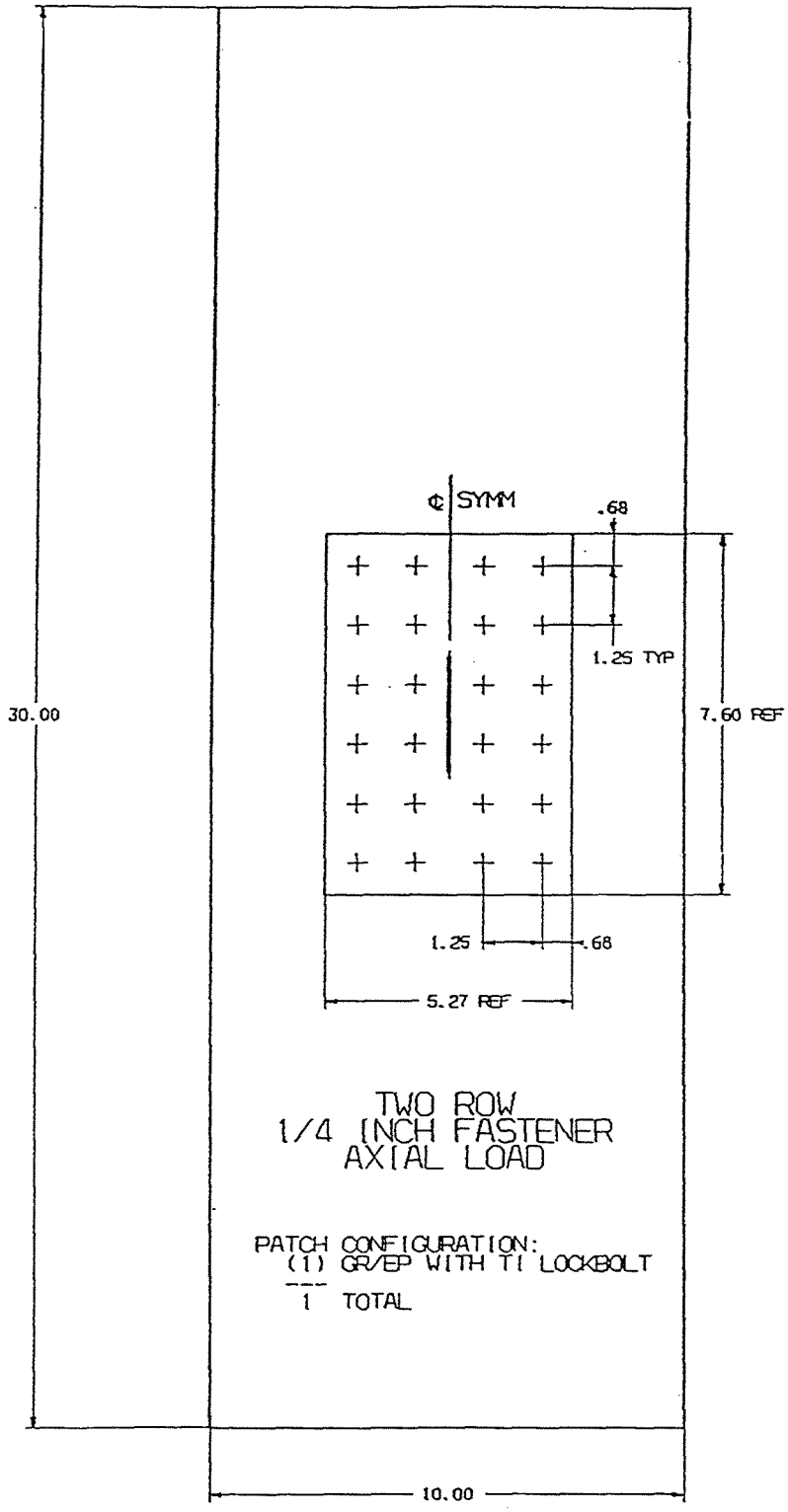

Figure A2-5: Repaired Coupon Case 13

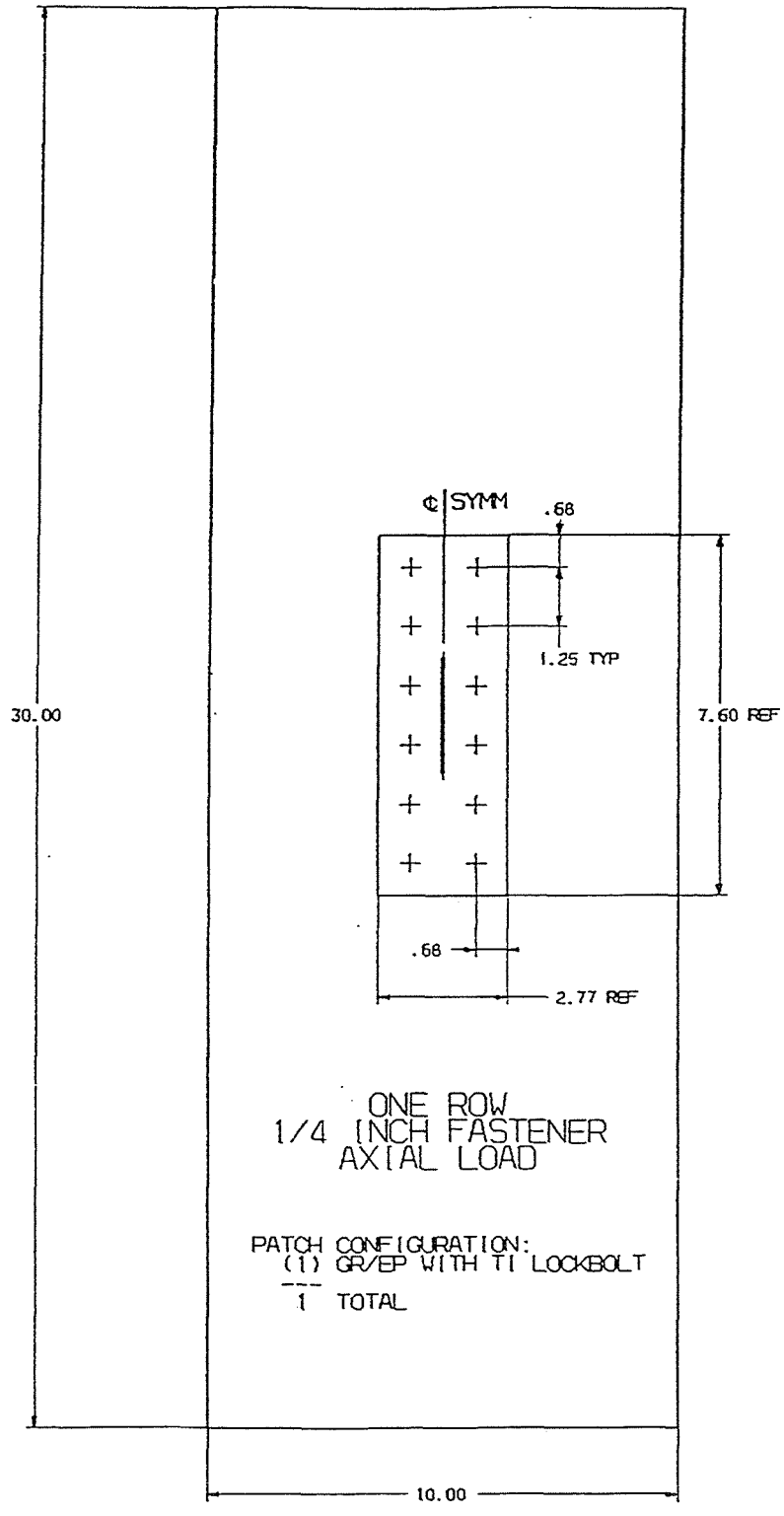

Figure A2-6: Repaired Coupon Case 14

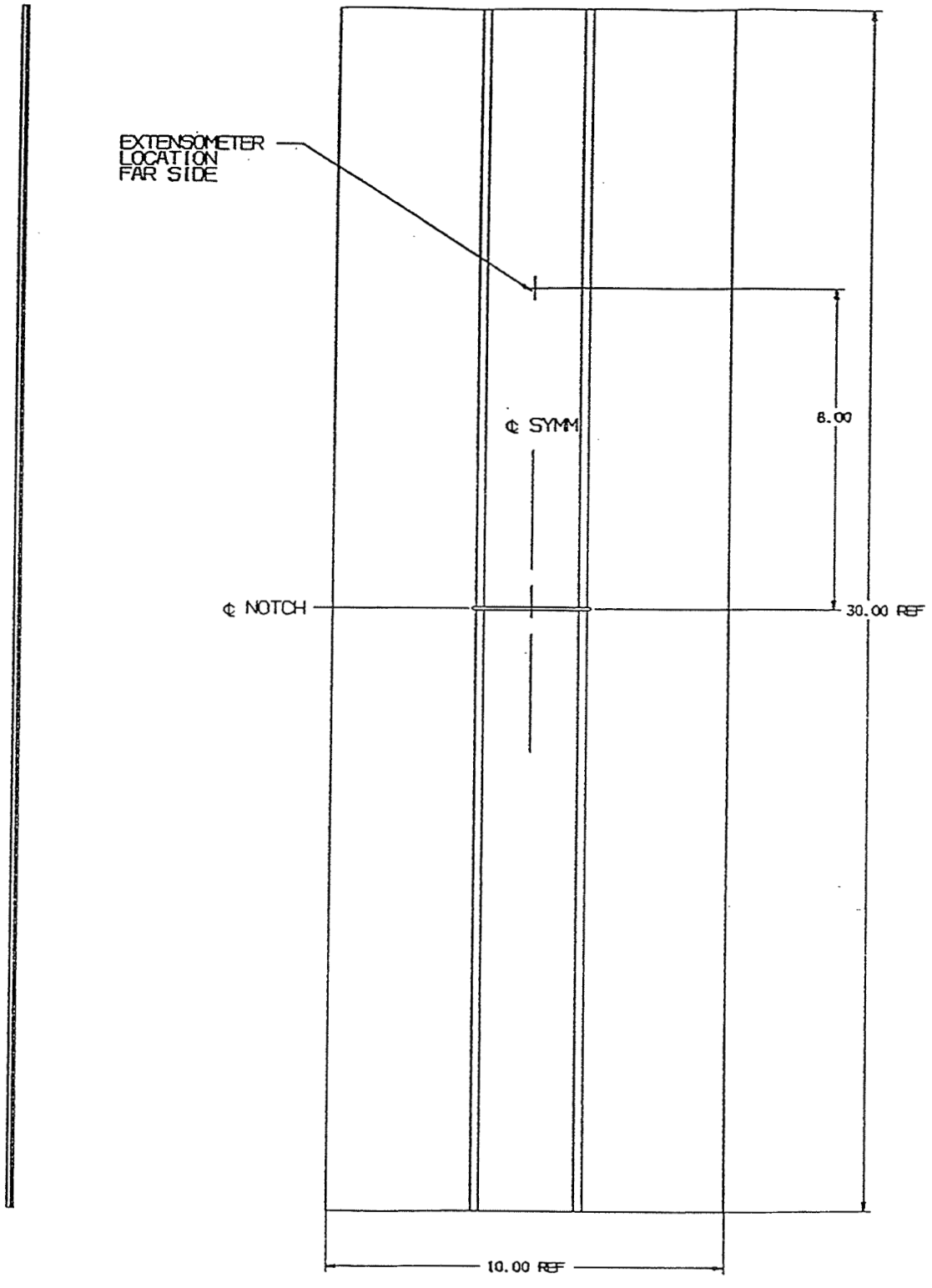

Figure A2-7: Repaired Coupon Case 15

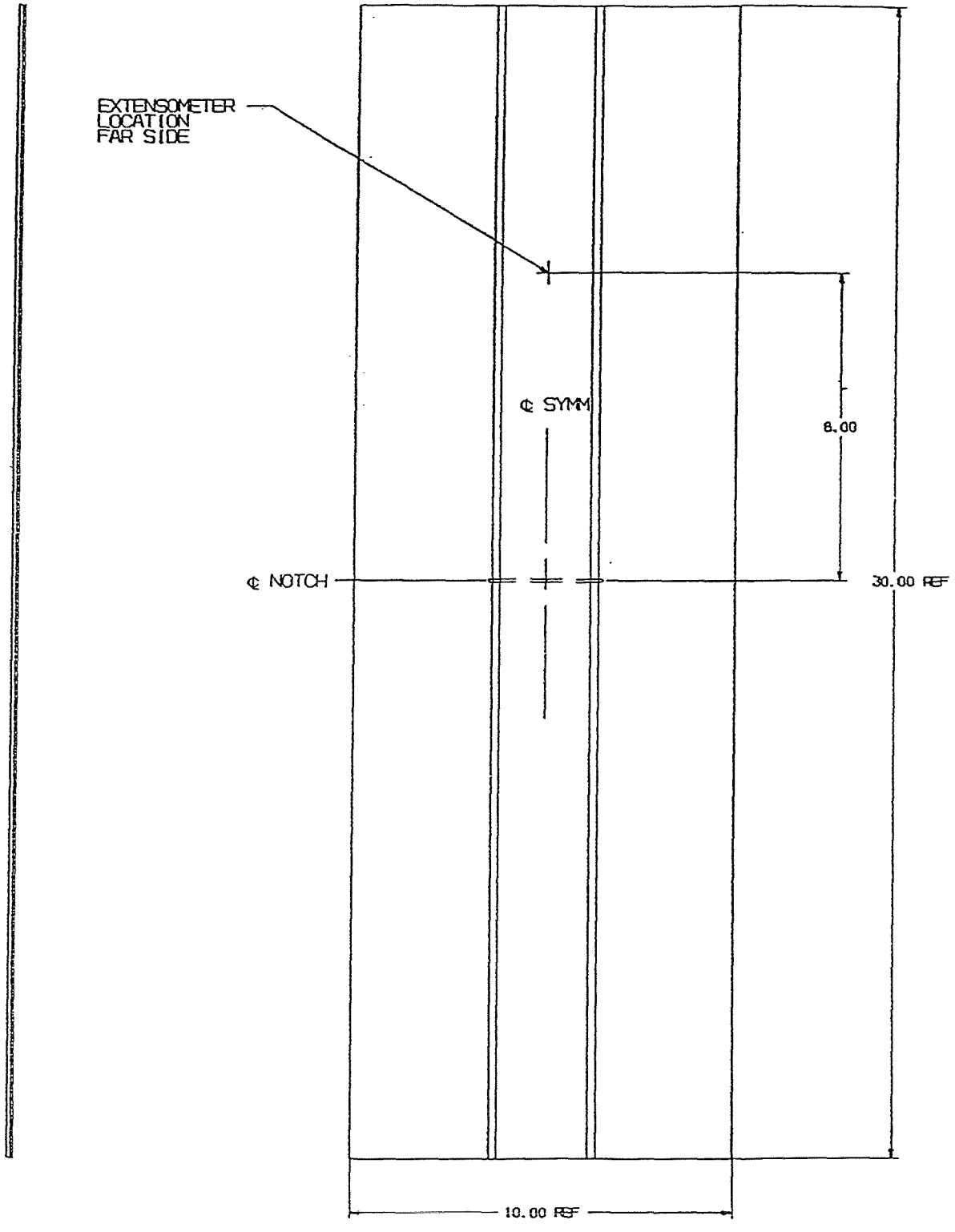

Figure A2-8: Repaired Coupon Case 16

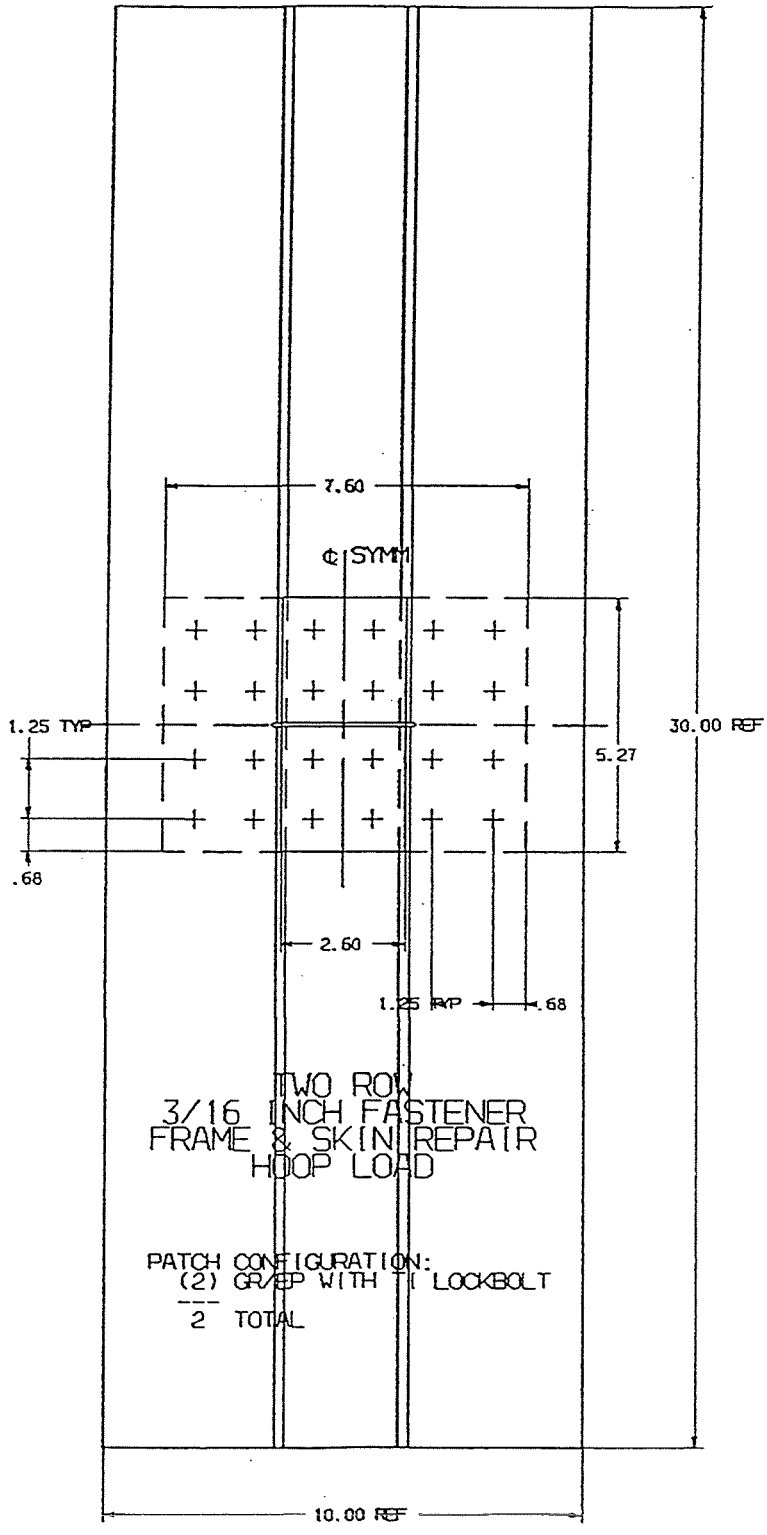

Figure A2-9: Repaired Coupon Case 17

elements was taken as the distance between the middle surface of the coupon and the middle surface of the patch. The ends of the beams were rigidly connected to the coupon and patch material. All material response was assumed to be elastic. The mesh for an unrepaired coupon is shown in Figure A2-10. A very dense mesh is used in the vicinity of the notch tip. To determine the adequacy of the mesh density, stresses near the crack tip were calculated and compared with the analytical solution with a finite width correction factor. Figure A2-11 shows that there is reasonably good agreement between the analytical and finite element solutions.

When the repaired coupon is loaded, there are two possible failure modes. One is propagation of the 2.5"-long notch. The other is bearing stress/bypass strain failure at the bolt hole in the coupon. The Whitney-Nuismer (1974) point stress criterion with a critical stress of 130,300 psi at a characteristic distance of 0.0654" was used to predict notch failure. The bearing/bypass failure curves for Cases 13 and 14 are given in Figure A2-12 and the remaining cases in Figure A2-13. The strains at the locations of the strain gages were calculated as functions of load. As will be discussed in the next subsection, it was necessary to perform a nonlinear analysis that took into account large deflections in the finite element calculations. Thus, load versus strain curves are not necessarily linear. The load required for failure was also calculated.

A2.1.3 Comparison of Theory and Experiment

Plots of the measured and predicted strains as functions of load were generated for all of the coupons. The agreement between theory and experiment ranged from fair to excellent. In this subsection we will focus on just a few representative cases. The strain gage locations for Case 7 are shown in Figure A2-14. The measured and predicted strains for gages 5 and 13, which are closest to the notch tip, are shown in Figure A2-15. Both linear and nonlinear (large deflection) analyses were performed. It is clear from the figure that large deflection effects are significant, and the large deflection solution is in considerably better agreement with experimental results than the linear solution. This apparently occurs because the out-of-plane displacements caused by the eccentric load path through the patch produce a restoring moment that reduces the total amount of bending. Because of this significant effect, large deflections were taken into account in all of the calculations.

The predicted (nonlinear analysis) and measured strains for several gages in Case 7 are shown in Figures A2-16 and A2-17. The agreement between theoretical and experimental results is good for these gages. An example of only fair agreement between theory and experiment is shown in Figure A2-18 which comes from Case 2. Gage 11 is located on the coupon 1.25" from the crack tip. Gage 5 is in a similar location but on the patch. From the figure it can be seen that the measured strain on the patch is lower than predicted. Thus, the load transmitted through the patch is lower than predicted. This might have resulted from an unusually large gap between the bolt and the hole coupled with low friction between the patch and the coupon. Neither bolt/hole gap nor coupon/patch friction are accounted for in the finite element model.

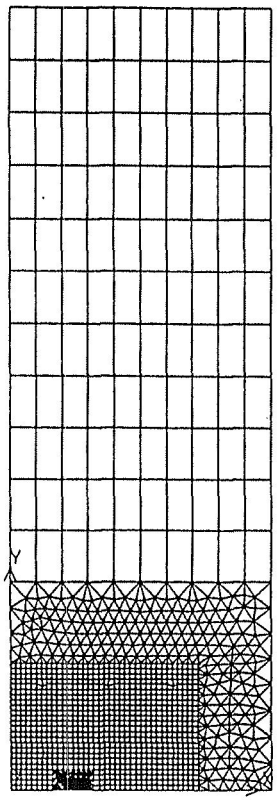

a) full mesh

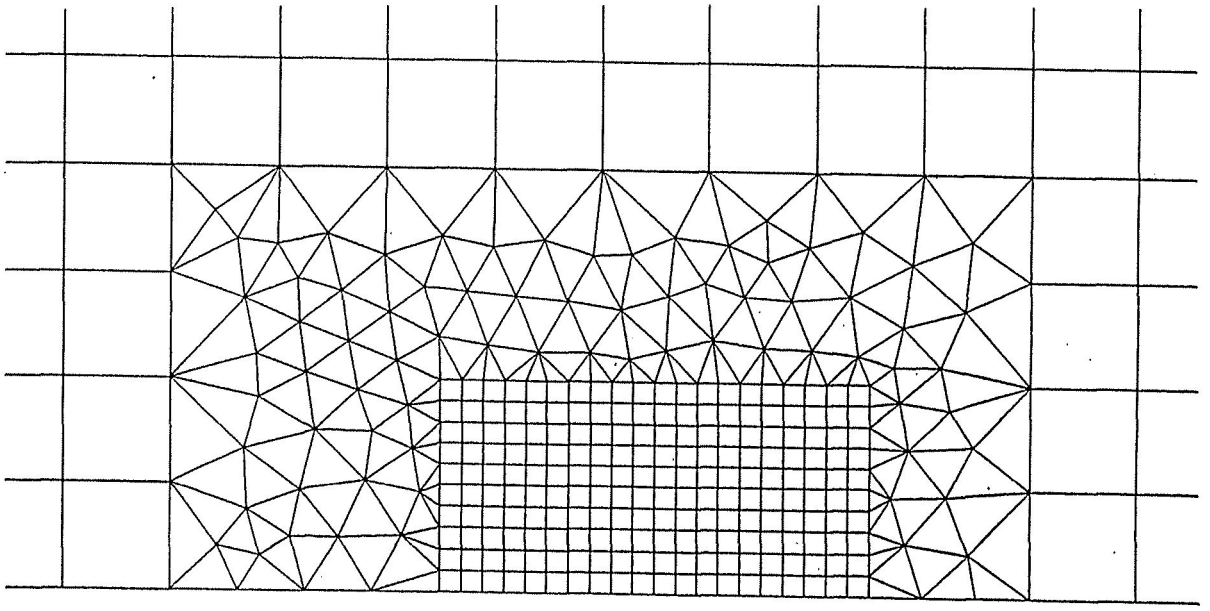

b) enlarged view of the mesh near the crack tip

Figure A2-10: Finite Element Mesh for Unrepaired Coupon

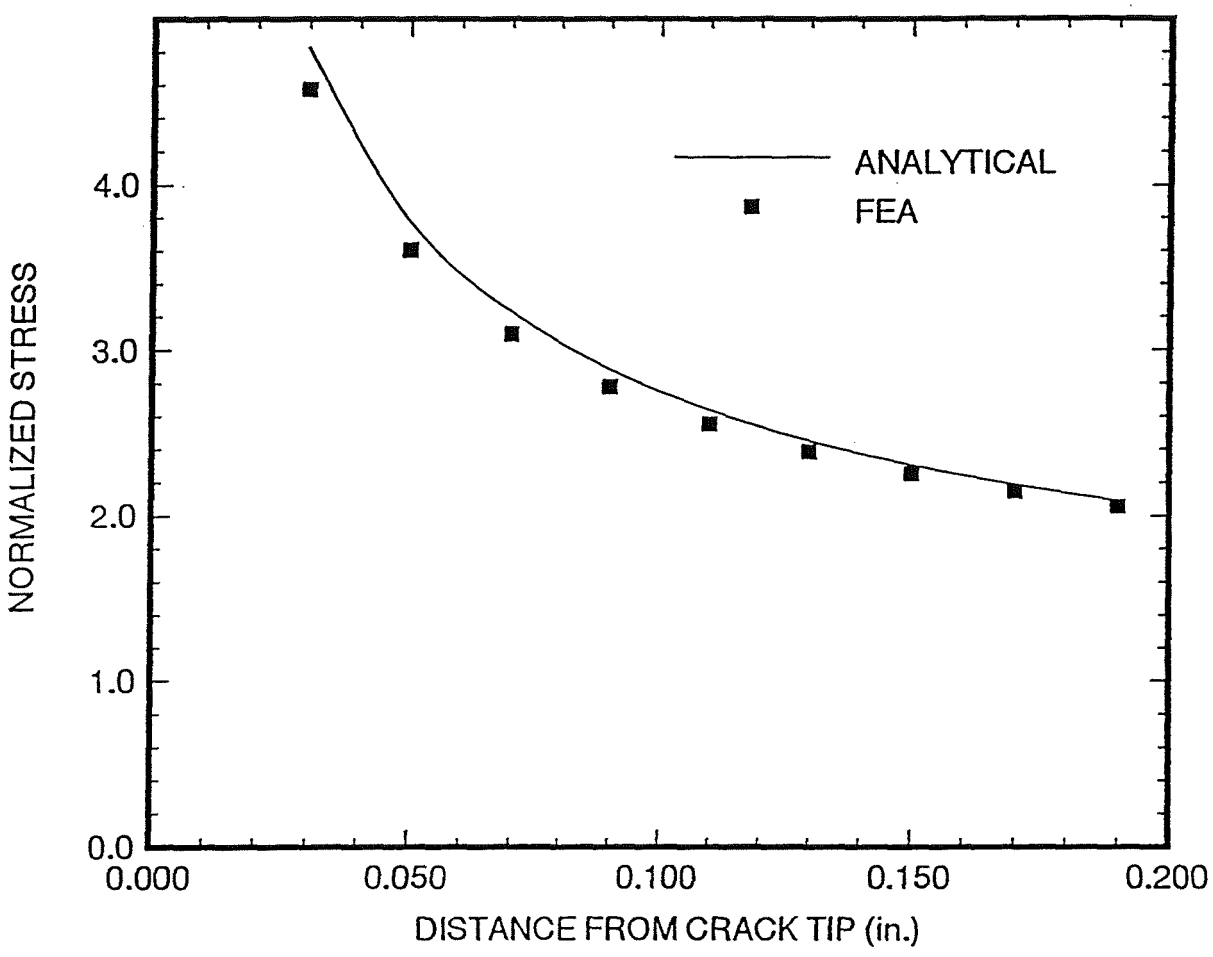

Figure A2-11: Comparison of Analytical and Finite Element Analysis (FEA) Results for an Unrepaired Coupon

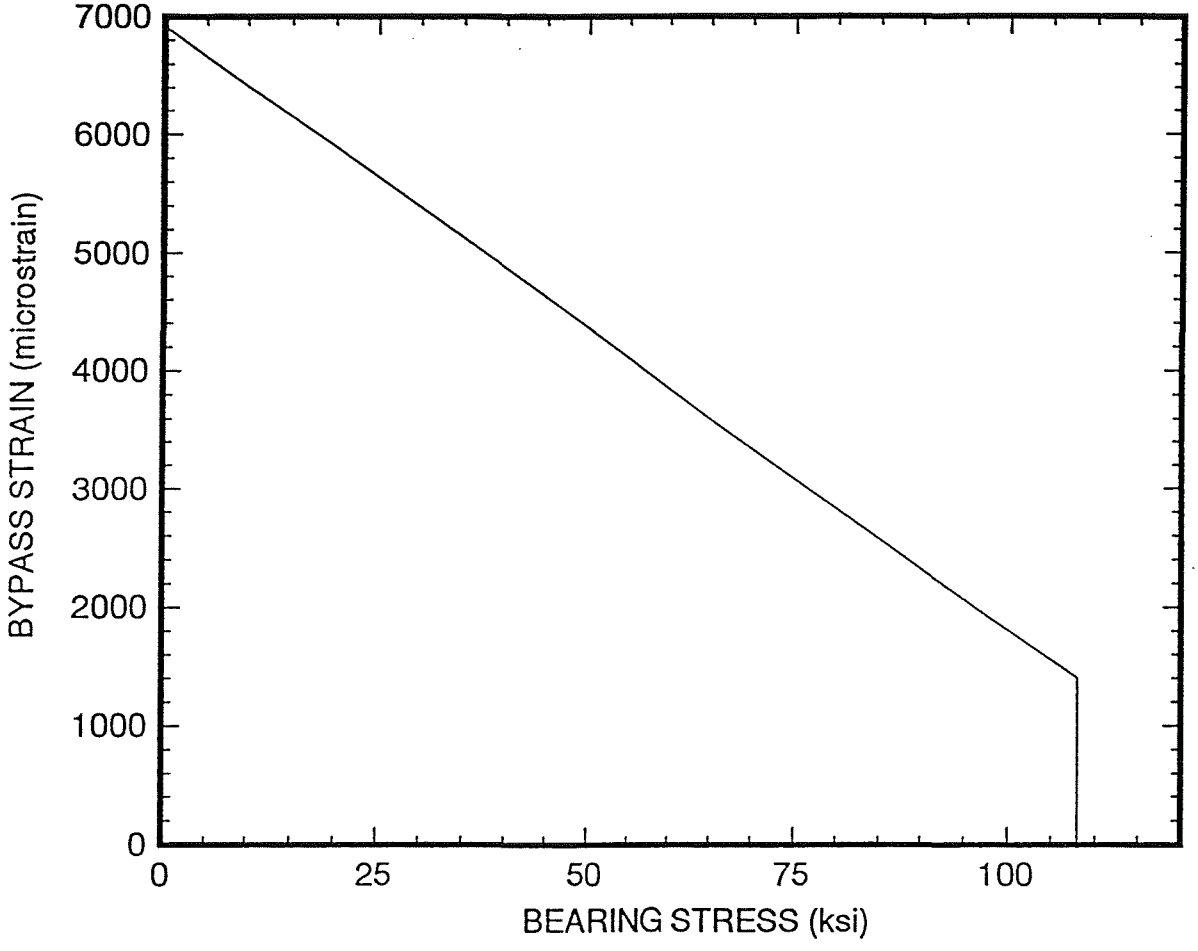

Figure A2-12: Bearing Stress/Bypass Strain Failure Curves for Cases 13 and 14

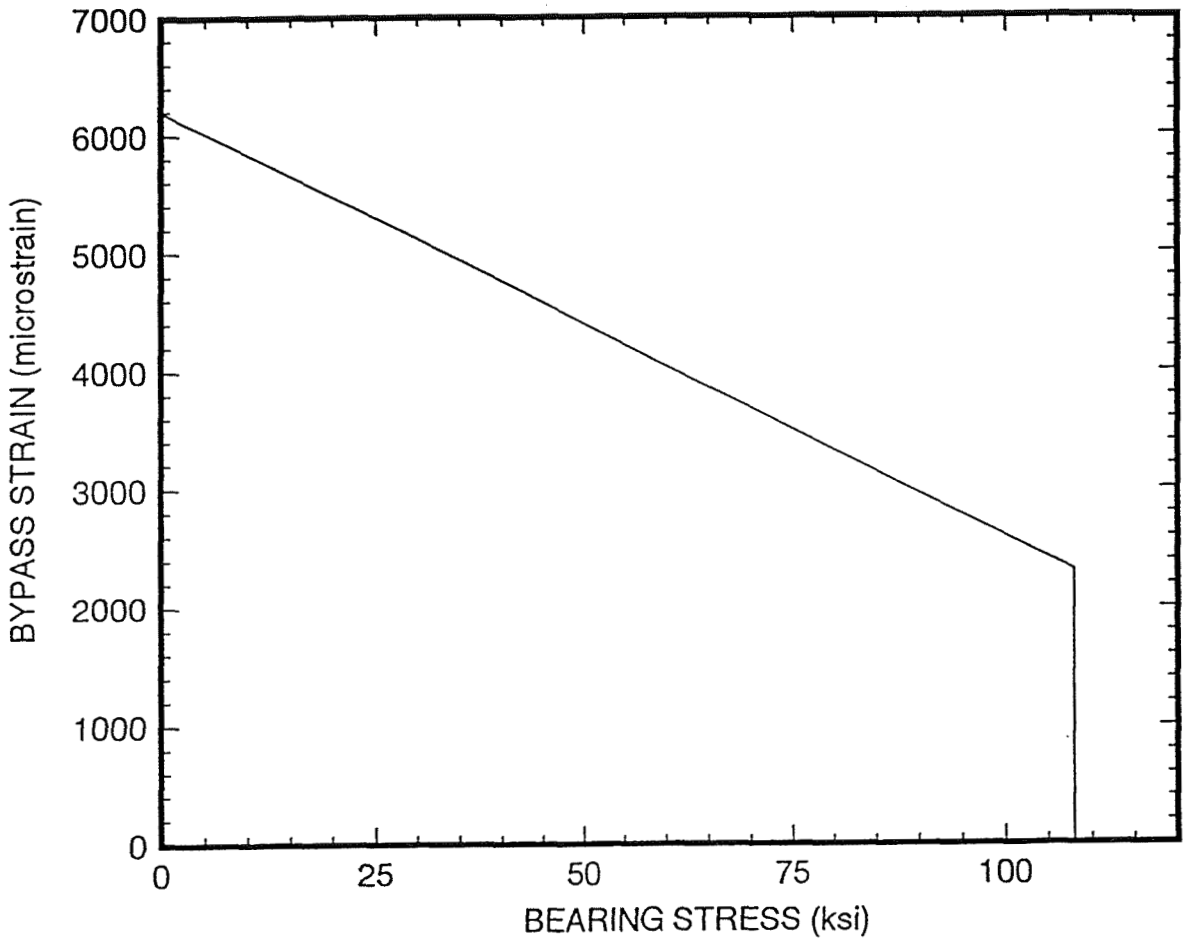

Figure A2-13: Bearing Stress/Bypass Strain Failure Curves for Cases 1-12 and 15-17

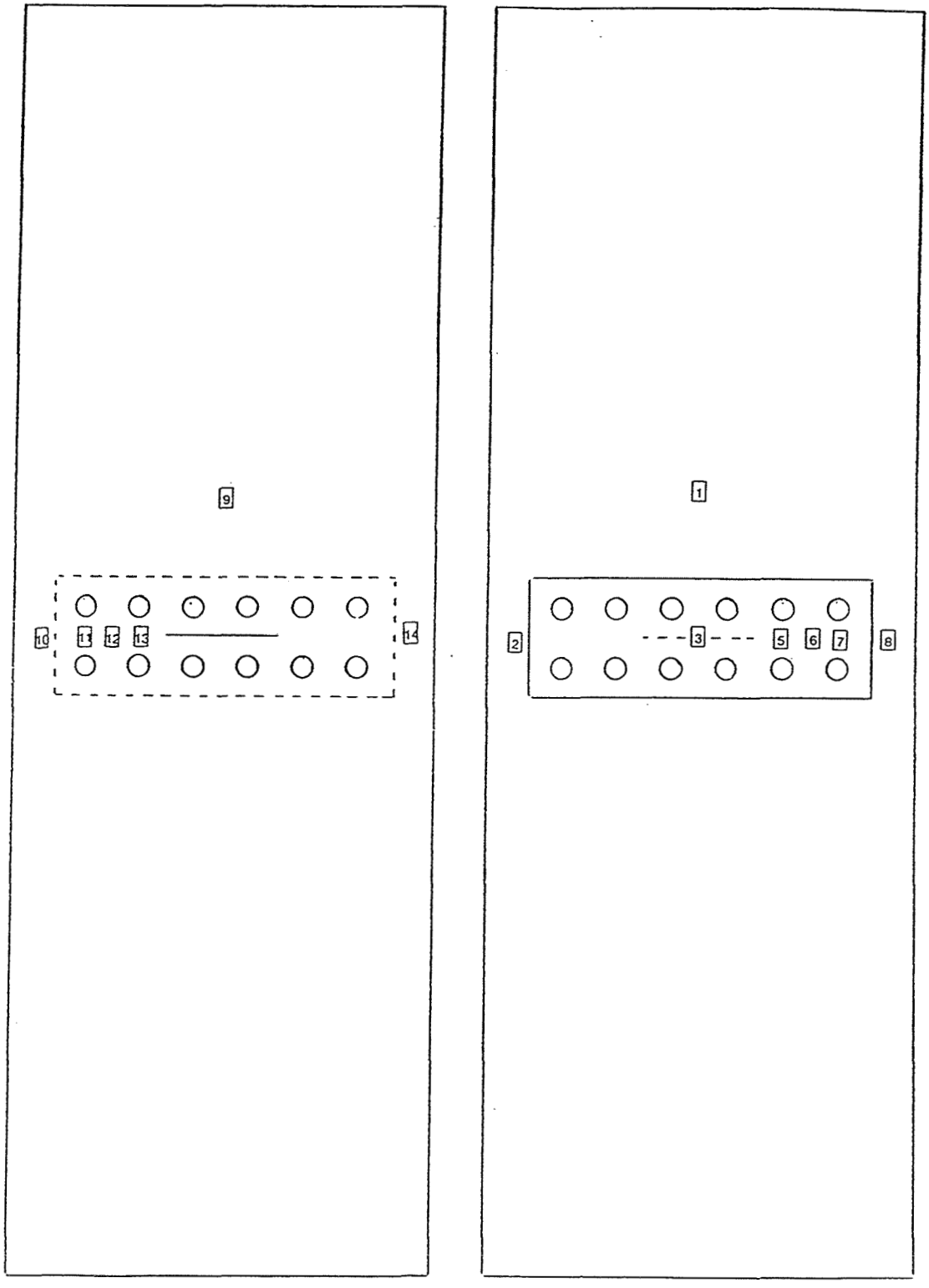

Figure A2-14: Strain Gage Locations for Case 7

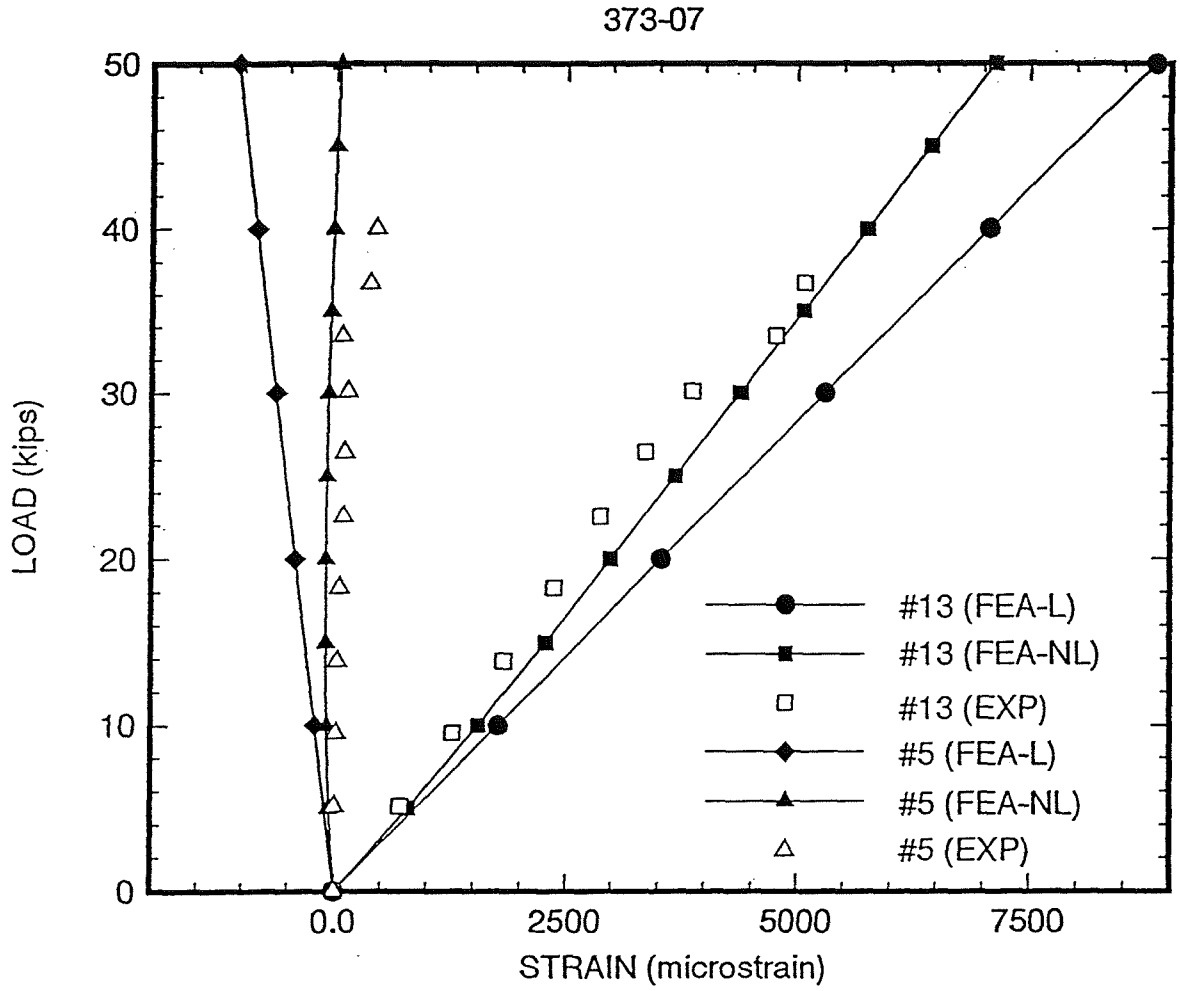

Figure A2-15: Comparison of Linear (FEA-L) and Nonlinear (FEA-NL) Theoretical Results with Experimental (EXP) Results for Gages #13 and #5 for Case 7

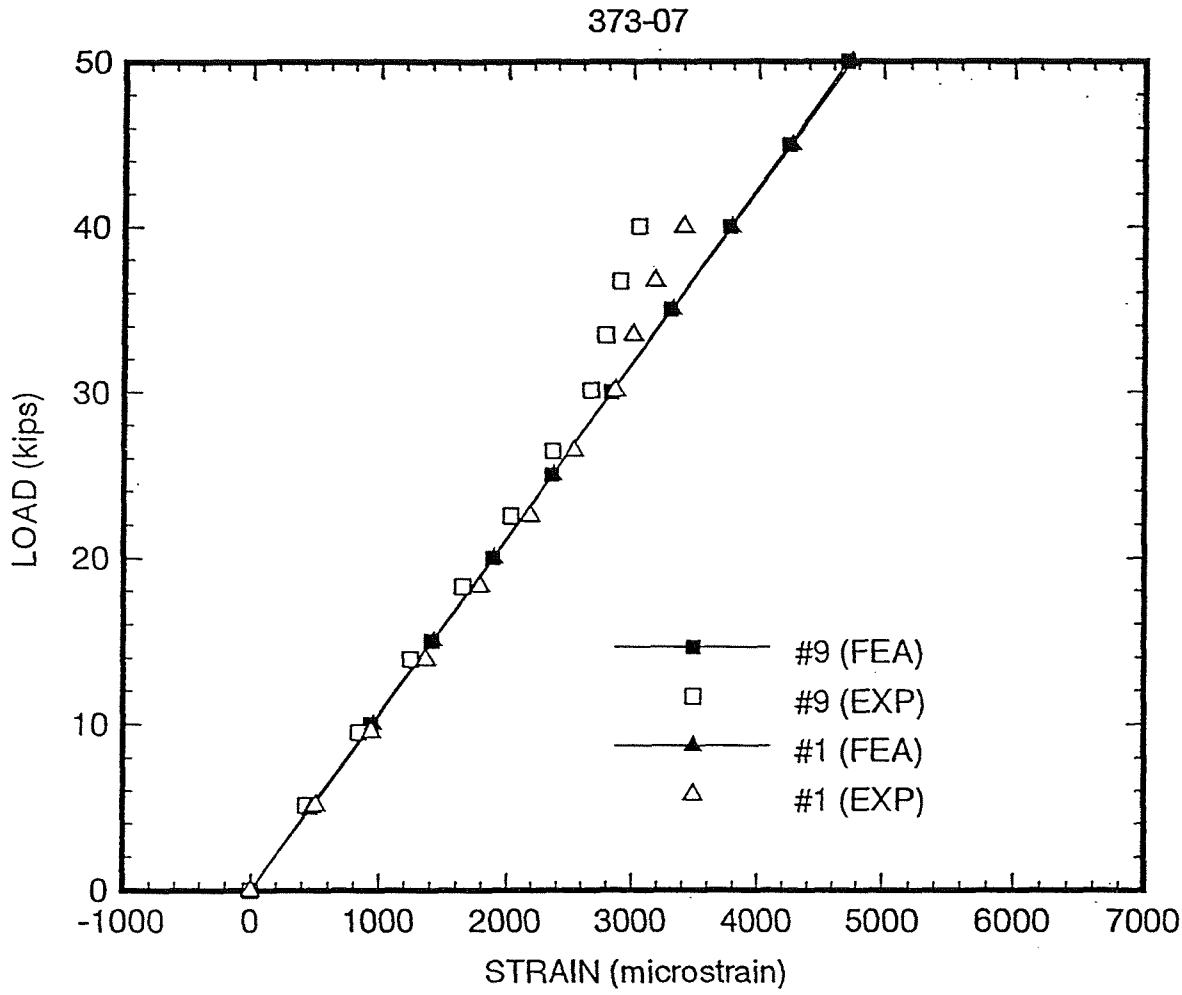

Figure A2-16: Comparison of Nonlinear Finite Element Analysis Predictions (FEA) and Experimental Results (EXP) for Gages #1 and #9 for Case 7

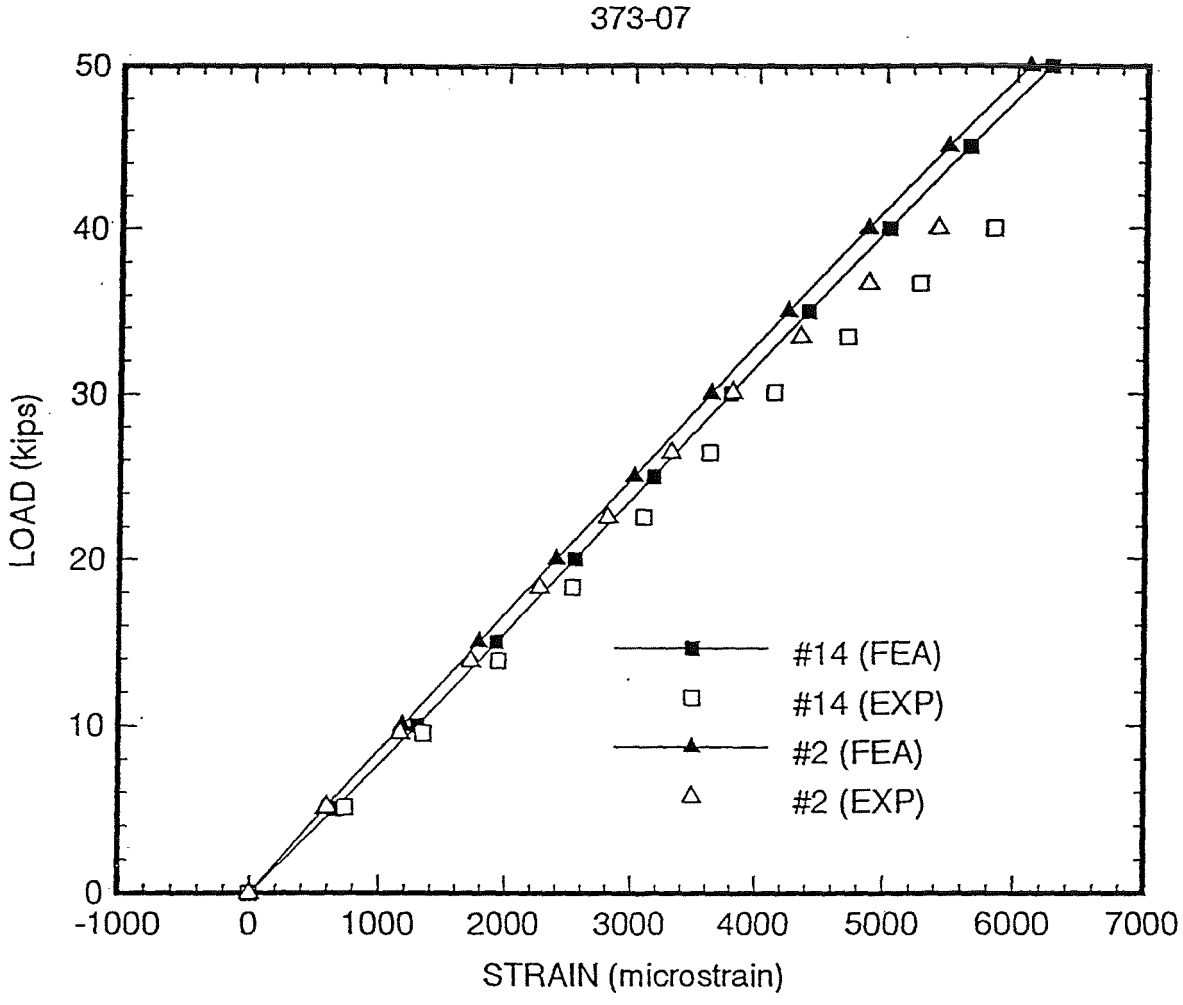

Figure A2-17: Comparison of Nonlinear Finite Element Analysis Predictions (FEA) and Experimental Results (EXP) for Gages #2 and #14 for Case 7

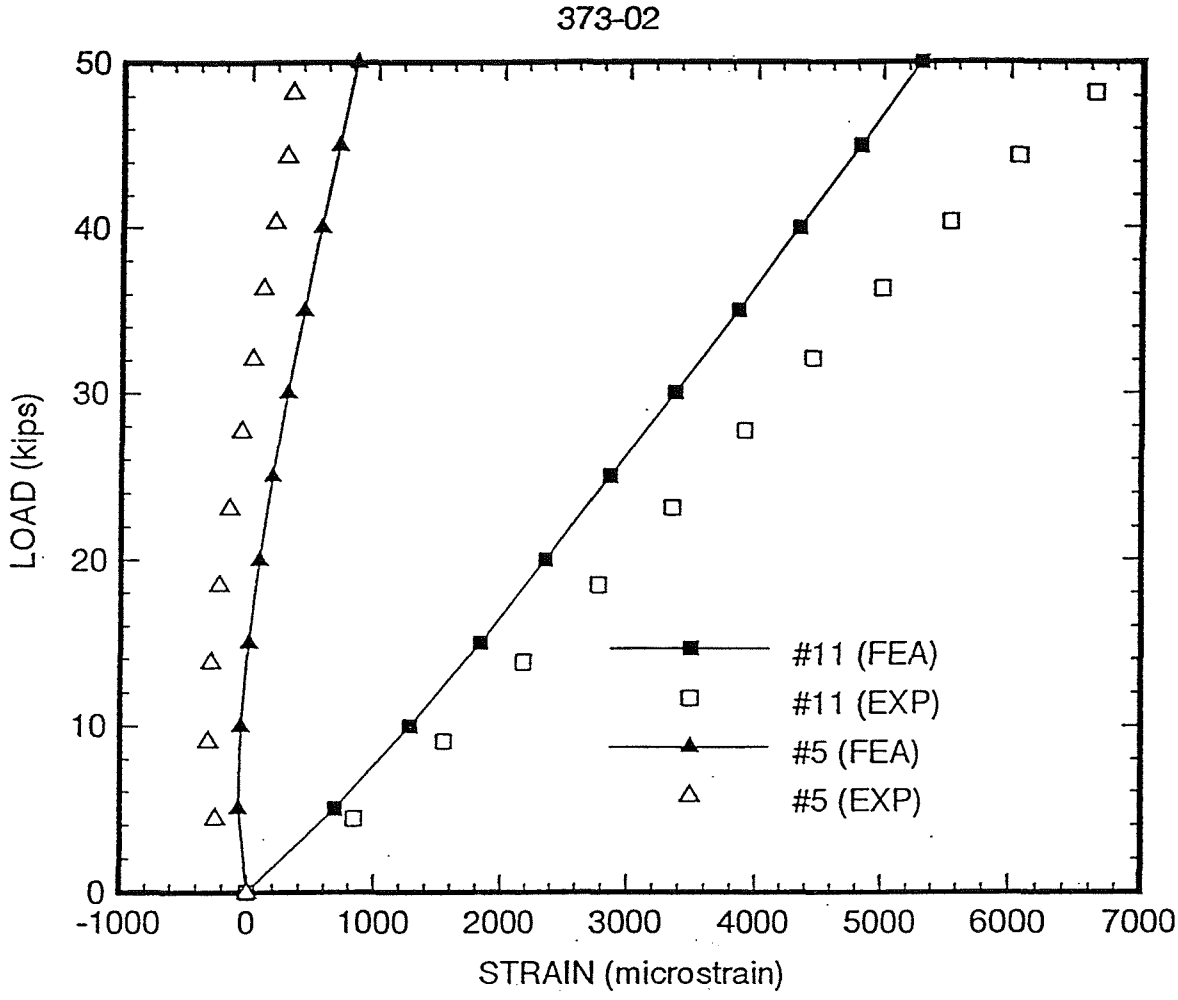

Figure A2-18: Comparison of Nonlinear Finite Element Analysis Predictions (FEA) and Experimental Results (EXP) for Gages #5 and #11 for Case 2

The predicted and measured (averaged if more than one test is performed for a case) failure loads for each coupon are listed in Table A2-1. The origin of failure is also indicated with either a "B" for bearing/bypass failure or an "N" for notch failure. The predicted and measured failure loads for an unrepaired coupon were 38,200 lb and 38,900 lb, respectively. All of the patches were effective in increasing the strength of the coupon. Before comparing the finite element predictions to the experimental results, it should be pointed out that the coupon used in Case 8 came from a defective panel, and its results are clearly not consistent with the rest of the data. Also, the part-through nature of the notch in Case 16 results in a complex three-dimensional phenomenon that the finite element analysis had no chance of properly modeling with shell elements. If Cases 8 and 16 are discarded, a comparison of predicted and measured results indicates an average difference of 12.4 percent.

In examining the failure loads, it can be seen that the agreement between theory and experiment was best for the 7.60" x 2.77" patches which contained only one row of fasteners above and below the notch. For the other cases there were two rows of fasteners above and below the notch, and the theory predictions of failure were less than the measured failure loads in all but one case. For all of these cases the theory predicted failure to originate at the fastener hole due to bearing stress/ bypass strain limitations. In actual fact, failure usually initiated at the notch tip. This would indicate that the bolt loads are actually more uniformly distributed throughout the fasteners than predicted. This could be the result of a materially nonlinear response of the coupon at the fastener hole. This type of nonlinearity was not accounted for in the finite element analysis.

An examination of the theoretically predicted failure loads does not indicate any particular trends regarding the effect of patch size, patch material, or fastener type. However, the experimental results indicate that large patches are more effective in raising the failure load than small ones and that titanium bolts are more effective than thermoplastic rivets. The experimental results do not indicate any particular trend regarding patch stiffness.

A2.2 Biaxial Loading Tests and Analysis

Biaxial loading tests and analysis were conducted to determine the effectiveness of analysis methods in predicting repair behavior under complex loading conditions. Also, such tests would provide further experience with the behavior of the tow-formed laminate in its role as fuselage skin. Finite element analysis was performed on the single repair and baseline no-repair specimens. Both linear and nonlinear (large-deflection) analyses were exercised. Analysis predictions were compared with test results. Details are given below.

A2.2.1 Test Specimens and Biaxial Tests

Both repaired and unrepaired tests were conducted upon a notched flat specimen of crucifix configuration (40 in. x 40 in.). The repaired version is shown in Figures A2-19 and A2-20. The center circular region of the specimen consists of the 13-ply graphite/epoxy-tow laminate utilized as fuselage skin. It is also the same as that defined,

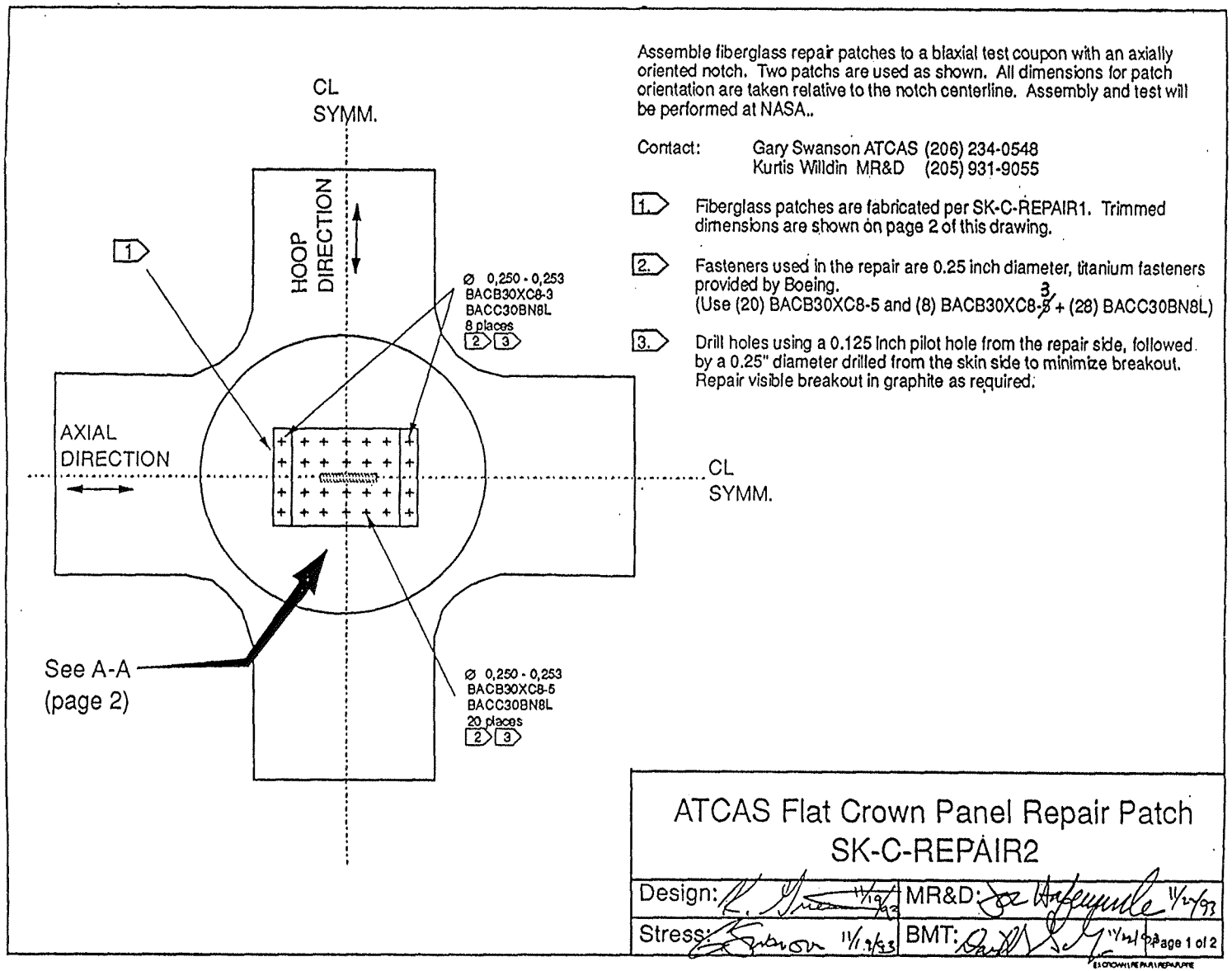

Figure A2-19: Repaired Biaxial Test Specimen

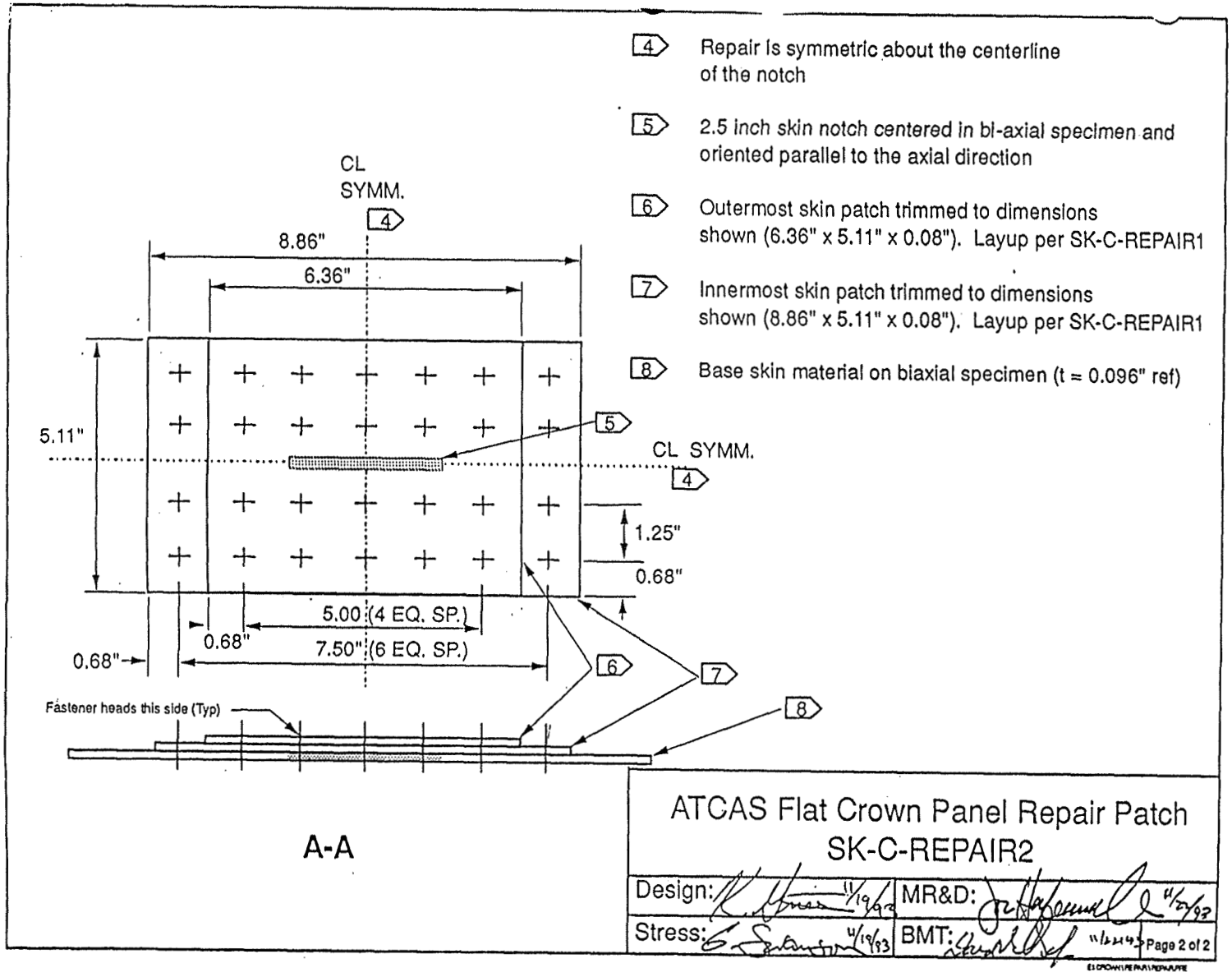

Figure A2-20: Repaired Biaxial Test Specimen

tested uniaxially, and reported upon in the previous section. Outside of the repair region, doublers were bonded to the specimen. Within the specimen test region, a 2.5-inch notch was cut. The notch was aligned parallel to the laminate's axial fuselage direction.

A two-tiered patch configuration was bolted to one side of the specimen over the specimen notch area using titanium protruding head fasteners. The patching consisted of the same glass/epoxy fabric as that incorporated in the uniaxial repair tests but of 8 ply quasi-isotropic layup of 0.08 inch thicknesses. The axial ends of the patches were staggered with the cover (top) patch set back from that of the base (bottom) patch. The bi-level repair configuration was expected to improve the bearing/bypass strength of the critical leading axial row of fasteners.

An unrepaired specimen was tested under biaxial load. As identified in Table A2-3, the ratio of hoop directed load to axial load was 1.19. Also, the specimen ultimately failed due to fracture at the notch-tip as desired. The specimen was instrumented with strain gages at various locations including a series ahead of the notch tip. For brevity, the test instrumentation data has not been included in this report.

A repaired specimen was tested under a series of four load conditions as indicated in Table A2-4. The final two test runs were truly biaxial and reflected the two critical load conditions representative of fuselage crown structure. As indicated the test specimen was loaded to failure in the fourth test run. Its ratio of hoop to axial loading of 0.52 represented the most critical fuselage crown condition and is representative of an ultimate high-g maneuver. The repair specimen was instrumented with strain gages. Final load levels for test runs 1 through 3 were controlled by limits set for certain strain gage combinations. For the first run, the average axial strain ahead of the patch (back-to-back gages #24 and #45) was to be limited to 2000 microstrains. For the second and third test runs, the hoop strain ahead of the notch (gage #0) was to be limited to 3000 microstrain.

A2.2.2 Finite Element Analysis of Specimens under Biaxial Loading

A finite element model was constructed for use in subsequent small and large deflection (nonlinear) analysis. The model for the repaired specimen is shown in an expanded display in Figure A2-21. As evident in the figure, only one quarter of the specimen was modeled, taking loading and geometry symmetry into consideration. Model specifics such as code, element types and material properties are the same as those used in the uniaxial repair analysis an discussed in Section A2.1.2. Stiffness properties of the graphite/epoxy tow were an exception in that a slightly greater ply stiffness was used. The ply properties were: E_{11} = 19.8E6 psi, E_{22} = 1.37E6 psi, G_{12} = 0.68E6 psi, and ν_{12} = 0.321. The specimen, base patch, and cover patch were modeled independently and joined by beam elements representing the fasteners. The mesh densities within the patch region and about the notch-tip are indicated in the figure. The patch area element size (0.125"x0.125") enabled a density of 10 elements between fasteners which was judged more than adequate. The notch-tip element size (0.02"x0.02") was the same used in the uniaxial repair analysis, and its rationale was discussed in Section A2.1.2.

Table A2-3: Unrepaired Biaxial Test Summary

Test Run No.	Loading P_{hoop}/P_{axial}	Result
1	1.19	Notch Fracture

Table A2-4: Repaired Biaxial Test Summary

Test Run No.	Loading P_{hoop}/P_{axial}	Result
1	P_{axial} only	No damage $P_{axial\ peak}$=15,000 lbs
2	P_{hoop} only	No damage $P_{hoop\ peak}$=10,700 lbs
3	1.19	NO damage $P_{hoop\ peak}$=12,750 lbs
4	0.52	Failure at specimen edge round-out, away from repair $P_{axial\ peak}$=79,500 lbs

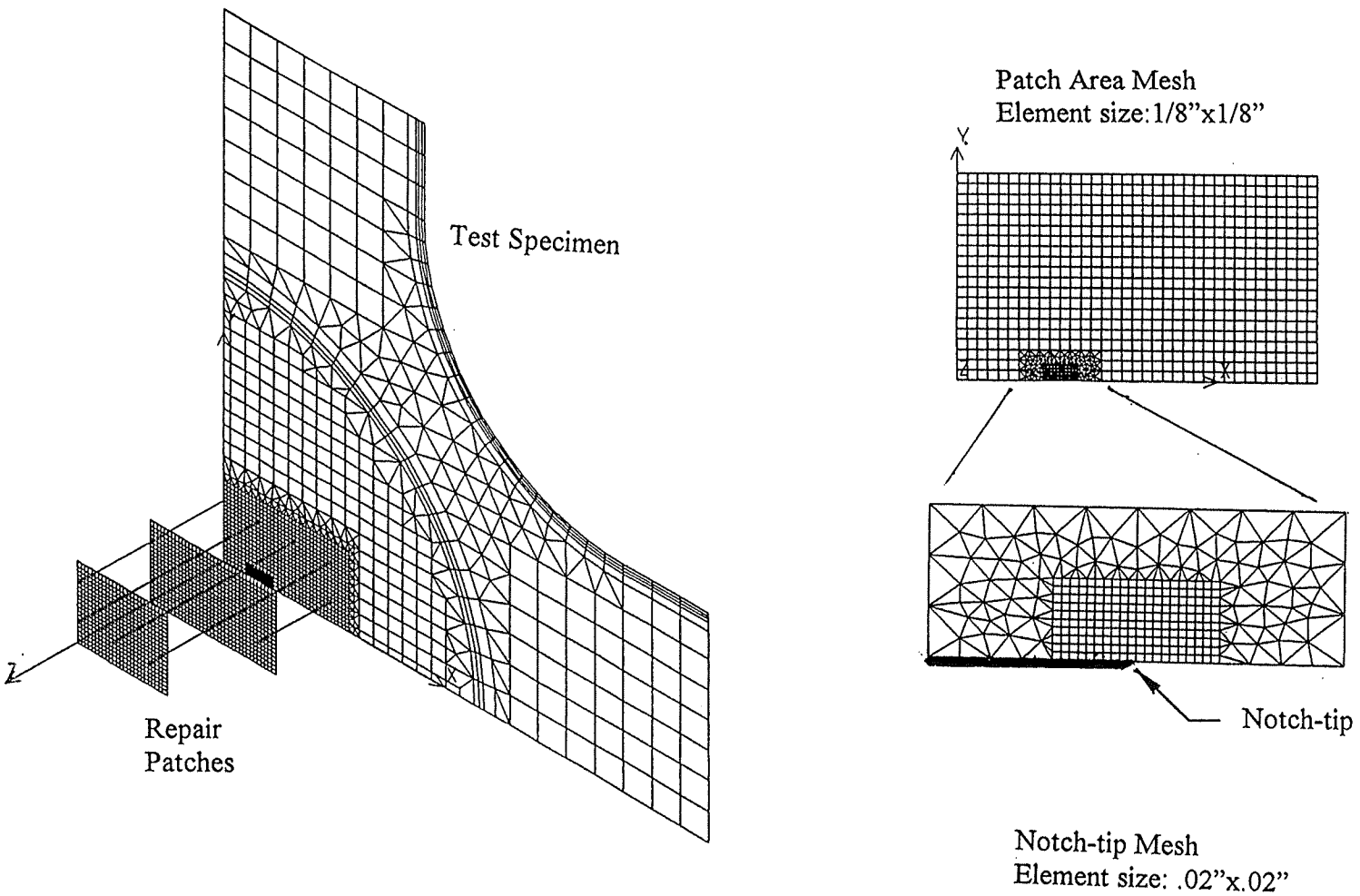

Figure A2-21: Finite Element Model for Repaired Specimen

Analysis of the unrepaired specimen was based on small deflection analysis. Nonlinear analysis would not produce results significantly different since no one-sided patch existed to create unbalanced stiffness and resultant large deflection behavior. Two possible failure modes were identified for the specimen, i.e. notch fracture and peak strain failure along the large radius round-out edge between the axial and hoop legs of the specimen. Notch fracture analysis employed the Whitney-Nuismer point stress failure criteria as discussed in Section A2.1.2. Peak strain analysis attempted to address maximum strain realized away from the notch and due to any strain concentration and/or flexure. Peak failure strains were extracted from the ATCAS Side Quadrant Material Property Design Data. A 15 percent B-basis knockdown from coupon failure loads was assumed for the allowables therein, and thus peak failure strains were factored up a corresponding amount. It is stressed that the 15 percent value was assumed as reasonable based upon other composite strength studies but could well be otherwise. Resultant peak failure strains of 8670 and 7640 microstrain were thus derived for the axial and hoop laminate directions respectively.

Nonlinear analysis of the repaired specimen was made necessary because the patching created an imbalance of in-plane stiffness. When in-plane loads are applied, the combined repair section of patch and specimen attempts to align itself with that of the applied load as shown in Figure A2-22. This phenomenon is nonlinear in that the lateral deflection of the specimen, needed for section alignment, develops at a high rate under initial loading but abates as the sections approach alignment. The corresponding bending moments caused by the stiffness offset behaves similarly. Comparison of the lateral deflection predicted by linear and nonlinear analysis for the specimen center is shown in Figure A2-23. Note that the nonlinear deflection behavior correctly approaches the dimension of the axial directed stiffness offset for the axially dominate load condition. Analysis of the repaired specimens addressed two possible failure modes in addition to those relevant to the unrepaired specimen: specimen fastener bearing/bypass strain failure and patch bearing failure. These criteria were also applied in the uniaxial repair analysis and reported upon in Section A2.1.2.

A2.2.3 Comparison of Theory and Experiment

The unrepaired specimen was tested at a load ratio of hoop/axial = 1.19. It failed due to fracture emanating from the notch at a hoop load level of 98,000 lbs. Failure analysis of the specimen addressed notch fracture and peak strain failure. Comparison of predicted versus actual failure loads is listed in Table A2-5. The point-stress fracture criteria based upon finite element stress ahead of the notch predicted a higher failure load than the peak strain criterion. However, both were within 6 percent of the actual failure load. A possible reason why the fracture criterion predicted too high a strength may be that it was based upon parameters derived from uniaxially loaded experiments. Biaxial loading may generate greater damage resulting in reduced strength. A possible reason for why the peak strain criterion predicted an erroneously low strength may be that the assumed 15 percent B-basis knockdown factor used deriving peak failure strain from allowables data was too high. The slopes of strain versus applied loading were derived from strain gage

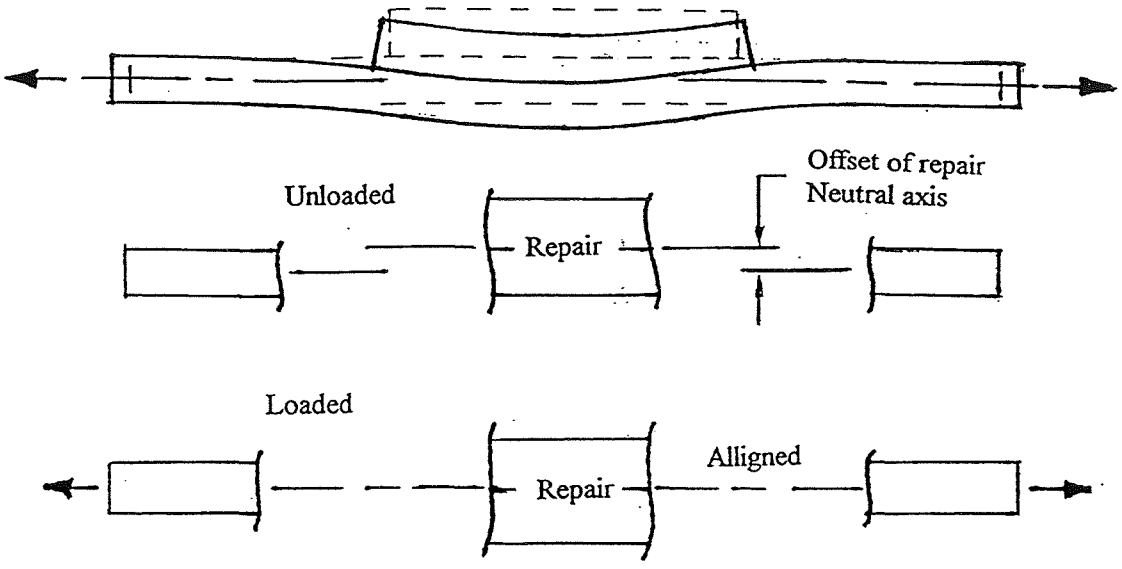

Figure A2-22: Repair Section Alignment with Plane of Applied Loading Responsible for Nonlinear Large Deflection Behavior

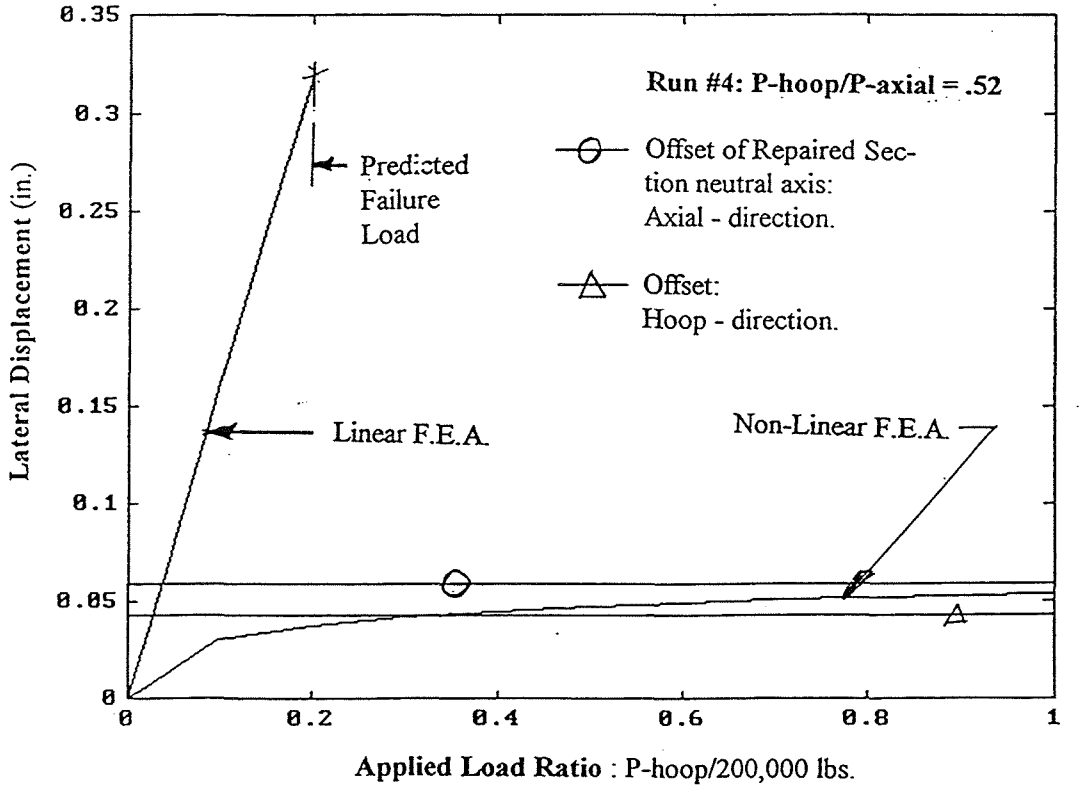

Figure A2-23: Nonlinear Analysis Correctly Predicts Repair Section Alignment

Table A2-5: Unrepaired Specimen, Predicted vs. Test Failure

	No Repair Phoop/Paxial = 1.19	
Failure Criteria	Linear FEA	Test Result
Peak Strain	95,320 lbs.	non-failure mechanism
Notch Fracture	103,600 lbs.	98,000 lbs

data and compared with finite element analysis results. Finite element analysis predicted half the strain rate at the notch tip as that realized from the gage nearest the notch-tip. Generally, however, the finite element analysis predicted a response 0-15 percent more stiff than realized by the gages. This result is consistent with other ATCAS material and structural tests.

The repaired specimen was run through three nondestructive tests and a final test to failure. To ascertain whether the specimen would survive the nondestructive tests, margin-of-safety checks were made. The ultimate load level for each of the three runs was arrived at by limiting certain strain readings as discussed in Section A2.2.1. Finite element analysis prediction of the peak load based upon gage readings at the notch-tip location are prone to two-fold over-estimation. The reason for the inaccuracy is discussed below. The analysis nevertheless predicted that the specimen would survive the tests but with some bearing/yield damage likely. Upon reviewing the actual load levels attained for the three nondestructive tests, analysis would indicate that no damage should have occurred.

Following the nondestructive tests, the specimen was tested to failure. Linear and nonlinear FEA were employed in predicting specimen failure. Results of the predictions and test are listed in Table A2-6. Interestingly, the linear analysis came very close to predicting the actual failure load for the correct failure mode; that is, the specimen failed due to strain concentration at the large radius round-out edge between the axial and hoop legs of the specimen. Nonlinear analysis, however, predicted a significantly higher load level for this failure mode and a lower load level for the specimen bearing/bypass failure mode. Unfortunately, no instrumentation was placed at the peak strain location. Nevertheless, indirect instrumentation supports the nonlinear analysis prediction as follows.

The repair section should align itself with the plane of loading and in doing so exhibit more in-plane stiffness. This should cause more load to be absorbed by the repair and divert loading from the outer peak strain location. Linear analysis is unable to reflect this behavior and also generates erroneously high bending moments. Strain gage data, as discussed below, agrees very well with the nonlinear analysis outside of the patch area. Comparison of linear and nonlinear strain prediction in this area showed that greater concentration of strain developed ahead of the repair for the nonlinear analysis which could be associated with the increased stiffness of the repair under large deflection behavior, thereby indirectly indicating that less peak strain should have been realized than predicted by linear analysis. As for the bearing/bypass failure analysis, it could be argued that it is conservative in multi-fastener joints due to fastener load redistribution. Yet even if this occurred, the nonlinear peak strain failure analysis still overestimated the actual failure by 15 percent. Scrutiny of the analysis peak strain failure value would suggest that a lower value is justified; however, this runs contrary to the results of the unrepaired specimen test. The only remaining rationale for the low peak strain failure is the a test load imbalance or specimen flaw, both of which are speculative possibilities.

Of great interest are the actual loads transferred into the repair via fastener shear. Unfortunately, instrumentation does not exist to measure fastener shear loads. However, fastener loads as derived by the nonlinear analysis at the failure load are presented in Table A2-7 according to the fastener chart in Figure A2-24. It is evident that the peak fastener load is that in the outermost corner of the repair and principally of axial orientation. The rationale for such a peak load location is that in addition to being a leading-edge fastener, the corner fastener must also pull at a section of patch without the beneficial assistance of an adjacent fastener. Mid-side fasteners on the other hand share their influence.

Measured and predicted (nonlinear analysis) strains as a function of load were compared. The agreement between nonlinear theory and experiment ranged from excellent to marginal, with excellent agreement at gage locations outside of the patch area. In the outer area little flexure was realized, and a pronounced peaking of in-plane strain in front of the patch was in contrast with linear analysis predictions. This suggests that alignment of the repair section with the plane of loading generated bending local to the repair area. Within the repair area the general agreement in the trend of strain development was found between nonlinear analysis predictions and experimental results. However, only marginal agreement on the actual values was obtained. Locations of several gages within the repair are shown in Figure A2-25 and A2-26. All identified gages are of axial orientation, parallel to the notch. Gages #6 and #34 represent average values of the three symmetric locations indicated. Plots of the nonlinear prediction versus experiment for the gages are shown in Figures A2-27 and A2-28 (Test Run No. 4, $P_{hoop}/P_{axial} = 0.52$). From examination of the experimental values, it is evident that strain on the top surface of the patch increases at greater distances toward its center. This behavior, a product of shear lag, was expected and was predicted by the nonlinear analysis. Although nonlinear analysis agreed with trends of the strain development, actual strain values showed poor correlation. Surprisingly the repair area realized higher strain than predicted. This suggests a coupling between patch and specimen that is more stiff than that modeled. This phenomena could in part be explained by friction between the fayed surfaces. This behavior was also realized in the uniaxial tests but to a much lesser extent.

Correlation of notch-tip gage results with nonlinear analysis was also marginal. As experienced with the unrepaired specimen, experimental strain was generally twice as high as predicted. An exception to this was with the gage nearest the notch-tip which during the test failure run experienced strain 3.6 times that predicted.

A2.3 Application of Coupon Experience to Crown Repair

From the uniaxial coupon tests it was evident that titanium fasteners were superior to thermoplastic rivets. Also, patches having multiple fastener rows returned greater strength to the damaged specimen. These are clear-cut results that should be carried forward. Not clear is the best patch material choice and the expected influence of the various nonlinear phenomena. However, a degree of confidence can be assumed with regard to small notch fracture, bearing/bypass failure and peak strain.

Table A2-6: Repaired Specimen, Test Failure vs. Linear and Nonlinear Analysis

	Repaired Specimen Phoop/Paxial = 0.52		
Failure Criteria	**Linear FEA**	**Non-linear FEA**	**Test Result**
Specimen Peak Strain	40,230 lbs	48,190 lbs	41,700 lbs
Notch Fracture	388,000 lbs	---	non-failure mode
Specimen Bearing/By-Pass	41,000 lbs	37,070 lbs	non-failure mode
Patch Bearing	50,720 lbs	---	non-failure mode

Table A2-7: Fastener Loads for Repaired Specimen as Derived from Nonlinear Analysis (Listing Refers to the Failure Load Level)

Bolt Number ==	1	2	3	4	5	6	7	8
	Fastener loads (lbs) at cover patch level							
hoop shear force	-	-	-180	-74	-127	-68	-92	-86
axial shear force	-	-	552	478	277	207	0	0
bolt axial tension	-	-	50	38	-19	-14	-5	-6
	Fastener loads (lbs) at base patch level							
hoop shear force	-51	-64	122	-5	236	154	326	454
axial shear force	1461	1352	827	682	401	321	0	0
bolt axial tension	138	122	20	16	-18	-7	-8	2

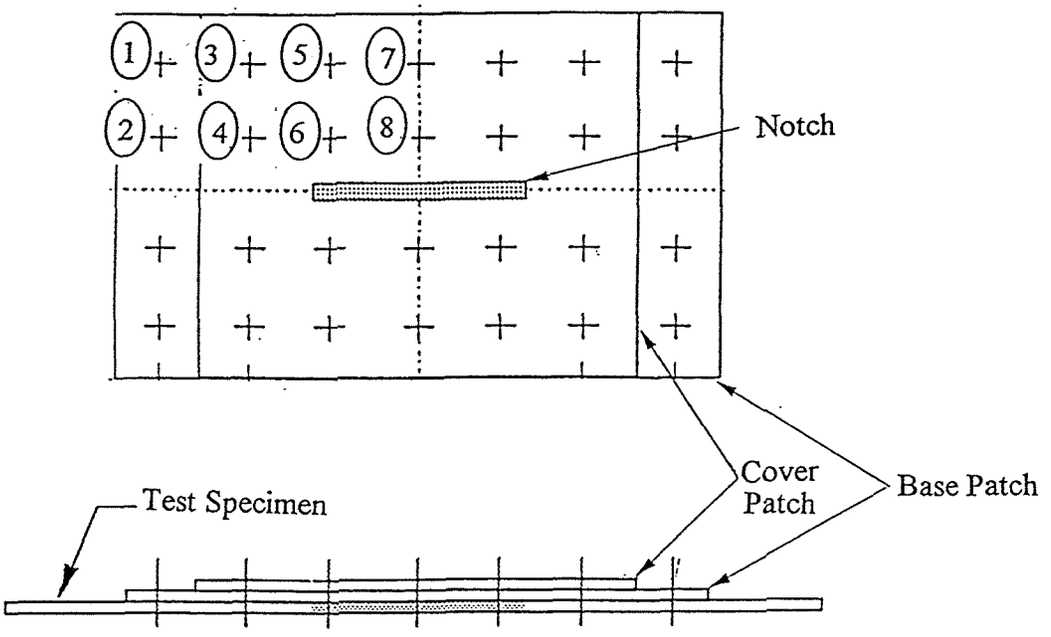

Figure A2-24: Repair Fastener Identification

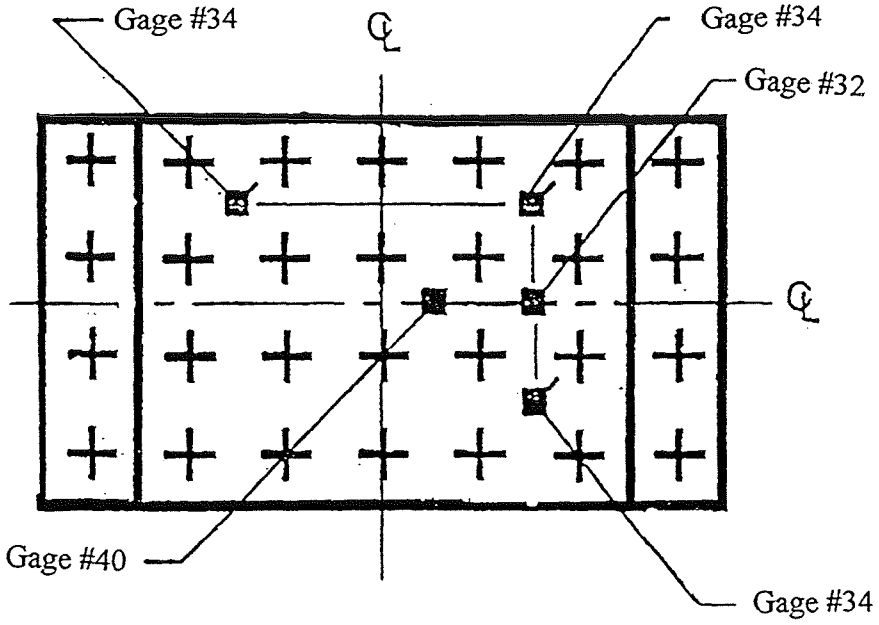

Figure A2-25: Strain Gages on Top of Repair Patches

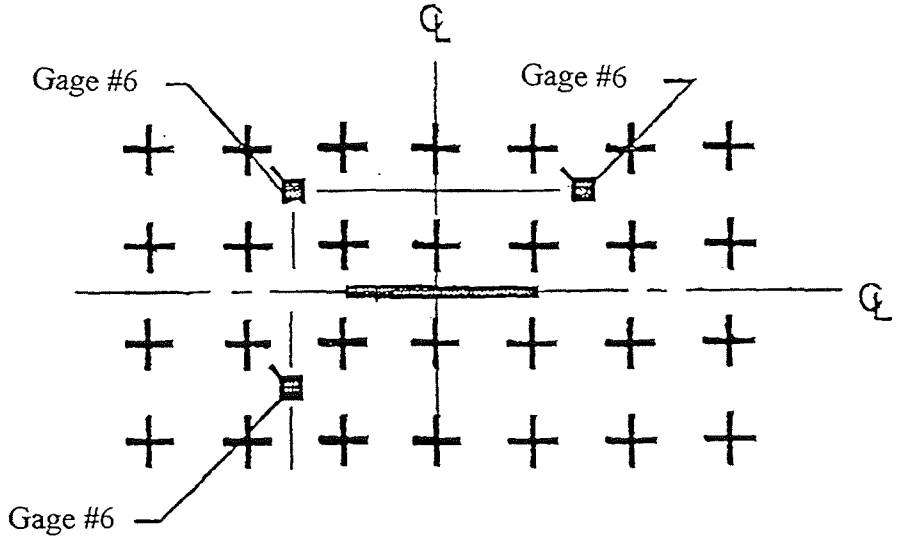

Figure A2-26: Strain Gages Below Repair on Specimen

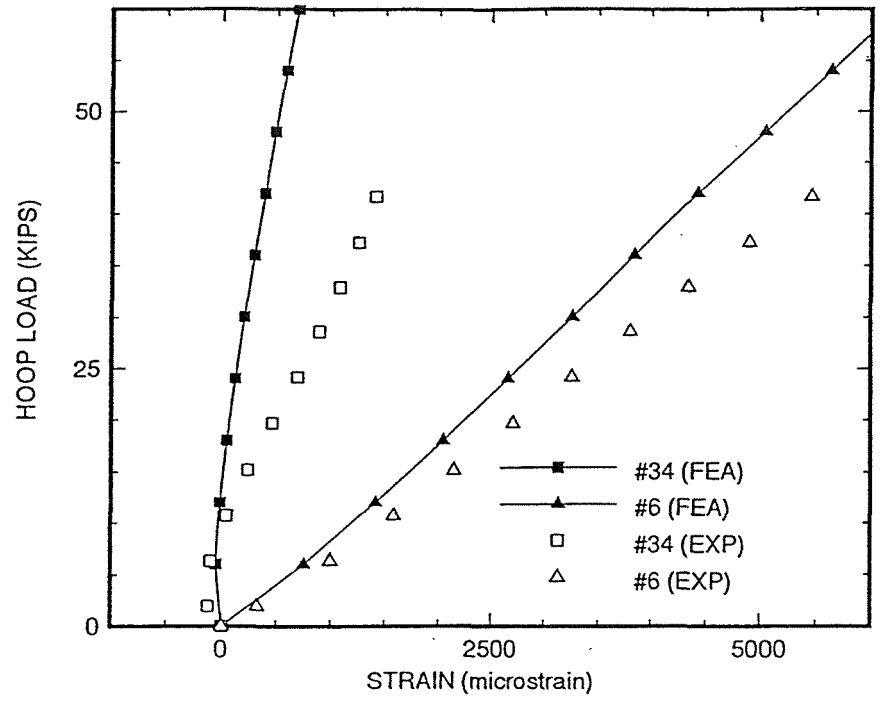

Figure A2-27: Comparison of Nonlinear Finite Element Analysis Predictions (FEA) and Experimental Results (EXP) for Averaged Gages #34 and #6

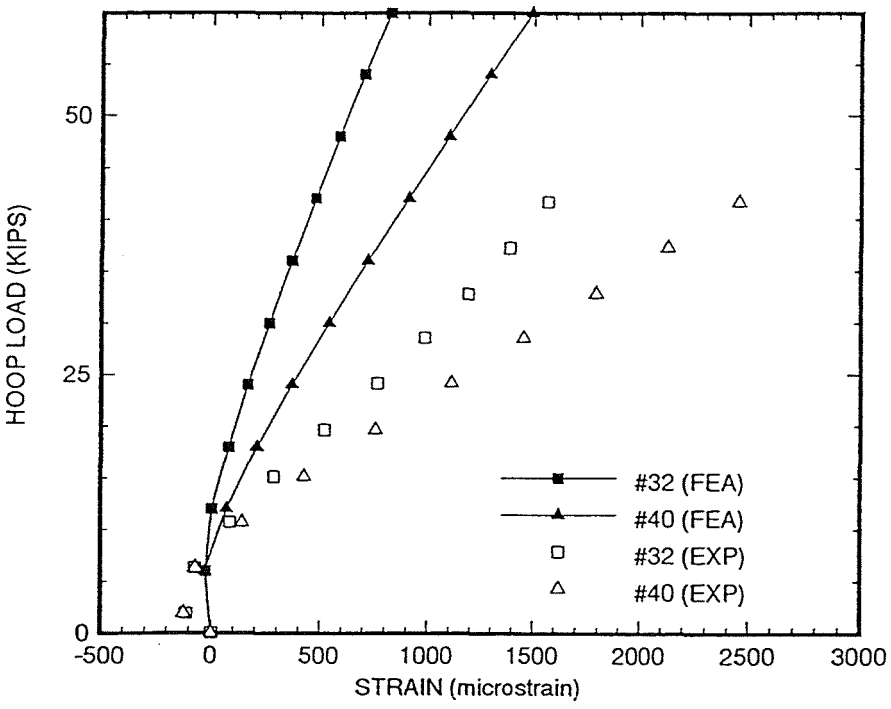

Figure A2-28: Comparison of Nonlinear Finite Element Analysis Predictions (FEA) and Experimental Results (EXP) for Averaged Gages #32 and #40

The three patch materials and their respective patch thicknesses represented a range of patch stiffness which would absorb more or less load depending upon its stiffness and thickness. For large repair application, stiffness consideration can be more significant and thus results of tests with patches of equal stiffness would have better extended to crown repair.

The various nonlinear phenomena can be significant to detail within the repair area. This detail is of great importance with respect to bearing/bypass strain failure. However, the sometimes marginal predictive capability and limited experimental tools makes understanding of the repair behavior difficult. However, it has been shown that nonlinear analysis based upon large deflection can provide good predictive results which are superior to linear analysis, but additional unrepresented phenomena can be significant within the repair area. Additionally, nonlinear, large deflection analysis seems to do a good job of correctly modeling the evolution of the repair area stiffness which has an effect on regional load path behavior. For stiffness critical structural repair, nonlinear analysis is recommended. Thus nonlinear, large-deflection analysis should be extended to the crown repair as the best tool available.

A3.0 FUSELAGE PANEL REPAIR DESIGN AND ANALYSIS

As described in the introduction of this report, the primary emphasis of the project has been to develop an efficient design for the repair of a 22"-long, through-penetration notch in the aft section of a composite fuselage. This section describes the development of this design.

A3.1 Composite Crown Panel Geometry and Load Cases

The section of crown panel for which the repair design is being developed is shown in Figure A3-1. The skin material is a 13-ply graphite/epoxy laminate whose properties were described in Section A2.1. The stiffeners are composed of a 15-ply graphite/epoxy laminate with a [45/90/-45/0/45/-45/0/90/0/-45/45/0/-45/90/45] layup. The frame members are composed of a graphite fabric composite with a thickness of 0.155" and moduli E_1=6.23x10^6 psi, E_2=8.89x10^6 psi, G_{12}=1.66x10^6 psi, and ν_{12}=0.144. A 22"-long line notch, severing both the skin and frame, lies at the center of the panel.

The response of the panel to the four load cases listed in Table A3-1 will be considered. Load Case 1 consists of a uniform internal pressure of 18.2 psi. This results in the usual hoop and axial loads present in a cylindrical pressure vessel. Load Case 2 consists of a uniform internal pressure of 13.65 psi and an axial load of 5,000 lb/in. Load Case 3 consists of an axial compressive load of 1,690 lb/in. Load Case 4 consists of a uniform internal pressure of 13.65 psi (resulting in the usual hoop and axial loads in a cylindrical pressure vessel) coupled with an edge shear load of 773 lb/in.

A3.2 Finite Element Model Of the Crown Panel

A finite element model was constructed for the notched crown panel using COSMOS/M. Four-node quadrilateral and three-node triangle, layered shell elements were used throughout. The development of the finite element model can be simplified by taking advantage of symmetry in the structure and the loading (except for Load Case 4). We first note that there is symmetry about a plane along a radial line passing through the notch parallel to the notch. Thus, only the lower half of the panel in Figure A3-l(b) needs to be modeled. Symmetry boundary conditions (i.e., zero displacement along an axis normal to the edge and zero rotations along axes parallel to the edge) were used on all four edges of the panel. This choice appears to be reasonable for all of the edges except for the lower edge in Figure A3-l(b). Ideally, the boundary conditions on this edge should be representative of the conditions on a similar line in the complete cylinder forming the fuselage. To determine how well the symmetry boundary conditions represent the true boundary conditions at this edge, an analysis was performed on an enlarged panel with double the arc length of that in Figure A3-1 for Load Case 1. The hoop stress contours for the original panel and the enlarged panel are shown in Figure A3-2. It can be seen that the stress fields are almost identical. In fact, near the notch tip the difference is less than 1

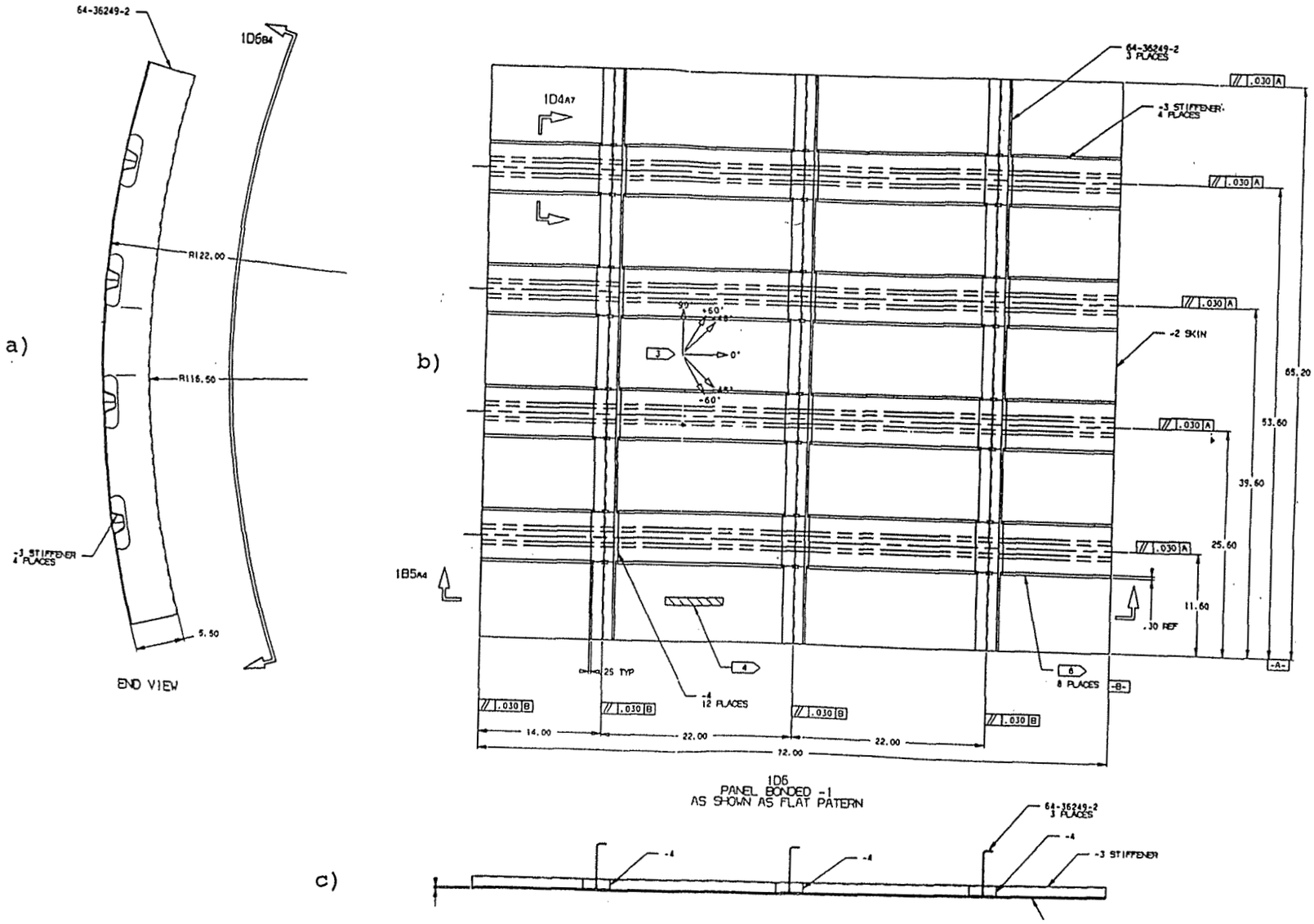

Figure A3-1: Section of Crown Panel with a Central Notch

Table A3-1: Load Cases Used in Repair Analysis

Load Case	Description	N_x (axial) lb/in	N_y (hoop) lb/in	N_{xy} (shear) lb/in	Pressure psi
1	maximum pressure acting alone	1110	2220	0	18.2
2	maximum axial load - 2.5g maneuver	5000	1665	0	13.65
3	maximum shear load	833	1665	773	13.65
4	maximum compression load	-1690	0	0	0

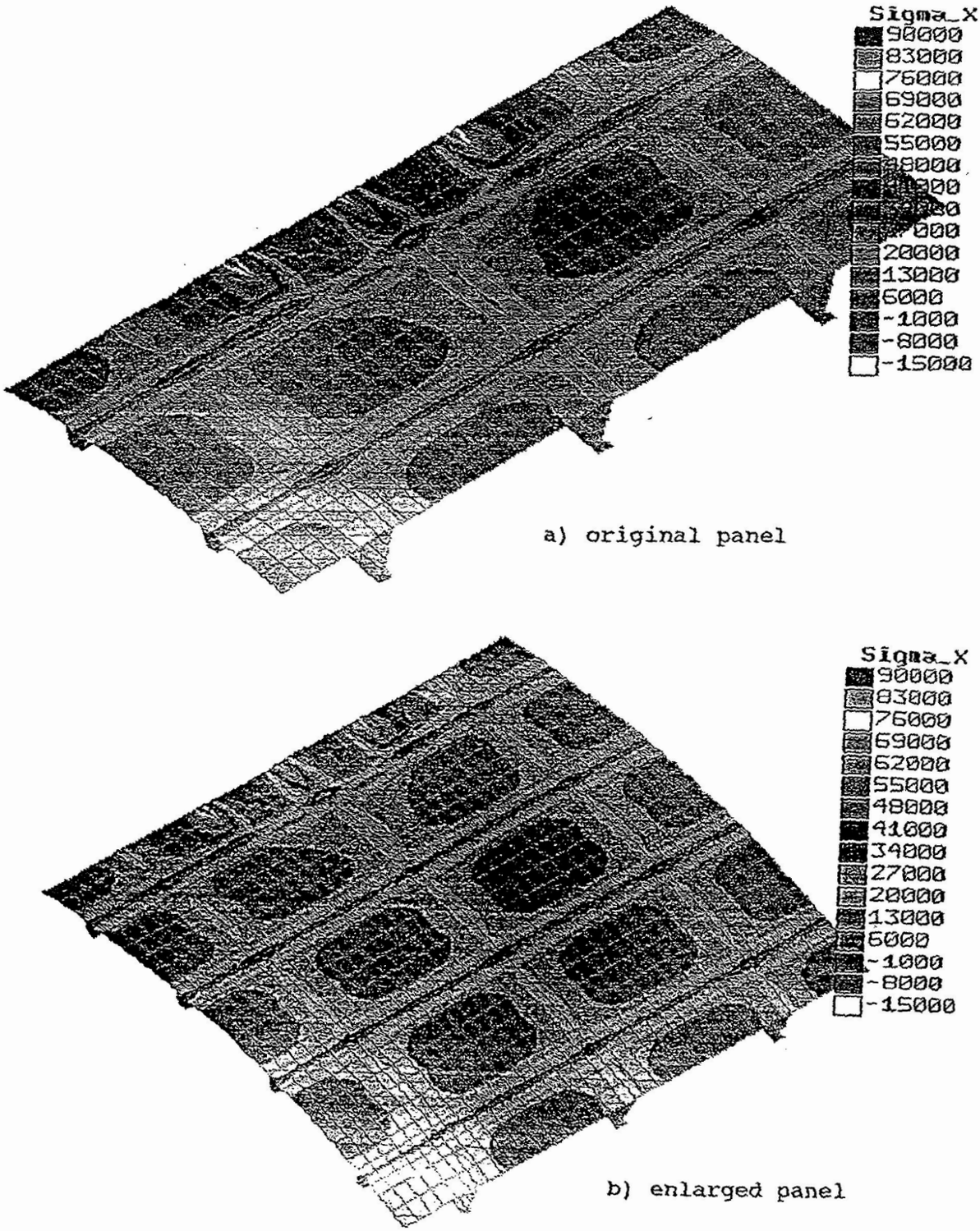

Figure A3-2: Comparison of Hoop Stress Contours in the Original Panel and the Enlarged Panel

percent. Thus, we conclude that our choice of boundary conditions should not introduce significant error in the analysis.

It is also interesting to note that if a vertical plane parallel to the frames is passed through the centers of the panels in Figure A3-2, the stress field on the left is virtually a mirror image of the stress field on the right (near the crack tip the difference is less than 1 percent). Thus, although geometric symmetry does not quite exist about such a plane (because the frame has a "J" shape), the assumption of such symmetry should still give reasonably accurate results. Consequently, only one-quarter of the panel was modeled in the finite element analysis. The mesh for this model is shown in Figure A3-3.

The criterion for failure at the notch tip that was used in the analysis was the Poe-Sova (1980, 1983) point strain criterion with a critical strain of 0.143 at a characteristic distance of 0.0585". This criterion was found to work well with this size of notch (Walker et al, 1992). To determine the adequacy of the mesh, a flat, two-dimensional version of the panel with the stiffeners and frames omitted was modeled under simple tension. The normalized strain near the crack tip calculated by the finite element analysis was compared with the analytical solution [Lekhnitskii, 1968]. The good agreement between these two results shown in Figure A3-4 indicates that the density of the mesh is adequate.

In the analysis of repaired coupons (Section A2), it was found that large-deflection considerations could have a significant effect on the response. To ascertain the importance of large deflections on the response of the notched crown panel, we performed both linear and nonlinear (large deflection) analyses on the model shown in Figure A3-3 for Load Case 1. The hoop and axial strains predicted by these two analyses on the inner and outer surfaces of the panel near the notch tip are shown in Figures A3-5 and A3-6. The difference between the inner and outer strains is considerably smaller in the nonlinear analysis than it is in the linear analysis. This indicates that the nonlinear analysis predicts significantly less bending. Also, for the hoop strain the bending directions are reversed. The reason for this is illustrated in Figure A3-7 which shows the shape of the deformed panel predicted by the two analyses. The linear analysis predicts that the panel dishes inward just ahead of the notch tip. This behavior is absent in the nonlinear analysis. Figure A3-8 shows the strains at the middle surface of the fuselage skin predicted by the two analyses. Here, we observe that the difference in response predicted by the two analyses is considerably smaller than it was for the surface strains. Since the prediction of failure is based on the middle surface strains, the use of a linear analysis for failure prediction should result in a small error. Consequently, in arriving at a repair design, a linear analysis was used to develop the design, and then its adequacy was verified with a nonlinear analysis.

In developing a repair for the notched crown panel, we will design patches that will carry load across the severed components. Before developing these patch designs, it is desirable to reduce the intensity of the stress/strain riser at the notch tip. This can be done by blunting the tip by cutting out material to form an elongated hole with rounded ends. For example, a finite element model for the panel with an elongated hole with a 2"-radius tip is

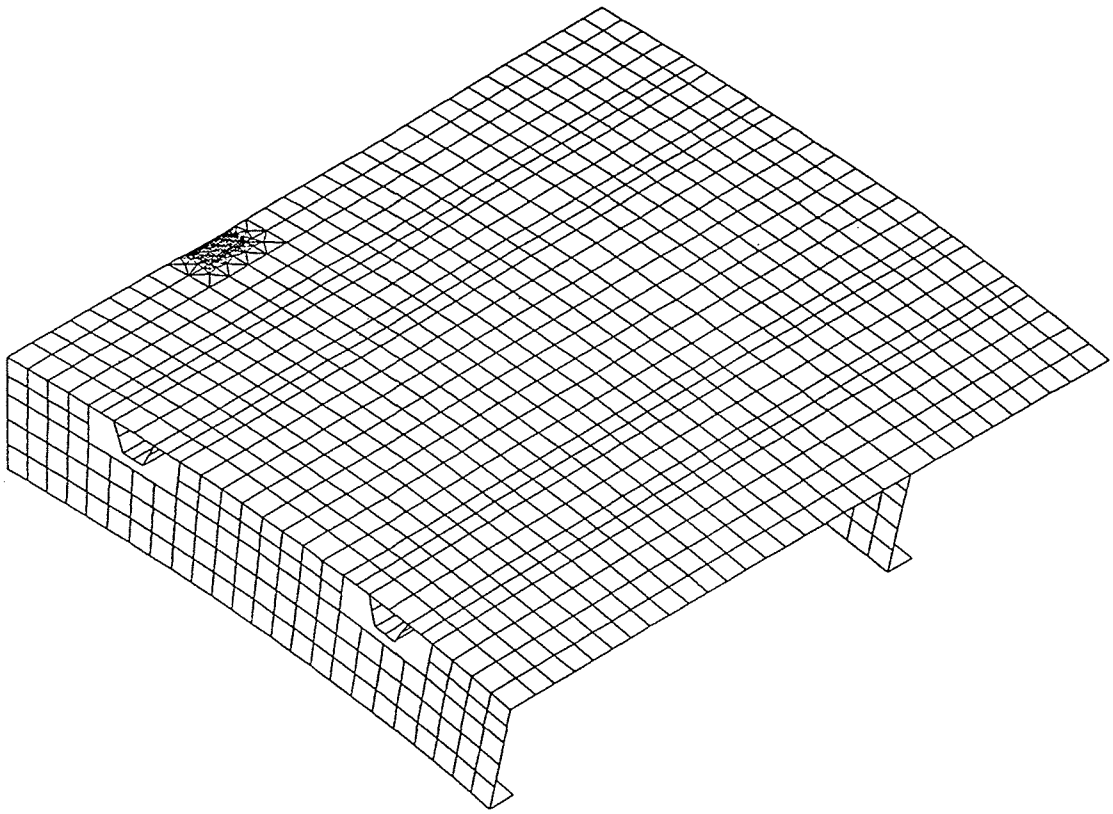

Figure A3-3: Quarter-Symmetry Model of the Notched Panel

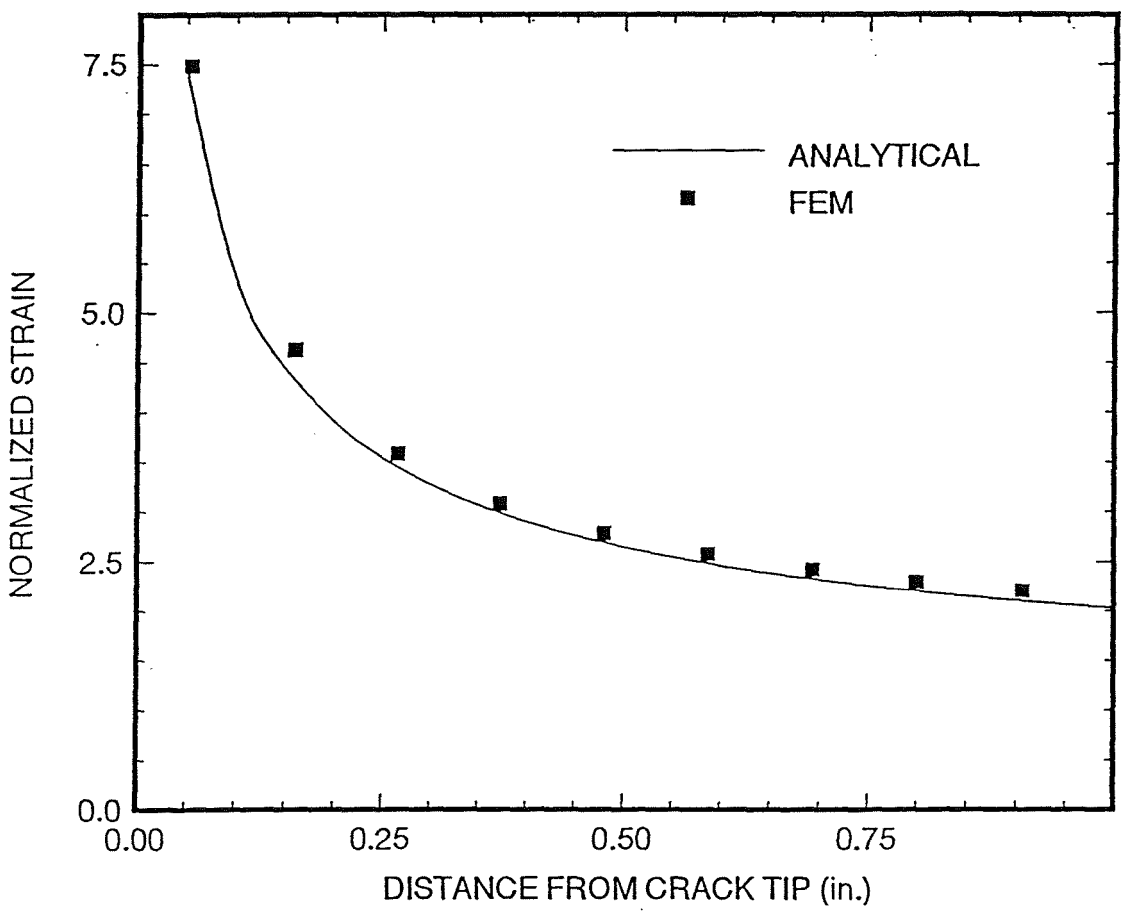

Figure A3-4: *Comparison of Analytical and Finite Element Analysis (FEA) Strains Near the Crack Tip in a Flat Unstiffened Panel*

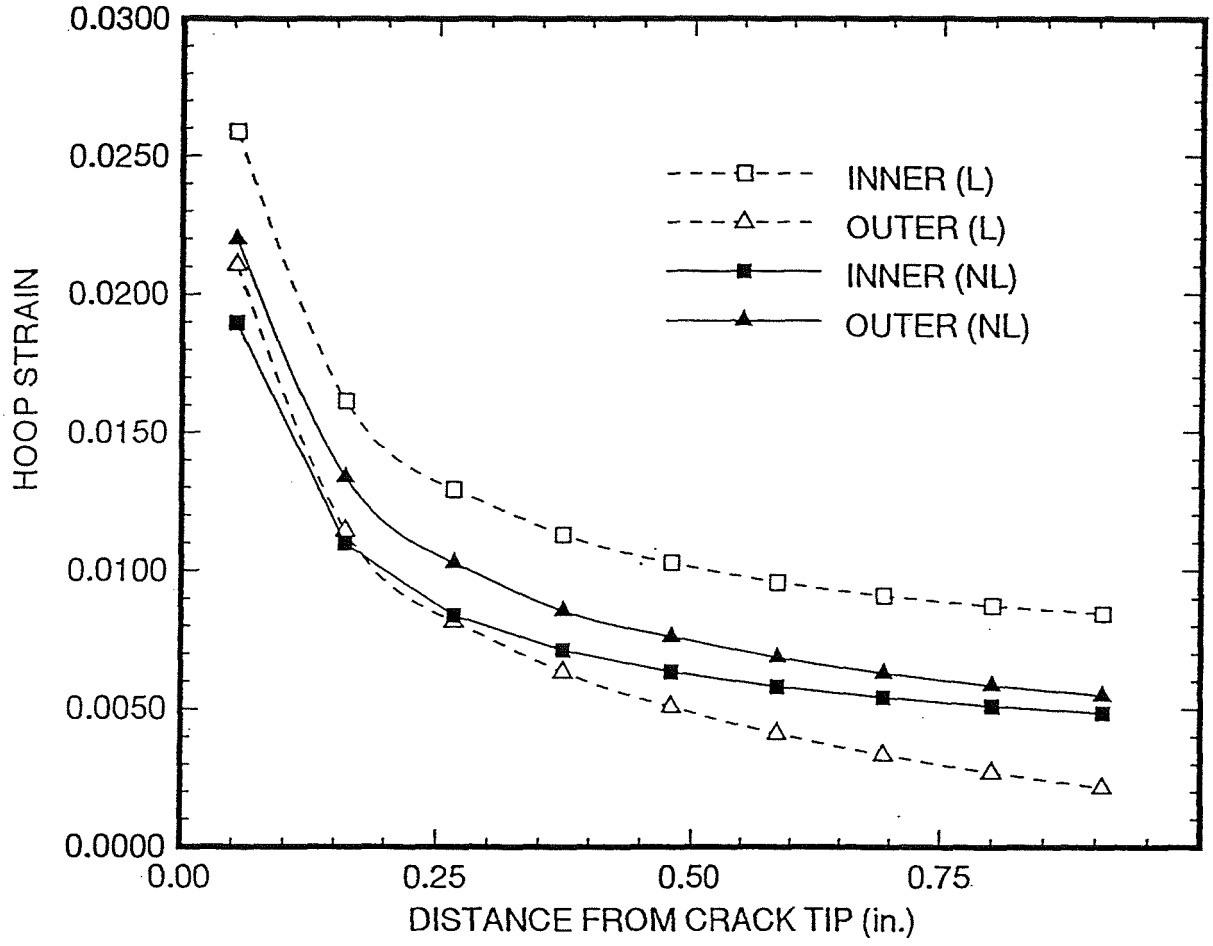

Figure A3-5: Hoop Stains on the Inner and Outer Surfaces Predicted by Linear (L) and Nonlinear (NL) Analyses

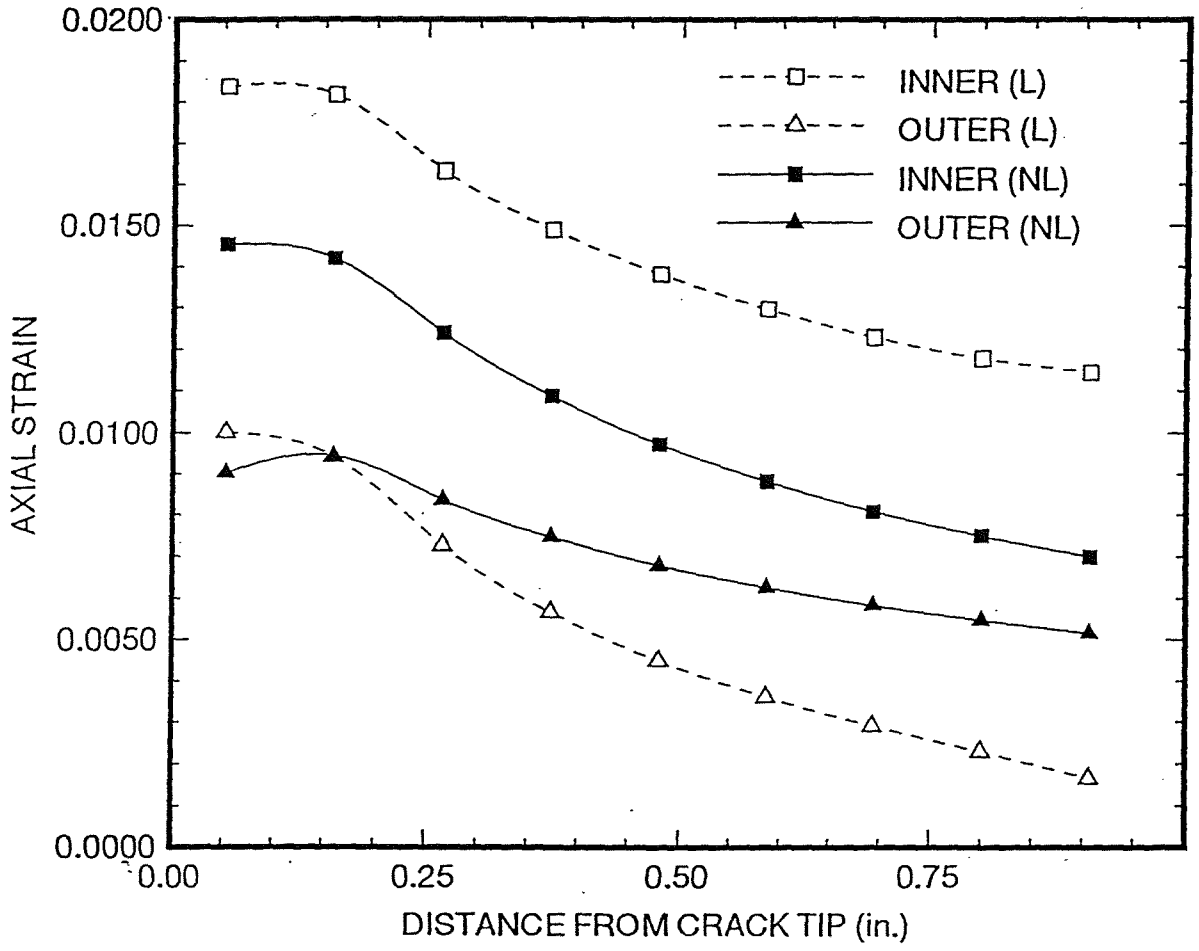

Figure A3-6: Axial Stains on the Inner and Outer Surfaces Predicted by Linear (L) and Nonlinear (NL) Analyses

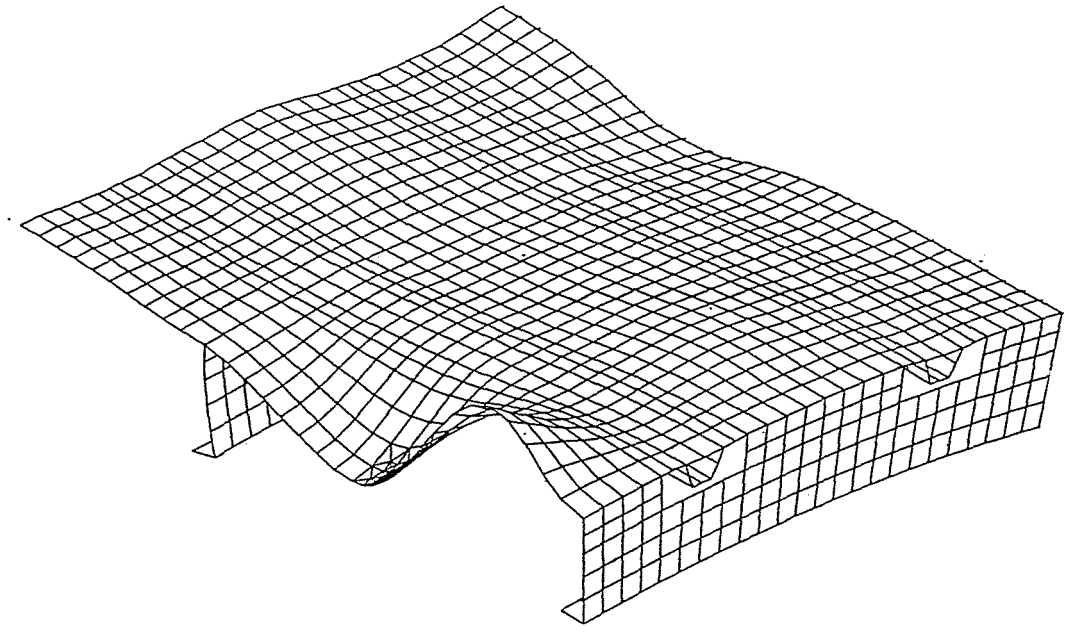

a) linear analysis

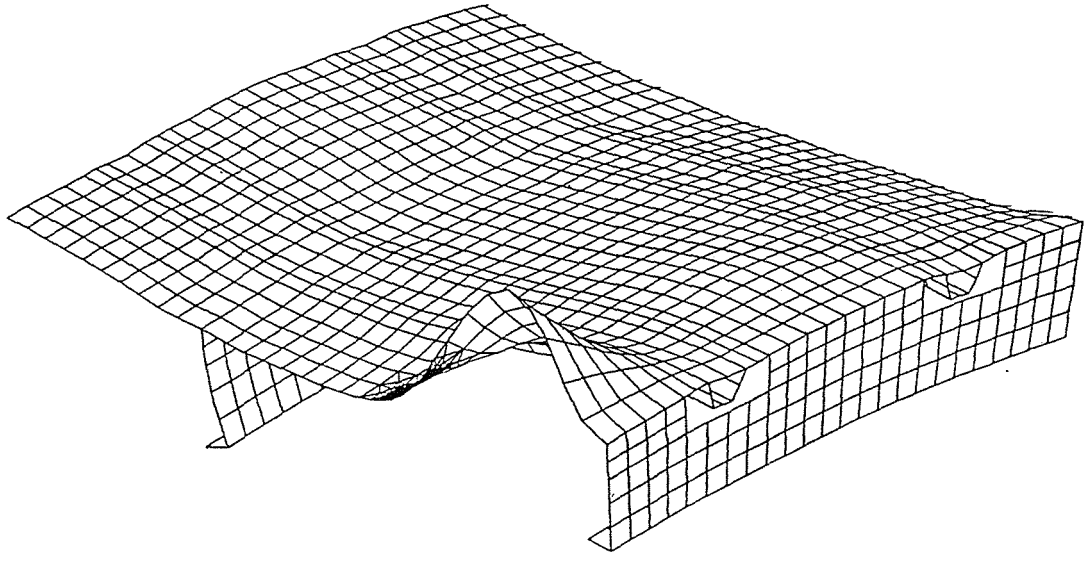

b) nonlinear analysis

Figure A3-7: Deformed Panel Shapes Predicted by Finite Element Analysis

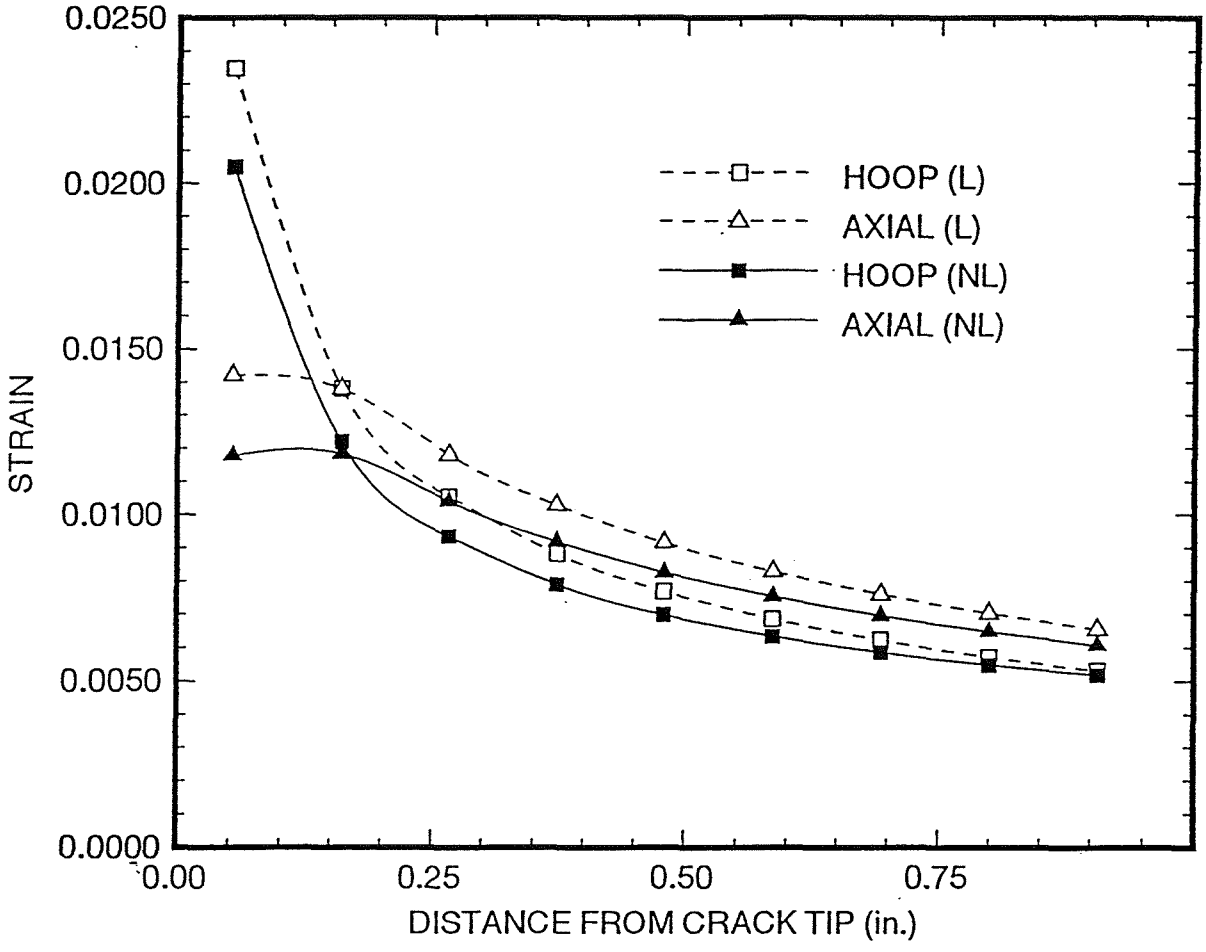

Figure A3-8: Hoop and Axial Strains in the Middle Surface of the Skin Predicted by Linear (L) and Nonlinear (NL) Analyses

shown in Figure A3-9. An analysis of this model for Load Case 1 was performed. A comparison of the strain near the notch tip for the original line notch and for the elongated hole is shown in Figure A3-10. The strain near the edge of the hole is considerably smaller than the strain near the tip of the line notch. Specifically, at the characteristic distance the strain is reduced by 66 percent. Thus, blunting the notch is an important factor in developing an efficient repair design.

A3.3 Final Repair Designs

A final repair design was arrived at which would become the subject of upcoming full-scale crown panel testing. Two additional designs are presented to illustrate the impact of repair material selection and fuselage design. All three repair designs are closely related. In pursuit of a practical repair, a general repair approach was developed. The approach argues that damage cut-out and repair strategies should be incorporated into the original fuselage design. Also cost-design trade studies are needed to identify where and when repair is preferred over factory replacement. Also, damage cut-out shape and repair building-block strategies are fuselage design dependent.

A3.3.1 General Approach

The general approach recommended below for fuselage repair should be an integral part of fuselage design development to ensure product long-term affordability. It should employ techniques that are broadly feasible and affordable to the entire family of airline customers. It should address only that damage for which repair is shown to be cost effective, and the infinite range of probable damage scenarios must be addressed by a finite hierarchical set of discrete cut-out repairs. Finally, definition of the discrete cut-out set and corresponding repair designs should be made part of the delivered aircraft product. A summary of the approach issues are listed in Table A3-2. The use of pre-cured and stocked laminate sheets should be employed in single or more layers to transfer load about damage cut-out areas. Also, fuselage and repair should be joined using mechanical fasteners. These recommendations are intended to avoid customer material storage and tooling costs as well as enhance reliability. Patching of fuselage skin should be placed external to the aircraft, and splicing of the internal substructure (stringers, frames, etc.) should be placed internally as a practical rule. Repair designs, specific to preconceived damage cut-out patterns over the various zones of the fuselage, would be developed as part of the aircraft product. The customer could then associate any potential and critical damage with a specific predefined cut-out pattern for which a repair design already exists. This method is obviously intended to minimize customer costs of repair development and aircraft down-time.

The range of damage scenarios for which cost effective repair is feasible would be determined by a cost study considering damage probabilities and costs of repair versus installing factory manufactured replacements or aircraft retirement. This exercise should define the range of cut-out sizes for the various sections of the fuselage for which repair is

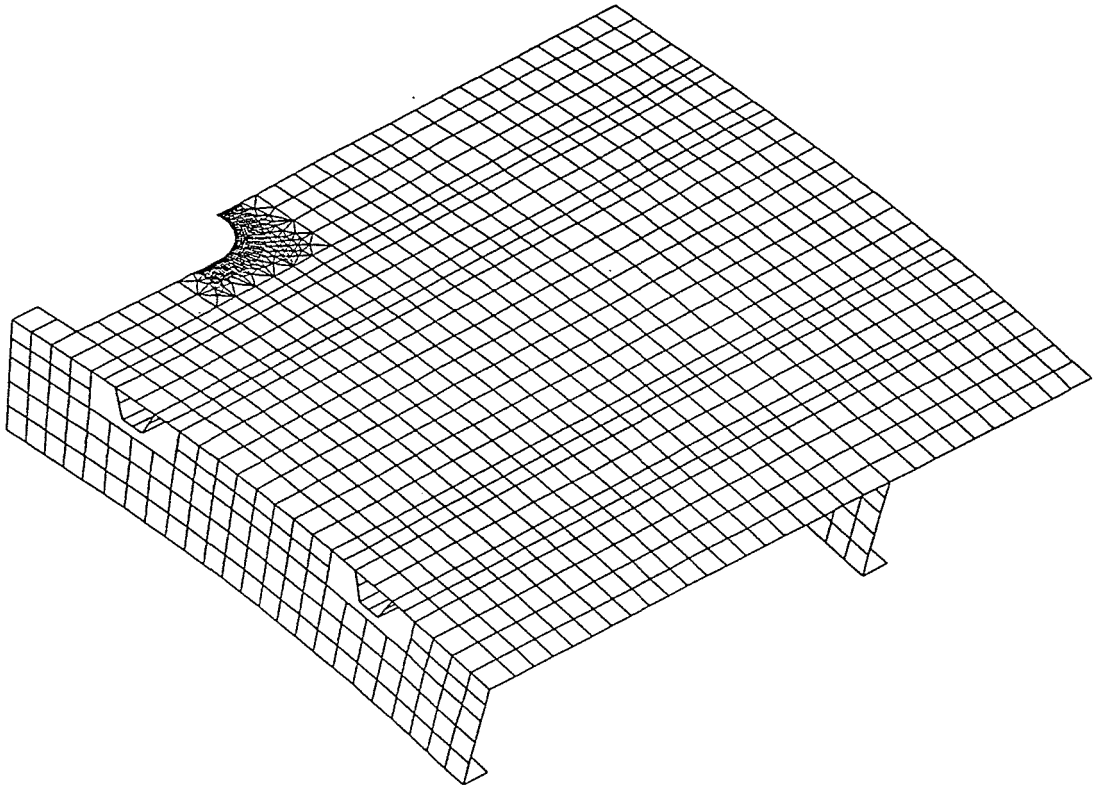

Figure A3-9: Finite Element Model of the Crown Panel with an Elongated Hole

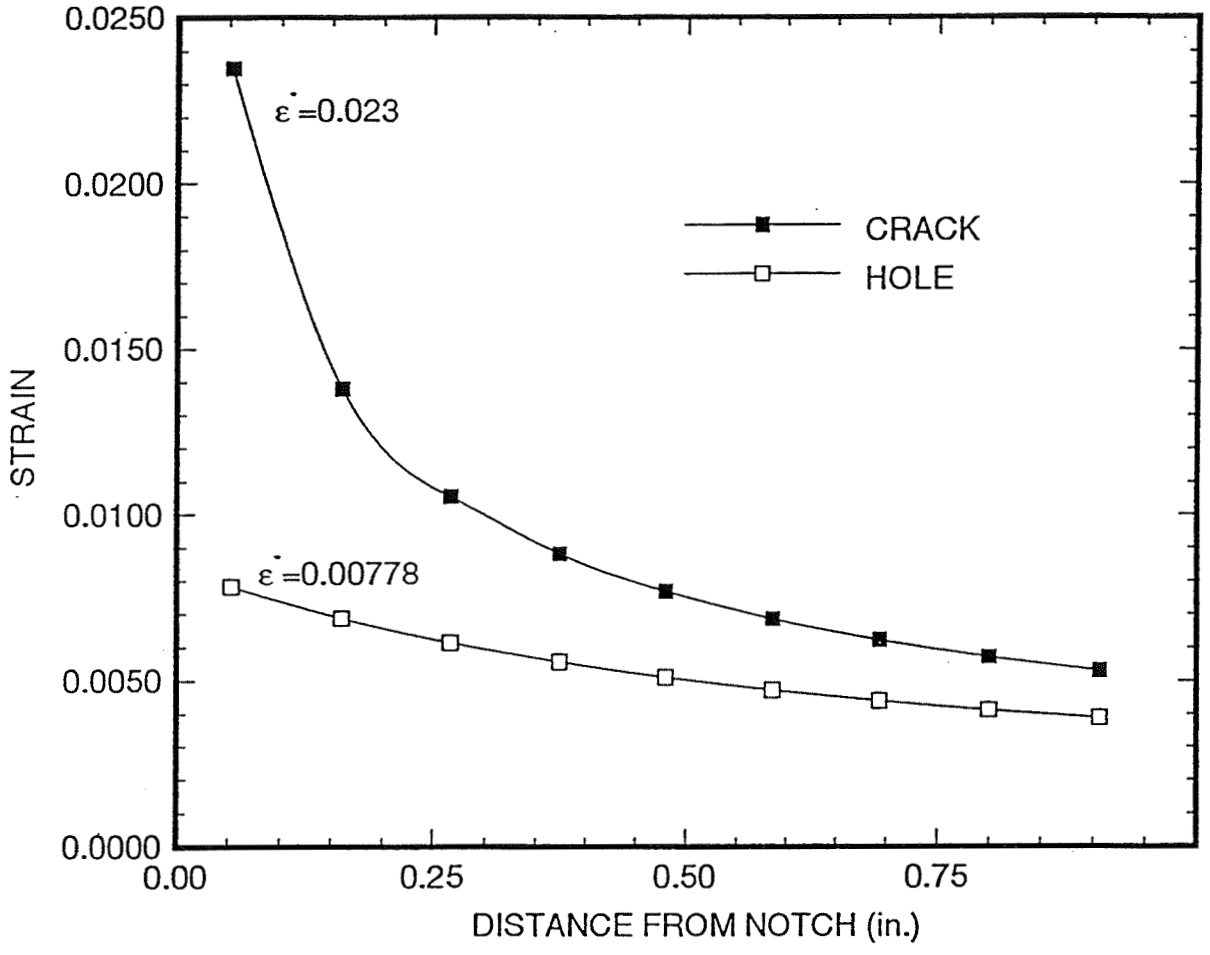

Figure A3-10: Comparison of Strain Near the Tip of a 22"-Long Line Crack and a 22"-Long Elongated Hole

Table A3-2: Summary of Approach Issues for Fuselage Repair

Damage Repair - Approach

Incorporate minimum field repair capabilities

- mechanical attachments
- pre-cured stock elements (patch laminates, composite or metal angles)
- eliminate material shelf life constraints (less waste)
- reduced refrigeration storage requirements

Predetermine damage cutout pattern

- address a range of damage severity
- patch size and placement pre-defined relative to the repair cutout
- patch size and bolt pattern adjusted to address fuselage location specific conditions
- skin patching external and sub-structure patching internal

Design stock laminate for most severe damage condition

- stiffness constraints
- strength requirements
- flexibility (single vs. multi-layer patches)
- repair vs. factory replacement costs (avoid factory replacement until very large damage scenarios)

called for. A further cost study is needed, however, to determine the best stock laminate material and respective set of gage thicknesses. It is conceivable that the largest cut-out repair might employ multiple layers of a stock laminate while the least disruptive cut-out repair employs only one. Repair and fuselage material stiffness anisotropy should also be considered at this stage.

The above approach has been referred to as the "Damage Level Approach". As described above it should be developed from the top-down direction as depicted in Figure A3-11. However, it would be applied from the opposite perspective; i.e. an incurred damage would be matched to the smallest pre-defined cut-out pattern. Levels of damage could be categorized by area of cut-out size, number of structural members involved in cut-out, and/or number of layers of stock laminate defined in the repair. Specific category definition was not warranted in the effort described herein. However, a limited example is described in Table A3-3.

3.3.2 Crown Panel Repair Design

A repair which reflects the above general approach was developed for the fuselage crown panel and damage defined in Section A3.1. This repair, shown in Figure A3-12, is the subject an upcoming full-scale pressure box test. The damage (22-inch axial notch) was cut-out using a general pattern shape. Patching of the skin employed layers of a quasi-isotropic stock laminate. Splicing of the frame employed yet another stock laminate. Mechanical fasteners were used to join the repair and fuselage, and no special preparation or assembly procedures were required.

Two additional repair designs were also developed and are reported herein. An alternative to the repair described above is distinguished by patch material exhibiting stiffness anisotropy. The other repair reflects the implications of a repair-friendly fuselage design.

Cut-out Configuration

The same cut-out pattern was employed for all three repair designs mentioned above. As illustrated in Figure A3-12, the cut-out has an hour-glass shape. This pattern is actually a union of three general cut-out (block) patterns as follows: two complete skin bay cut-outs and a joining cut-out of the severed frame and skin assembly. Choice of the block shapes reflects maximum areas of uniform structure which implies uniform patch design. Block shapes do not reflect any anticipation of damage type, shape or orientation; thus they are generalized. Large damage size would be addressed by assembling a union of cut-out blocks.

The cut-out block of the frame should have included the full breadth of structure between the stringer flanges as did the skin cut-out block. This would have enabled the arrived-at repair to address frame damage other than that contained within the central two inches. The shortened breadth of the version employed in this effort was an artifact of the limited size of the crown panel employed in testing. The larger frame cut-out would have necessitated a longer frame splice which would have extended outside of the panel area in

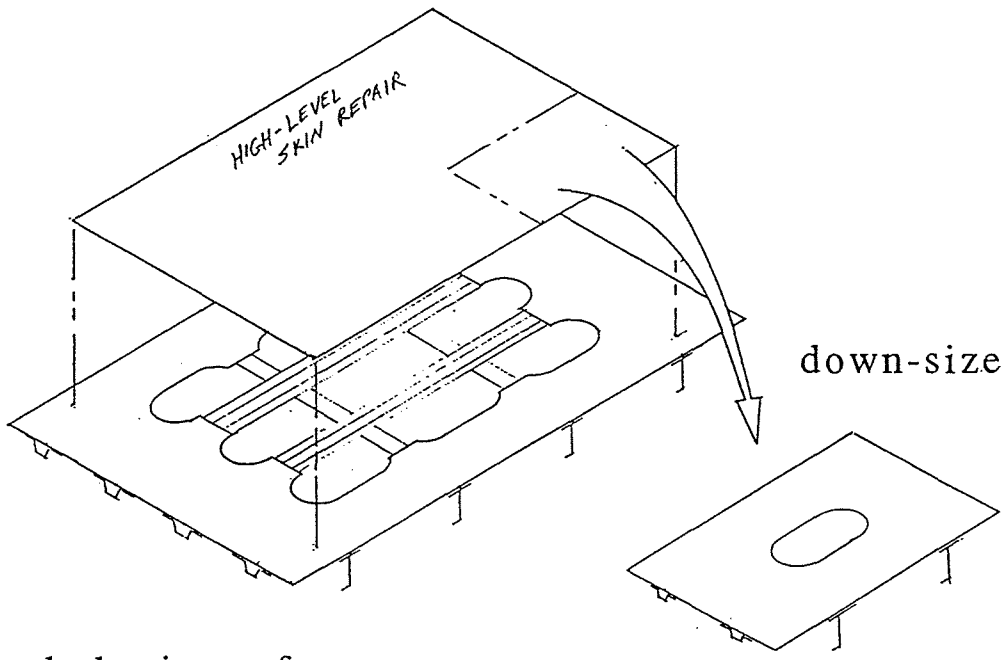

Figure A3-11: ***Stock Patch Material Sized for Severe Damage and Down-Sized for Lesser Conditions***

Table A3-3: Damage Level Approach to Repair Identification

Designation	Damage Description	Repair Approach
Level 0	Skin delamination or debond from stiffening elements	Fastener restraint
Level 1	Critical damage to a single structural element (skin or stiffener)	Mechanically fastened patch and/or splice
Level 2 (and higher)	Multiple occurences of Level 1 damage	same as Level 1

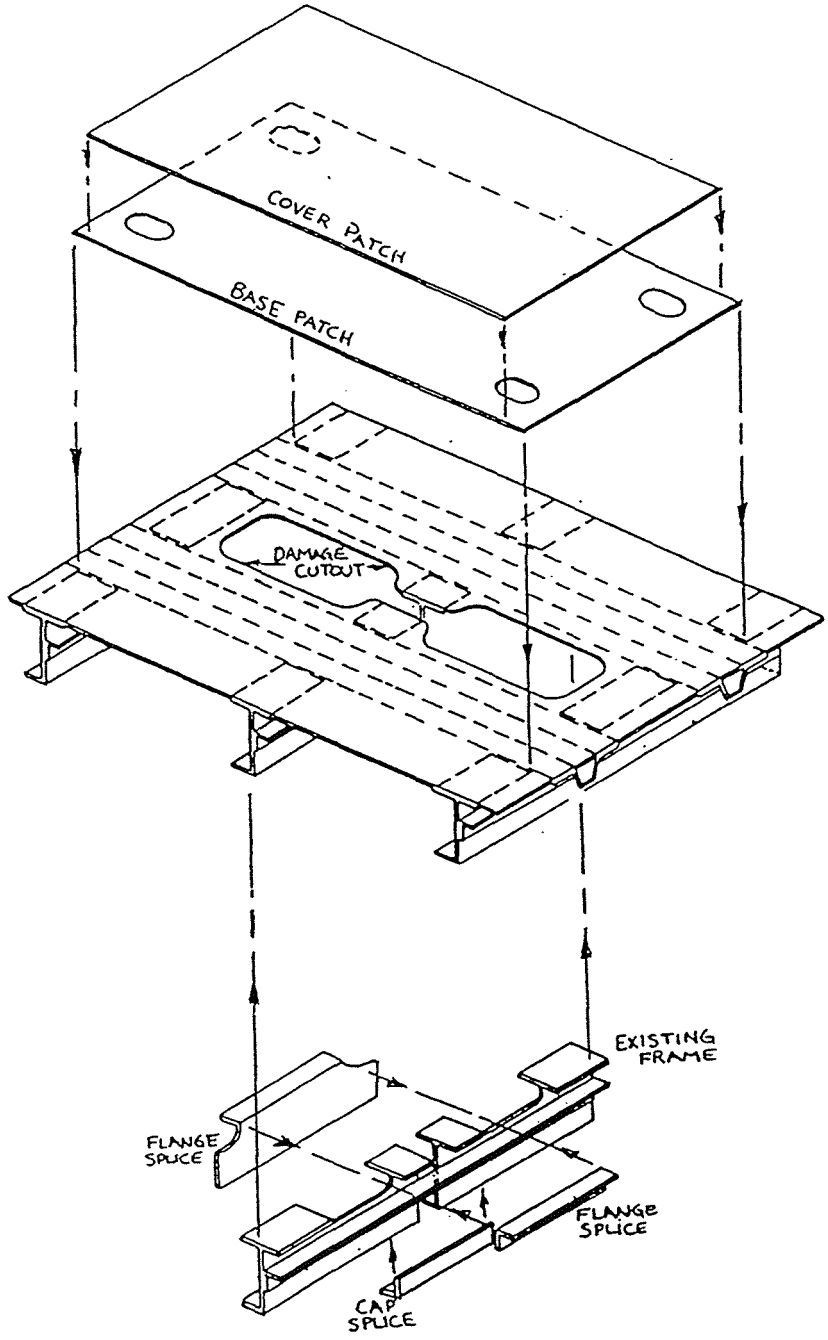

Figure A3-12: Final Repair Design Configuration

which flight load conditions could be simulated. The shortened frame cut-out and splice design were chosen as adequate for demonstration of the repair concept.

External Patches

The two layers of external patching, shown in Figure A3-12, are composed of E-glass/epoxy fabric lamination. The function of an external patch is to transfer the load that had been conducted through the removed (cut-out) skin. It also contains fuselage pressure. To avoid complications to surrounding structure, the external patch also serves to return the damaged area to its original stiffness.

Ideally, the external patch should make a multiaxial stiffness contribution that equals that of the cut-out fuselage structure. In practice this goal is complicated by geometrical constraints and limited range stiffness modulus available in structural materials. Fuselage cut-out and repair patch stiffnesses (modulus x area) are listed in Table A3-4. As listed, the final E-glass fabric patch was more stiff axially and more soft circumferentially than the cut-out fuselage skin. It should be noted that the listed fabric patch stiffnesses are based on experimental testing of the actual repair laminate and are 5% less than anticipated.

Depending on how close the original structure was designed to the limits of its allowable strains, the significance of the patch stiffness can vary. For the ATCAS fuselage crown, under the ultimate high-g maneuver load condition, little margin existed between nominal (no damage) axial strain levels and strain allowables that reflected damage tolerance and fastener bearing/bypass strain interaction criteria. Thus, the axial stiffness of the repair patch was critical. As evident from stiffnesses listed in Table A3-4, the achieved axial stiffness of the fabric repair patch was significantly higher than that of the cut-out skin. This was the case even though the employed E-glass/epoxy is the least stiff structural material available.

The external patching was composed of two layers: a base and a cover patch, as shown in Figure A3-12. Use of the multi-layered approach was dictated by the need to reduce peak fastener shear loads at the axial leading edge of the patch. A somewhat low allowable fastener load was realized due to the limited margin between nominal strains in the fuselage and strain allowables accounting for fastener bearing/bypass interaction fracture. Using the multi-layered patch approach, the base patch could be extended ahead of the cover patch. In this configuration the leading row of fasteners joins only half the patch stiffness and thus realizes half the resistance to stretching. Also noted on the sketch in Figure A3-12 are oblong cut-out holes in each corner of the base patch. Because fasteners could not be anchored into the closed hat-sectioned stringer cavity, increased duty was placed on fasteners at adjacent locations. The holes serve to reduce the stiffness of the combined repair at the leading axial edge over each stringer and thus are an artifact of the closed nature of the hat-section stringer design.

E-glass/epoxy was chosen as the patch material because its stiffness (lowest modulus structural material on the market) could best satisfy the stiffness constraints mentioned above. Patch stiffness is the product of cross-sectional area and modulus of elasticity.

Table A3-4: Final Repair Design — Stiffness Comparison of Damaged Structure Cut-Out vs. Attached Repair

Fuselage Direction	Cut-out Skin E x A (Mips)	Patch E-glass Fabric E x A (Mips)	Cut-out Frame (Mips)	Splice Frame (Mips)
Axial	3.30	8.24	-	-
Hoop	33.39	19.94	9.18	12.19

The circumferential cross-sectional width of the patch had to extend to three times that of the cut-out in order for a second column of fasteners to be anchored into the far stringer flange either side of the repair. A lesser patch width would be required for stringer designs other than the hat-section configuration of the present fuselage design. The patch width constraint combined with the bi-level objective mentioned above would dictate a low stiffness (thickness x width x modulus) of each laminate layer. Practical limits exist as to how thin laminates and sheet metal can be made. Additionally, patch thinning is not desired from a stability and pressure bulging perspective. E-glass/epoxy offered the lowest modulus of elasticity; and thus, the greatest patch thickness was possible while satisfying the cut-out stiffness matching criteria. Use of graphite/epoxy or titanium materials would have dictated a single layered patch approach and thus realized fastener bearing/bypass strain failure at a lower axial load than that required and that achievable using E-glass/epoxy.

Frame Splice

Design of the frame splice consisted of a four component assembly as depicted in Figure A3-12. The splice laminate was designed to match the stiffness of the severed woven-graphite/epoxy frame. Splice members employed a standard graphite/epoxy fabric because of its general availability, sufficient strength/stiffness performance, and ability to be draped and formed to complex curvatures as required of this repair.

Use of multiple splice members was influenced by the benefits of double shear load transfer from the severed frame via splicing on either side of the frame. Splice member count could have been reduced using continuous C-sectioned members, but these encounter practical dimensional tolerance limitations. Not shown in the sketches are shim plugs placed to occupy the space vacated by the cut-out frame damage.

Alternate Patch Material Design

An alternative to the above final repair design is a repair consisting of external patch laminate exhibiting stiffness anisotropy. Judicious tailoring of the external patch stiffness could enable a repair that best matched that of the cut-out fuselage structure and would thus make possible a repair of greater strength. A repair of this concept was not chosen as the final design because the chosen fabric patch material does not enable appreciable stiffness anisotropy. Also, it could be argued that a repair should be of isotropic stiffness in order to maintain generality to the array of stiffnesses realized over the entire fuselage structure. Although a tape material would have enabled stiffness anisotropy, it could not be made available within program time constraints, was more costly due to minimum order conditions and had a lesser track record than that of the fabric material.

The alternative patch design was developed using a ply material of E-glass/epoxy tape. Resultant patch and cut-out stiffnesses are listed in Table A3-5. The frame design reflected in this and the following repair effort did not contain a fail-safe chord. Also, the frame splice utilized a graphite/epoxy tow material laminate equal to that of the skin. As is evident, the tape patch stiffness is somewhat better than that of the fabric patch which

Table A3-5: Optimized Repair Design — Stiffness Comparison of Damaged Structure Cut-Out vs. Attached Repair

Fuselage Direction	Cut-out Skin E x A (Mips)	Patch GR/EP Tow E x A (Mips)	Cut-out Frame (Mips)	Splice Frame (Mips)
Axial	3.30	7.77	-	-
Hoop	33.39	23.12	6.89	6.21

was itself 5% better (axially) than predicted from ply property data. Thus, as made evident in the structural analysis of Section A3.3.3, a tape repair exhibiting stiffness anisotropy should result in greater strength than an isotropic repair.

The E-glass/epoxy tape material, G/913 manufactured by Ciba-Geigy, was chosen for the alternate design because a good bolted-joint strength database was available (Kretsis and Matthews, 1985). The reported ultimate bearing strengths (bearing stress at peak load) were significantly higher than that of the E-glass fabric material used in the final design. However, bearing yield stresses were lacking from the tape material database. Analysis of the fabric patch showed bearing yield to be critical. Thus the E-glass/epoxy tape material appears to be a superior material choice but certainty would require additional testing.

Modified Fuselage Repair

A repair design was requested for a modified crown panel which was identical to that of the other repair efforts except that its skin and stringer laminations were modified to radically change stiffness characteristics. Impetus for this effort arose from discussion of fuselage design characteristics that were impediments to repair. The modified fuselage design was formulated using the ATCAS design-cost trade analysis program COSTADE and thus was more than a simple example of a repair friendly fuselage design. The modified fuselage addressed two difficulties encountered in the above repair effort. First, the margin between nominal (no damage/no repair) strains and allowable strains was increased. Second, the skin was hardened (i.e., made stiff) axially. This, combined with the aspect ratio of the damage cut-out, resulted in skin cut-out stiffnesses that better matched what was feasible in a patch. Cut-out and patch stiffnesses for the modified fuselage are listed in Table A3-6.

Because of the increased margin between nominal and allowable strains, it was possible to place a column of fasteners along the perimeter of the cut-out. In the previous designs, fastener bearing/bypass interaction criteria were easily violated for fasteners at these locations. A second column of fasteners could now be placed into the stringer flange adjacent to the cut-out. Thus, unlike the previous repair patches, the patch did not have to be extended to the far stringer flange. The modified fuselage patch was thus much narrower axially and was thus better able to match the stiffnesses of the cut-out.

The increased margin between nominal versus bypass strain also made possible the use of a single layer patch design. The greater margin allowed for increased fastener bearing which made the tiered bi-level patch approach unnecessary. Thickness of the single layer patch would be twice that of a bi-level patch. Thus, the minimum thickness gage limitations of graphite/epoxy and titanium were not confronted. Graphite/epoxy tow laminate, equal to that of the original fuselage skin, was chosen for the repair patch due to its good stiffness matching and an existing database of bolted-joint strengths.

Table A3-6: Modified Fuselage Repair Design — Stiffness Comparison of Damaged Structure Cut-Out vs. Attached Repair

Fuselage Direction	Cut-out Skin E x A (Mips)	Patch GR/EP Tow E X A (Mips)	Cut-out Frame (Mips)	Splice Frame (Mips)
Axial	8.31	10.07		
Hoop	21.49	23.7	6.89	6.21

A3.3.3 Structural Analysis

All structural analysis was based upon solutions to finite element analysis (FEA). Both linear and nonlinear (large deflection) FEA were performed. Large deflection FEA did not allow for interactive data retrieval and was thus used only for results found to be of significant variation from linear FEA. The finite element model employed 1/4 symmetry and is shown in exploded form in Figure A3-13. Details of the finite element modeling technique can be found in Section A3.2.

The designs were analyzed for strength under ultimate load conditions listed in Table A3-1. Analysis calculations have not been included in this report for brevity. Analysis of the three repair designs identified margins-of safety for various criteria. The resultant margins-of-safety are summarized in Table A3-7. Criteria for bearing/bypass strain interaction were based upon interaction envelopes provided by Boeing. Cut-out strength criteria was based upon the Poe-Sova point strain fracture analysis method for composites. Laminate strength criteria addressed peak strain concentration as well as basic strain levels, for which allowables ensured tolerance to unobtrusive damage. Tolerance to large damage, a fail-safe load criteria, was factored for inclusion in ultimate load condition analysis. Stability was confirmed for the ultimate loads, but no effort was made to obtain final buckling loads.

Bearing/Bypass

The interaction of bearing stress and bypass strain was considered in analysis of the mechanically fastened composite joints. In particular the joined graphite/epoxy laminates were analyzed as such; however, the E-glass/epoxy laminates were not since their fracture toughness far exceeded the fuselage strain levels of interest. Thus, E-glass/epoxy laminates were analyzed for pure bearing failure.

The analysis addressed the interaction of bearing with tensile bypass strain only. The ultimate compression load condition did not induce strain levels sufficient to warrant concern. The tensile bypass strain and bearing interaction envelopes were made available by Boeing. For brevity only the envelope corresponding to bearing and bypass in the axial direction is shown in Figure A3-14. Based upon limited coupon testing, a Boeing computer program extrapolated to define a continuous iteration envelope. The program analysis method was based upon calculating stress concentration about a fastener hole undergoing bearing and bypass strain. The resultant envelope was then truncated at a level of bearing strength considered realistic. Boeing provided mean, room temperature, dry interaction envelopes. OSU applied 0.8 reduction factor to the interaction portion of the envelope which reflected B-basis, environmental effects. The 0.8 factor and the B-basis bearing cut-off stress were derived from previous Boeing, B-basis, interaction envelope definition for the same material. The effect of fastener diameter versus edge margin and bolt spacing were taken into account via a knockdown factor.

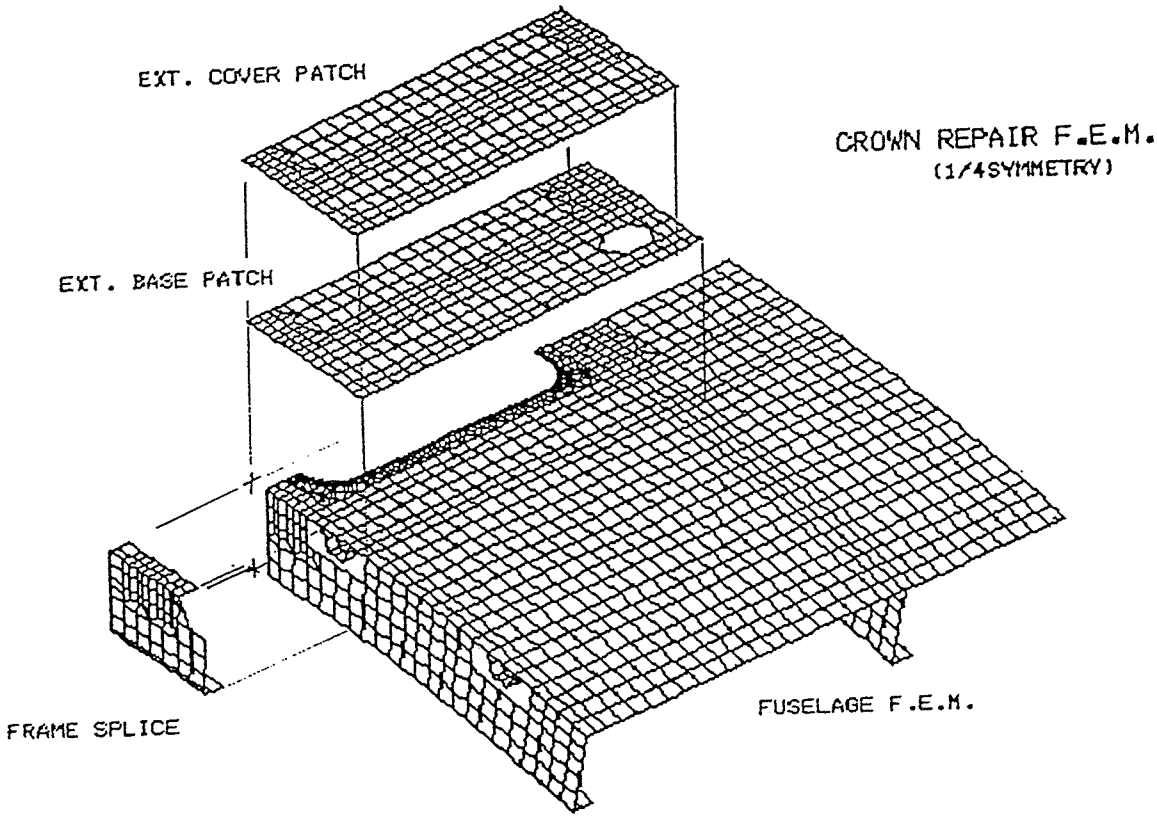

Figure A3-13: Finite Element Model for Crown Panel Repair

Table A3-7: Summary of Repair Margins of Safety

Graphite/Epoxy

Criteria	Final Repair	Alternate Repair	Alternate Fuselage
Bearing/By-pass	-0.02	-0.01	+0.10
Basic Strain	-0.14	-0.12	+0.34
Peak Strain	+0.03	+0.07	+0.25
Damage Tolerance	+0.04	+0.06	-
Cutout	+1.03	+0.92	+2.3
Buckling	None	None	None

Glass/Epoxy

Criteria	Final Repair	Alternate Repair	Alternate Fuselage
Bearing-Ult.	-0.18	+0.23	-
Bearing @ 1.15 xDesign	-0.30	-	-
Shear-out	-	+0.21	-
Pull-Through	-	-	-

Bearing / By-Pass Interaction Envelope - Skin

*Graphite/epoxy: AS4/938 Tow

* Layup: 45/-45/90/0/60/-60/90/-60/60/0/90/-45/45

* Width/bolt diameter ratio - w/d = 6

* By-pass strain in 90 degree (axial) direction

* Bearing load orientation: alpha = 0 degrees (axial)

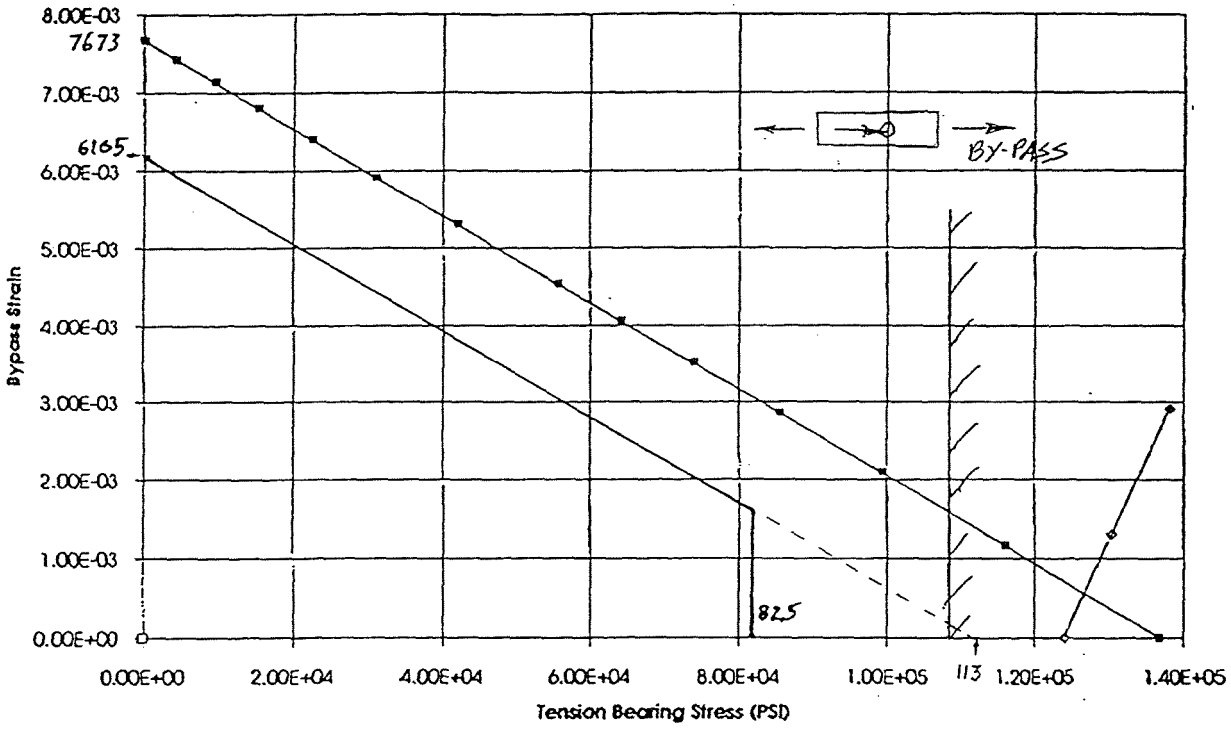

——— Allowable (B-Basis, sever environment)

—■— R.T.D., Mean

Figure A3-14: Example Bearing/Bypass Strain Interaction Envelope Allowable

Cut-out

The Poe-Sova point-strain fracture criterion discussed in Section A3.2 was applied in the analysis of the cut-out of each design. All design cut-outs strengths exceeded the criterion by at least a factor of 1.92. The point-strain criteria makes the allowance for damage development in the zone of peak strain. In doing so, it is more representative of fracture in composites than methods based upon LEFM stress intensity factorization. The identified characteristic dimension, d_o = 0.0585", and critical strain of 0.143 were applied at all locations along the cut-out edge.

It should be recognized that the point strain criterion is an ultimate strength criteria and does not attempt to address damage tolerance. Therefore, such issues as edge delamination, impact, etc. were not addressed. Boeing ATCAS has applied a damage tolerance based criterion to such details as window cut-outs. This criterion was not utilized by direction of Boeing ATCAS.

Laminate Strength

Strength criteria were applied to the repaired fuselage skin and stringer laminates. The analysis applied to the stringer identified insufficient strength at ultimate loads. However, this apparent strength deficiency is also associated with the nominal, no-damage/no-repair fuselage. The criteria addressed tolerance to concentrated strain and hidden damage. No data for such criteria was available for the frame members. However, in light of their low strain, their safety was of little concern. Strength analysis calculation for the E-glass/epoxy patch laminates was also not made. This was primarily due to the lack of concern considering the high strain capability of the material. "B" basis tensile strain allowables of 0.01 surpassed all strains developed in the patch under ultimate load conditions.

A basic strain criterion was applied to the repaired fuselage skin and stringer laminates. The criterion addressed tolerance to hidden damage, fastener holes and extreme environments. It was intended not to address concentrated strain areas or flexure. In regards to the axially directed strength, a skin laminate allowable of 5575 microstrain was satisfied for all conditions. However, the stringer allowable of 4660 microstrain was exceeded under the ultimate high-g maneuver load condition. The basic strain margin-of-safety for the stringer was M.S.=-0.14. However, the nominal fuselage would experience an average axial strain of 4960 microstrain for this load condition and thus realized a margin-of-safety of as least M.S.=-0.06. The allowables were calculated from formulae provided by Boeing specific to the fuselage material AS4/938 Tow.

A peak strain criterion was also applied to the repair fuselage. The criterion applied "B" basis unnotched laminate strength to strain concentrations including that associated with flexure. The criterion was not applied in the vicinity of the cut-out. Allowables in the critical axial direction of 7680 microstrain for the skin laminate were satisfied uniformly. Calculations were not applied to the stringer considering that it experienced little variation of strain and would have realized a significant positive margin-of-safety.

Damage Tolerance

Damage tolerance was addressed for two levels of damage defined as detectable and nondetectable. Tolerance to nondetectable damage was incorporated into the ultimate basic-strain/strength criteria discussed above. Detectable damage definition varied from that of visible impact indentation to complete structural unit failure. With respect to the fuselage crown area, the critical structural unit of concern was that of two adjacent skin bays plus central stringer or frame member. Tolerance to detectable damage was treated as a safety-of-flight load criterion. The analysis was conducted by Boeing for the nominal fuselage design and resulted in allowables for far-field strain levels. These allowables were factored up to reflect ultimate load conditions analyzed in the repair design. Repair damage tolerance analysis then determined whether the disturbed fuselage strain field exceeded the damage tolerance allowable.

Damage tolerance analysis of repaired fuselage indicated a minimum margin-of-safety of MS = +0.04 for axially directed strain under the ultimate high-g maneuver load condition. In general, the repair damage tolerance analysis focused on the fuselage structure just outside of the repair area. At these areas one can expect the greatest disturbance of the nominal strain field. Axial and hoop strains were determined over cross-sections in these areas using finite element analysis results. The cross sections included skin of one bay length positioned symmetrically over the substructure member of concern. Strains over the cross-section varied, and an average was arrived at for comparison to the allowable. Averaging implies a weighting of terms, and in this case strain was weighted according to the stiffness of the laminate. Thus, strain of the hard stringer laminate was given proportionately higher weighting than that of the skin.

Stability

Stability of the repaired fuselage was analyzed for the ultimate conditions generating an axial compressive load of -1686 lbs./in. Stability was confirmed for all repair designs considered. Further analysis sought to determine the load level at which initial buckling of the skin or patch laminate would occur. Skin buckling was generally initiated at 113 percent of limit load. The modified fuselage was an exception since no initial buckling was predicted below the ultimate load mentioned above.

Stability analysis was based upon nonlinear, large deflection finite element analysis. The incremental load level at which the model stiffness matrix becomes singular was taken as the instability. Compressive loading of the model was incremented up to the ultimate load identified above. Initial buckling of the skin would produced nonconvergence of the analysis. This condition was recognized for what is was, and its load level noted. To load beyond this level, mode-one skin buckling shape was given a small assistance which enabled convergence of solution iteration. Loading was then incremented up to the ultimate load defined above.

A4.0 CONCLUSION

The goal of this project has been the development of cost-effective repair techniques for damaged composite fuselage. The primary focus has been the repair of a 22-inch, through-penetration notch in the aft crown-section of the fuselage. Only mechanically fastened repair concepts were considered because of their advantages over bonded repairs.

To gain some understanding of the critical variables that effect performance without the expense of full scale tests, experiments were performed on uni- and biaxially loaded, notched coupons with various repair patches, fasteners and load conditions. The tests indicated that large patches with multiple rows of titanium bolts were more effective than small patches with a single row of bolts around its periphery. Additionally, titanium fasteners were superior to thermoplastic rivets. Comparison of test results with finite element predictions gave an indication of the reliability of computer analysis. In general it was found that strains in repaired composites could be predicted with reasonable accuracy, provided that geometric nonlinearities (large deflections) were taken into account. Likewise large deflection analysis better modeled the nonlinear evolution of the repair's in-plane stiffness. Strain predictions were less accurate within the repair for biaxial load conditions. Failure analysis considered notch fracture, fastener bearing/bypass strain, and peak strain outside of repair. Prediction of failure load and mode of failure was less reliable than that of strains. The inaccuracy of the failure and strain predictions were apparently due to material and/or part contact nonlinearities. Bearing yield, initial non-uniformity of fastener-hole alignment, and friction between patch and specimen were anticipated but not modeled due to complexity of these phenomena and lack of analysis methods. Nevertheless, bearing yield should enable bolt loads in the repair to become more uniformly distributed. This should result in tested bearing/bypass strength greater than that predicted, a comparison which was realized. Also, strains within the repair area were greater than predicted for both specimen and patch which suggested the influence of friction coupling.

During the development of the fuselage repair design, it became apparent that a general approach to fuselage repair should be an integral part of fuselage design development. It should result in detailed procedures for damage removal and repair that would be made part of the deliverable aircraft. Design costs studies of fuselage configurations should include repair costs influenced by substructure spacing and design, stiffness anisotropy and resultant operational strains. The studies should weigh costs associated with repair versus factory replacement of damage cut-out areas.

The resultant repair procedure should include a damage cut-out plan that defines discrete increments of fuselage removal for which repair is at hand. This is not unlike a jig-saw puzzle from which more and more pieces are removed depending on the extent of damage. Repair design would be made available as part of the deliverable aircraft, where depending on the cut-out size and location, patching of specific size, layering and stock material

would be identifiable. Repair components and strategy would be defined by design costs studies to ensure return of ultimate strength for the even the most extreme damage condition while minimizing costs associated with the more probable small damage conditions. It was envisioned that multiple layers of stock material could be assembled to address severe cut-out conditions. A simple reduction of layers would then address less severe damage. The procedure for assembling patch layering could then be defined in a building-block/damage level framework.

Repair in general should necessitate only those tools and skills that are widely available within the customer base. Thus, mechanical attachment would be employed over adhesive bonding for fuselage/repair joining. Repair material should be available in standardized stock forms to avoid costs of composite laminate fabrication and perishable material storage. A final design, reflective of the above approach, was arrived at and analyzed for safety under ultimate load conditions. The 22" axial notch was removed in block cut-out fashion. A simple laminate of quasi-isotropic stiffness was employed for external skin patching in a bi-level manner. Frame patching also used a simple laminate intended as stock material.

Protruding head fasteners were used throughout the repair. Return of the damaged fuselage to ultimate strength was not achieved from a severe environment, "B" basis, standpoint. A minimum margin-of-safety MS = -0.18 was identified and associated with bearing failure of the external base patch of E-glass/epoxy. Close behind was a MS = -0.14 associated with basic strain of the stringer laminate, followed by a MS = -0.02 for bearing/bypass failure of the fuselage. All of these negative margins-of-safety were associated with the ultimate high-g maneuver load condition. No negative margins were associated with the remaining load conditions. An additional criteria was imposed on the bearing strength of the E-glass/epoxy in that it should not yield at load levels of 115 percent of limit. Margins-of-safety associated with this condition under severe environmental, "B", basis were MS = -0.3.

Inability to derive a repair design which could return the fuselage to ultimate strength was directly tied to the small margin existing in the nominal fuselage design between operational strains and allowables. In other words, the nominal fuselage was designed so close to the allowables for basic strain, damage tolerance, etc., that it could accept little perturbation of its strain field due to damage cut-out and repair.

Further analysis showed that optimization of the above repair was possible using a patch laminate exhibiting stiffness anisotropy and a higher performing E-glass/epoxy material. However, applicability of any specific stiffness anisotropy to fuselage repair in general is open to question. A minimum margin-of-safety for the optimum design was MS = -0.16 associated with basic ultimate strain of the stringer laminate, followed by MS = -0.01 associated with bearing/bypass of the fuselage laminate. It should be noted that the basic ultimate strain criterion applied to the nominal fuselage stringer should also produce negative margins-of-safety.

The nominal fuselage design was arrived at without the benefit of lessons learned in this repair study. An alternate fuselage design, derived by Boeing design-cost studies, was identified that seemed better suited to repair. In contrast to the nominal fuselage, its dominate stiffness was aligned with the dominant axial load and thus reduced peak operational strains. This allowed fasteners to transfer greater loads without violating bearing/bypass criteria and for them to be positioned where it was previously not possible. Additionally, the combination of the alternate skin stiffness anisotropy and the aspect ratio of the bay cut-out shapes made patch stiffness replacement more attainable. The resultant repair was more simple in that it required only one layer of external patch laminate and was of significantly reduced size. It also produced all positive margins-of-safety. Additional fuselage design improvement, from a repair perspective, would do away with hat-sectioned stiffener configurations.

A5.0 REFERENCES

Adkins, D.W. and Pipes, R.B., 1985, "End Effects in Scarf Joints," *Composites Science and Technology*, Vol. 22, pp. 209-221.

Bair, D.L., Hudson, P.O., and Ghanimati, G.R., 1991, "Analysis and Repair of Damaged Composite Laminates," 36th International SAMPE Symposium, pp. 2264-2278.

Baker, A.A., 1986a, "Joining Advanced Fiber Composites," *Composite Materials for Aircraft Structures*, Hoskin, B.C., and Baker, A.A. (Eds.), AIAA, pp. 115-139.

Baker, A.A., 1986b, "Repair of Graphite/Epoxy Composites," *Composite Materials for Aircraft Structures*, Hoskin, B.C., and Baker, A.A. (Eds.), AIAA, pp. 193-216.

Bohlmann, R.E., Renieri, G.D., and Libeskind, M., 1981, "Bolted Field Repair of Graphite/Epoxy Wing Skin Laminates," *Joining of Composite Materials*, ASTM STP 749, pp. 97-116.

Bohlmann, R.E., Renieri, G.D., and Riley, B.L., 1986, "Bolted Field Repairs Subjected to Biaxial or Shear Loads," *Composite Materials: Testing and Design*, ASTM STP 893, pp. 34-47.

Busch, J.D. and Dompka, R.V., 1991, "V-22 Composite Repair Development Program: Evolution of a Permanent Repair Design," Third DoD/NASA Composite Repair Technology Workshop, pp. 241-290.

Chandra, R. and Subramanian, A., 1989, "Stress-Intensity Factors in Plates with a Partially Patched Central Crack," *Experimental Mechanics*, Vol. 29, pp. 1-5.

Cripps, D.B., 1984, "Development of a Field Repair Technique for Mini-Sandwich Kevlar/Epoxy Aircraft Skin," M.S. Thesis, Naval Postgraduate School.

Deaton, J.W., 1991, "Evaluation of Repair Durability for Graphite/Epoxy Laminates after 7 Years of Outdoor Exposure," Third DoD/NASA Composites Repair Technology Workshop, pp. 393-418.

Dehm, S. and Wurzel, D., 1989, "Fast, In-Situ Repair of Aircraft Panel Components," *Journal of Aircraft*, Vol. 26, pp. 476-481.

Dodd, S.M. and Sandow, F., 1991, "Optimum Repair Design for Aircraft Battle Damage Repair," Third DoD/NASA Composites Repair Technology Workshop, pp. 148-167.

Hall, S.R., Raizenne, M.D., and Simpson, D.L., 1989, "A Proposed Composite Repair Methodology for Primary Structure," *Composites*, Vol. 20, pp. 479-483.

Hoehn, G. and Ramsey, C., 1986, "Test Verification of Improvements to Bolted Repair Design Methodology," Second Dod/NASA Composites Repair Technology Workshop, pp. 341-359.

Hunter, M.W., 1990, "Modeling and Analysis of Orthotropic Plate with Circular Cutout and Adhesive Bonded Patch," M.S. Thesis, Air Force Institute of Technology.

Jones, R. and Callinan, R.J., 1979, "Finite Element Analysis of Patched Cracks," *Journal of Structural Mechanics*, Vol. 7, pp. 107-130.

Jones, R. and Callinan, R.J., 1981, "A Design Study in Crack Patching," *Fiber Science and Technology*, Vol. 14, pp. 99-111.

Labor, J.D., 1981, "Composite Repair Concepts for Depot Level Use," 26th National SAMPE Symposium, pp. 705-715.

Labor, J.D. and Myhre, S.H., 1979a, "Repair Guide for Large Area Composite Structure Repair," AFFDL-TR-79-3039.

Labor, J.D, and Myhre, S.H., 1979b, "Large Area Composite Structure Repair," AFFDL-TR-79-3040.

Lin, K.Y. and Wang, F.X., 1988, "Development of Composite Repair Techniques," Boeing Advanced Systems Company, Contract No. GU2941.

Kretsis, G. and Matthews, R.J., 1985, "The Strength of Bolted Joints in Glass Fiber/Epoxy Laminates," *Composites*, pp. 92- 102.

Mahon, J. and Candello, J., 1981, "Development of Large-Area Damage Repair Procedures for the F-14A Horizontal Stabilizer," 26th National SAMPE Symposium, pp. 825-835.

Maman, S., 1989, "Composite Material Repair and Reliability," M.S. Thesis, Naval Postgraduate School.

Manno, A., 1981, "Review of Navy Composite Repair Program," 26th National SAMPE Symposium, pp. 695-704.

Myhre, S.H., 1981, "Advanced Composite Repair-Recent Developments and Some Problems," 26th National SAMPE Symposium, pp. 716-727.

Myhre, S.H. and Kiger, R.W., 1980, "Problems and Options in Advanced Composite Repair," *Composites in Structural Design*, Lenoe, E.M., Oplinger, D.W., and Burke, J.J. (Eds.), Plenum Press, pp. 354-380.

Paul, J. and Jones, R., 1989, "Analysis and Repair of Impact Damaged Composites," Aeronautical Research Laboratory, ARL-STRUC-R-435.

Poe, C.C., Jr. and Sova, J. A., 1980, "Fracture Toughness of Boron/Aluminum Laminates with Various Proportions of 0° and ±45° Plies," NASA Technical Paper 1707, 1980.

Poe, C.C., Jr., 1983,"A Unifying Strain Criterion for Fracture of Fibrous Composite Laminates," *Engineering Fracture Mechanics*, Vol. 17, pp. 153-171.

Polland, D.R. and Swanson, G.D., 1993, Private Communication.

Reisdorfer, D.A., 1992, "Evolution of Permanent Composite Repair Designs," *24th International SAMPE Technical Conference*, pp. T791-T805.

Renton, W.J. and Vinson, J.R., 1977, "Analysis of Adhesively Bonded Joints Between Panels of Composite Materials," *ASME Journal of Applied Mechanics*, Vol. 44, pp. 101-106.

Russell, S.G. and Kan, H.P., 1991, "Rapid Analysis Procedures for Combat-Damaged Composite Aircraft Structures," Third DoD/NASA Composites Repair Technology Workshop, pp. 1210-146.

Siener, M.P., 1992, "Stress Field Sensitivity of a Composite Patch Repair as a Result of Varying Patch Thickness," *Composite Materials Testing and Design*, ASTM STP 1120, pp. 444-464.

Shyprykevich, P., 1986, "Design and Analysis of Field Repairs for High-Strain Composite Wing," Second DoD/NASA Composite Repair Technology Workshop, pp. 315-337.

Shyprykevich, P., Rosenzweig, E., and Corrigan, M., 1991, "Bolted Repairs for High-Strain Wing: Analysis and Test Validation," Third DoD/NASA Composite Repair Technology Workshop, pp. 291-316.

Smith, P.J., Bodine, J.B., Preuss, C.H., and Koch, W.J., 1992, "Design, Analysis, and Fabrication of a Pressure Box Test Fixture for Tension Damage Tolerance Testing of Curved Fuselage Panels," *Third NASA Advanced Technology Conference*, NASA CP 3154, pp. 789-906.

Trabocco, R.E., Donnellan, T.M., and Williams, J.G., 1988, "Repair of Composite Aircraft," *Bonded Repair of Aircraft Structures*, Baker, A.A. (Ed.), Martinus Nijhott, pp. 175-211.

Walker, T.H., Ilcewicz, L.B., Polland, D.R., and Poe, C.C., Jr., 1992, "Tension Fracture of Laminates for Transport Fuselage - Part II: Large Notches," *Third NASA Advanced Technology Conference*, NASA CP 3178, pp. 727-758.

Whitney, J.M. and Nuismer, R.J., 1974, "Stress Fracture Criteria for Laminated Composites Containing Stress Concentrations, *Journal of Composite Materials*, Vol. 8, pp. 253-265.

REPORT DOCUMENTATION PAGE

Form Approved
OMB No. 0704-0188

1. AGENCY USE ONLY *(Leave Blank)*	2. REPORT DATE	3. REPORT TYPE AND DATES COVERED
	April 1997	Contractor Report

4. TITLE AND SUBTITLE
Advanced Technology Composite Fuselage - Repair and Damage Assessment Supporting Maintenance

5. FUNDING NUMBERS
C NAS1-18889
C NAS1-20013 (Task 2)
WU 510-02-13-01

6. AUTHOR(S)
B.W. Flynn, J.B. Bodine, B. Dopker, S. R. Finn, K.H. Griess, C.T. Hanson, C.G. Harris, K.M. Nelson, T.H. Walker, T. C. Kennedy, and M.F. Nahan

7. PERFORMING ORGANIZATION NAME(S) AND ADDRESS(ES)
The Boeing Company
P.O. Box 3707
Seattle, WA 98124-2207

8. PERFORMING ORGANIZATION REPORT NUMBER

9. SPONSORING / MONITORING AGENCY NAME(S) AND ADDRESS(ES)
National Aeronautics and Space Administration
Langley Research Center
Hampton, VA 23681-0001

10. SPONSORING / MONITORING AGENCY REPORT NUMBER
NASA CR-4733

11. SUPPLEMENTARY NOTES
Langley Technical Monitor: W.T. Freeman, Jr.

12a. DISTRIBUTION / AVAILABILITY STATEMENT
~~FEDD~~ Publicly Available
Subject Category 24

12b. DISTRIBUTION CODE

13. ABSTRACT *(Maximum 200 words)*

Under the NASA-sponsored contracts for Advanced Technology Composite Aircraft Structures (ATCAS) and Materials Development Omnibus Contract (MDOC), Boeing is studying the technologies associated with the application of composite materials to commercial transport fuselage structure. Included in the study is the incorporation of maintainability and repairability requirements of composite primary structure into the design. This contractor report describes activities performed to address maintenance issues in composite fuselage applications.

A key aspect of the study was the development of a maintenance philosophy which included consideration of maintenance issues early in the design cycle, multiple repair options, and airline participation in design trades. Fuselage design evaluations considered trade-offs between structural weight, damage resistance/tolerance (repair frequency), and inspection burdens. Analysis methods were developed to assess structural residual strength in the presence of damage, and to evaluate repair design concepts.

Repair designs were created with a focus on mechanically fastened concepts for skin/stringer structure and bonded concepts for sandwich structure. Both a large crown (skin/stringer) and keel (sandwich) panel were repaired. A compression test of the keel panel indicated the demonstrated repairs recovered ultimate load capability. In conjunction with the design and manufacturing developments, inspection methods were investigated for their potential to evaluate damaged structure and verify the integrity of completed repairs.

14. SUBJECT TERMS	15. NUMBER OF PAGES
Advanced Composite Technology Program; Maintenance; In-service experience; Skin/stringer; Sandwich; Bolted repair; Bonded repair; Inspection;	153
	16. PRICE CODE

17. SECURITY CLASSIFICATION OF REPORT	18. SECURITY CLASSIFICATION OF THIS PAGE	19. SECURITY CLASSIFICATION OF ABSTRACT	20. LIMITATION OF ABSTRACT
Unclassified	Unclassified	Unclassified	